QATAR UNIVERSITY

COLLEGE OF ENGINEERING

THE EFFECT OF WATER TABLE FLUCTUATIONS AND SOIL HYDROGEOCHEMISTRY ON THE DISTRIBUTION OF NAPLS IN GROUNWATER

BY

REEM ELFATIH ISMAIL

A Dissertation Submitted to

the College of Engineering

in Partial Fulfillment of the Requirements for the Degree of

Doctor of Philosophy in Civil Engineering

June [2023]

COMMITTEE PAGE

The members of the Committee approve the Dissertation of

[Reem Ismail] defended on 16/01/2023.

_____

[Prof. Riyadh Al-Raoush]
Thesis/Dissertation Supervisor

_____

[Dr. Hazim Ali Qiblawey]
Committee Member

_____

[Dr. Ahmad Khalaf Sleiti]
Committee Member

Approved:

_____

Khalid Kamal Naji, Dean, College of Engineering

ABSTRACT

Ismail, Reem Doctorate: June: 2023, Doctorate of Philosophy in Civil Engineering

Title: The effect of water table fluctuation and hydrogeochemical properties on NAPLs natural attenuation

Supervisor of Dissertation: Dr. Riyadh, Al-Raoush

Human activities have recently resulted in the degradation and contamination of groundwater. Petroleum spills, such as crude oil, gasoline, and diesel fuel, are a major source of groundwater contamination, especially along coastlines. Crude oil contamination causes major social, economic, and environmental problems around the world because it progressively changes the makeup of soil and groundwater.

Predicting the fate and transport of contaminants through the soil, as well as managing water resources, irrigation, and fertilizer all rely on accurate predictions of water movement in the saturated and unsaturated zones.

In this thesis, three experiments were performed to understand the effect of water table fluctuations on the distribution and natural attenuation of BTEX and the hydrogeochemical properties of the soil. Each one of the experiments were performed to understand the effect of the following parameters: salinity effect, soil layering, temperature, and the effect of aerobic and anaerobic conditions. Different pore water analyses were performed during the experiment which included ORP, EC, pH, cations and anions, and GC analysis for aqueous and soil samples. The experiments were performed in the laboratory using natural soil samples from the beach of simaisma in the eastern side of Qatar.

The first study investigating the impact of two salinities, brackish water and seawater, observed spatial and temporal variations in redox conditions within the soil columns. Moreover, ORP values showed consistent patterns in the stable column and bottom of the fluctuating column but varied in the middle of the fluctuating columns due to

organic presence and changing water table levels, while no significant differences were observed between high and low salinity columns. EC values decreased initially in the fluctuating columns, followed by an increase, while stable columns showed a consistent decline. The pH range was narrower in stable columns and became more alkaline over time in fluctuating columns. Sulfate was abundant as a major electron acceptor, while iron, manganese, nitrogen, and nitrate were present in low concentrations. Benzene and toluene concentrations decreased faster in fluctuating columns, resulting in a shorter lifespan for the source zone. The consumption of sulfate indicated improved natural attenuation in fluctuating columns. The study suggested the potential of water table fluctuations to expedite LNAPL remediation in contaminated aquifers, considering site-specific factors.

In the second study, soil layering lowers the enhancement of reducing conditions as BTEX are present in low permeability layer, same as the slower fluctuation's intensity, while temperature increase resulted in ORP reduction. Statistical tests showed significant differences in middle and bottom ORP values. EC values were greatly influenced by fluctuation and temperature, with statistical tests confirming significant differences. Statistical tests confirmed significant differences in sulfate concentrations. The positive correlation with ORP and negative correlation with DIC, combined with the association between BTEX and sulfate concentrations, indicated an increase in biodegradation in the columns.

DEDICATION

To Al mighty Allah,

My parents,

Awlla, Dena, Mohamed, Elfatih, and my husband

ACKNOWLEDGMENTS

I would like to express my gratitude to almighty Allah for bringing my vision to reality, all honor and glory are due to Him alone.

My deep gratitude to Prof. Riyadh Al Raoush my supervisors. Thanks to him for all his help, direction, encouragement and technical input during the course of this journey.

To the whole Civil Engineering department at Qatar University, I owe a debt of gratitude for their exceptional cooperation and assistance in enabling me to carry out my research aims. Special thanks to the technical staff of the department-in particular Mr. Abdul aziz, Mr. Siju Joseph. I would like to express my sincere thanks to Mr. Khalid al Jamal, for his assistance with the preliminary analysis of this work, and the technical staff of the central lab unit, in particular-Dr. Mohammed Ibrahim, Mr. Ahmed Al Ahmedi, Dr. Ahmed Abdelsalam, Mr. Mohammed Akkbik and Mr. Ahmed Suliman for their assistance throughout the experiment, as well as my fellow classmates and friends Safna, Ratiba, Hanadai, Fatima, Wamda, Hania and Malak for their encouragement and support during the course of the PhD. I would like to extend my sincere gratitude to Jamal Hannan and Ahmed Rahmani for all the assistance they provided. I would like to express my gratitude to Qatar National Research Fund (QNRF) for their financial support, which made this study feasible. Without their assistance, this project would have been impossible.

I would want to express my heartfelt thanks to my family, which includes my father, mother, sisters, and brothers, for their continuous support and encouragement throughout my life. My friends at home and abroad have each made a significant contribution to this achievement in their own manner.

my gratitude to my husband and children for their love, support, and for standing up for me while I was away.

TABLE OF CONTENTS

DEDICATION v

ACKNOWLEDGMENTS vi

LIST OF TABLES xi

LIST OF FIGURES xii

LIST OF ABBREVIATIONS xv

CHAPTER 1 INTRODUCTION 1

1.1 Research objectives 4

1.2 Outline of the thesis 5

CHAPTER 2 LITERATURE REVIEW 6

2.1 Groundwater Contamination and Non-aqueous phase liquids 6

2.1.1 Total petroleum hydrocarbons degradation (aerobic/anaerobic) 11

2.2 Water Table Fluctuations, its enhancement on TPHs and soil hydrogeochemistry 14

2.2.1 Soil and Groundwater hydrogeochemistry 21

CHAPTER 3 MATERIAL AND METHODS 27

3.1 Field sampling and soil analysis 27

3.2 Experimental setup of columns 28

3.3 Analytical methods 30

CHAPTER 4 THE SYNERGIC IMPACT OF WATER TABLE FLUCTUATION AND SALINITY ON LNAPLS DISTRIBUTION AND HYDROGEOCHEMICAL PROPERTIES IN THE SMEAR ZONE UNDER COMPLETELY ANAEROBIC

CONDITIONS 33
4.1 Introduction 33
4.2 Experimental Setup 36
4.3 Results and Discussion 39
4.3.1 Pore water geochemistry 39
4.3.1.1 Water table and redox regimes 39
4.3.1.2 Electrical Conductivity (EC) 43
4.3.1.3 pH 47
4.3.1.4 Concentration of electron acceptors 49
4.3.1.5 Dissolved Inorganic Carbon (DIC) 52
4.3.2 Concentration of dissolved organics 54
4.3.2.1 Concentration of dissolved and solid-phase Toluene 54
4.3.2.2 Concentration of dissolved and solid-phase Benzene 60
4.4 Conclusion 65
CHAPTER 5 THE CORRELATION BETWEEN BTEX ATTENUATION, AND SOIL HYDROGEOCHEMICAL PROPERTIES UNDER THE EFFECT OF WATER TABLE FLUCTUATION 67
5.1 Introduction 67
5.2 Experiment Setup 72
5.3 Results and Discussion 74
5.3.1 Pore water geochemistry 74
5.3.2 Electrical Conductivity (EC) 77

5.3.3 pH....80
5.3.4 Concentration of electron acceptors....81
5.3.5 Dissolved Inorganic Carbon (DIC)....84
5.3.6 Dissolve organics phase....85
5.3.7 Correlation between the hydrogeochemical parameters of dissolved organics 86
5.4 Conclusion....93
CHAPTER 6 THE INFLUENCE OF GROUNDWATER FLUCTUATION ON THE NATURAL ATTENUATION OF HOMOGENIZED CONTAMINATED SOIL UNDER AEROBIC AND ANAEROBIC CONDITIONS....99
6.1 Introduction....99
6.2 Experiment Setup....103
6.2.1 Soil Spiking....104
6.2.2 Column experiment....104
6.2.3 Water table regimes....105
6.3 Results and Discussion....105
6.3.1 Properties of groundwater and pore water geochemistry....105
6.3.2 Terminal electron acceptors and DIC....112
6.3.3 Dissolved organic phase....116
6.4 Conclusion....120
CHAPTER 7 SUMMARY AND CONCLUSIONS....122
CHAPTER 8 RECOMMENDATION FOR FUTURE WORK....125

REFERENCES 126

APPENDIX A: SOIL SAMPLING AND EXPERIMENT EQUIPMENT'S.....152

APPENDIX B: CALIBRATION CURVED FOR GC ANALYSIS 156

APPENDIX C: CHAPTER 5 FIGURES 159

APPENDIX D: STATISTICAL ANALYSIS – PARAMETERS EXAMPLE 162

APPENDIX E: CHAPTER 6 FIGURES 163

LIST OF TABLES

Table 1: Synthetic Groundwater properties 28

Table 2: The experiement Design 38

Table 3: Water table Column’s characteristics 74

Table 4: Correlation values and criteria 94

LIST OF FIGURES

Figure 1: Schematic diagram of the experimental set-up. Depth A (-10 cm), depth B (-30 cm), and depth C (-50 cm) from the top of the column. 30

Figure 2: Experiment Setup 39

Figure 3: Oxidation-Reduction potential (ORP) at (left) depth B and C for the columns S1 and F1(for the case of low salinity columns), (right) ORP at the depth B and C for the columns S2 and F2 (for the case of high salinity columns) 43

Figure 4: Electrical Conductivity (EC) concentrations at (left) at depth B and C for the columns S1 and F1(low salinity), (right) Electrical Conductivity (EC) concentrations at depth B and C for the columns S2 and F2 (high salinity).....46

Figure 5: pH for (left) at depth B and C for the columns S1 and F1(low salinity columns), (right) pH at depth B and C for the columns S2 and F2 (high salinity).....49

Figure 6: Dissolved sulfate concentrations at depth B of the stable columns (S1 and S2), and depth B, and C for the fluctuating columns (F1 and F2). 52

Figure 7: Dissolved inorganic carbon (DIC) concentrations at depth B for stable (S1 and S2) and fluctuation columns (F1 and F2).....55

Figure 8: Toluene concentrations for (a) depth A (b) for depth B, (c) for depth C, and (d) for final soil concentrations of the columns S1, S2, F1, and F2. 60

Figure 9: Benzene concentrations for (a) depth A (b) depth B, (c) depth C, and (d) the final benzene concentration of the stable and fluctuating water table columns S1, S2, F1, and F2. 65

Figure 10: ORP values at (left) the middle (depth B) and (right) the bottom (depth C) of the columns S, F1, F2, F3, and F4. 77

Figure 11: EC values at (left) the middle (depth B) and (right) the bottom (depth C) of the columns S1, F1, F2, F3, and F4 80

Figure 12: pH values at (left) the middle (depth B) and (right) the bottom (depth C) of the columns S1, F1, F2, F3, and F4 81
Figure 13: Sulfate concentrations at (left) the middle (depth B) and (right) the bottom (depth C) of the columns S, F1, F2, F3, and F4 84
Figure 14: Dissolved Inorganic Carbon (DIC) at the middle (depth B) of the columns S, F1, F2, F3, and F4 85
Figure 15: Benzene Correlation with pH, ORP, EC, sulfate concentrations, and DIC at the middle of the columns S, F1, F2, F3, and F4 95
Figure 16: Toluene Correlation with pH, ORP, EC, sulfate concentrations, and DIC at the middle of the columns S, F1, F2, F3, and F4 96
Figure 17: Ethylbenzene correlation with pH, ORP, EC, sulfate concentrations, and DIC at the middle of the columns S, F1, F2, F3, and F4 97
Figure 18: Xylene Correlation with pH, ORP, EC, sulfate concentrations, and DIC at the middle of the columns S, F1, F2, F3, and F4 98
Figure 19: Oxidation reduction potential (ORP) at the middle (depth B) and the bottom (depth C) of the columns S1 and F1 110
Figure 20: Electric conductivity (EC) at the middle (depth B) and the bottom (depth C) of the columns S1 and F1 111
Figure 21: pH values at the middle (depth B) and the bottom (depth C) of the columns S1, and F1 112
Figure 22: Dissolved sulfate concentrations at the middle (depth B) of the columns S1, S2, F1, and F2 114
Figure 23: Dissolved inorganic carbon (DIC) at the middle (depth B) of the columns S1, S2, F1 and F2. 115
Figure 24: Toluene concentrations at the middle (depth B) and the bottom (depth C) of

the columns S1 and F1.....117
Figure 25: Naphthalene concentrations at the middle (depth B) and the bottom (depth C) of the columns S1 and F1.....119

LIST OF ABBREVIATIONS

BTEX	Benzene, toluene, ethylbenzene and xylenes
Bss	Below soil surface
Ca^{2+}	Calcium
Si	Silicon
Mn	Manganese
CH_4	methane
CO_2	Carbon dioxide
DO	Dissolved oxygen
DOC	Dissolved organic carbon
DIC	Dissolved inorganic carbon
Eh	Redox potential
ORP	Oxidation reduction potential
Fe^{2+}	Ferrous iron
Fe(III)	Ferric iron
g	Gram
GC	Gas chromatography
GC/MS	Gas Chromatography/Mass Spectrometry
GC-FID	Gas Chromatography- Flame Ionization Detector
IC	Ion Chromatography
ICP-MS	Inductively coupled plasma-mass spectrometry
K^+	Potassium
L	Liter
mg	Milligram

Mg^{2+}	Magnesium
mL	Milliliter
N_2	nitrogen
Na+	Sodium
NA	Natural attenuation
NAPL	Non-aqueous phase liquid
NO_3^-	nitrate
O_2	Oxygen
PHC	Petroleum hydrocarbon
SO_4^{2-}	Sulfate
SRB	Sulfate-reducing bacteria
TEA	Terminal electron acceptor
TIC	Total inorganic carbon

CHAPTER 1 INTRODUCTION

Groundwater is one of the most valuable natural resources available on earth. Its existence is vital to life and a fundamental part of our natural environmental cycles of carbon, nitrogen, oxygen, water, and nutrients. In some areas of the world, groundwater is the only source of drinking and irrigation. In recent years, human activities have resulted in the degradation and contamination of groundwater. Petroleum spills, such as crude oil, gasoline, and diesel fuel, are a significant source of groundwater contamination, particularly in coastal locations. Petroleum hydrocarbons (PHs) have emerged as a pervasive environmental pollutant. The contamination resulting from crude oil presents global challenges, significantly impacting the environment, economy, and society. This contamination gradually alters the composition of both soil and groundwater. Furthermore, among the various hazardous chemicals, petroleum hydrocarbons, along with solvents, pesticides, lead, and other heavy metals, are recognized as some of the most perilous substances (Fent, 2004; Sookhak Lari et al., 2019). The pollution by Total petroleum hydrocarbons (TPHs) affects the nature of plants and animals, and human health (Newton, 1990; Q. X. Zhou, 1995). The International Agency for Research on Cancer (IARC) has recognized benzene (TPH compound) as carcinogenic to humans and benzo[a]pyrene and gasoline are probably and possibly carcinogenic to humans (Teramoto et al., 2020; Toxfaqs, 1999; Weelink et al., 2010; Yadav and Hassanizadeh, 2011). Without remedial activities that specifically target LNAPLs, the source zones may remain for decades at polluted sites, posing ongoing hazards to groundwater quality (Irianni-Renno et al., 2016; Logeshwaran et al., 2018).

The Qatar Peninsula is located on the Arabian Gulf's northeastern shore. Rainfall and groundwater are Qatar's only natural freshwater resources. According to the Human

Development Report (2005), Qatar is ranked first among Arab countries and 35th worldwide in economic growth. The generation of a large amount of waste and the wide use of chemicals since the industrial revolution has resulted in numerous contaminated sites across the globe. The Arabian Gulf has been affected for years by hundreds of oil spills, some of these accidents were reported but most unreported (Al-amirah, 1982).

As a result of oil spills, ecotoxicological problems at all levels arise, from molecular to the ecosystem. Sites with severe contamination offer major environmental risks to the ecological system and human health, particularly those with long-term effects. It affects human health directly by digestion and breathing of soil particles into the human body, or indirectly by the consumption of food or drinking contaminated water (Fent, 2004). Moreover, it alters the chemical, physical, and biological properties of these natural resources which affect its purpose for the sustainability of the living organisms (Prusty et al., 2017; Suk et al., 2022). Groundwater contamination is typically caused by leaking of underground storage tanks or waste from landfills, discharge of industrial waste to the soil, filtration of contaminated surface water to subsurface layers, or application of pesticides (Maliszewska-Kordybach, 1996). Heavy metals and organic contaminants are the most serious pollution, and, in some cases, the contamination is considered irreversible.

The groundwater in Qatar has been vulnerable to contamination due to the growth in gas, oil, and petroleum industries, overuse of groundwater, and saltwater intrusion. Oil spills from petroleum manufacturing facilities, pipelines, and gas stations are sometimes inevitable and are persistently released to soil and groundwater. Pollutants derived from petroleum hydrocarbons are highly toxic due to the composition of sulfur and nitrogen, which react with the environment to produce secondary poisonous chemicals. The arid and semi-arid coastal regions are known for their dynamic

environmental conditions such as temperature differences, salinity, and water table fluctuation endanger soil and water resources (Yadav and Hassanizadeh, 2011). Climate change will cause global tension especially in semi-arid regions with more frequent and intense droughts (Erdogan et al., 2020; IPCC, 2014).

Understanding water movement in saturated and unsaturated zones is important for the management of water resources, irrigation, fertilizer, and environmental studies such as prediction of fate and transport of material through the soil. The movement in the vadose zone is controlled by infiltration under the gravity force and redistribution by the capillary rise (Bunsri et al., 1974; Zanello et al., 2021). A wide variety of laboratory, modeling, and field studies have indicated that seasonal variations of groundwater, among other things, can affect contaminant movement and redistribution, dissolution rates, volatilization, and biodegradation. LNAPL compounds' vertical dispersion and redistribution at the capillary fringe has been shown to be affected by changes in groundwater level and in soil moisture (Cavelan et al., 2022; Dobson et al., 2007), hence altering their release into the surrounding environment. It is possible, however, the dynamic nature of groundwater level changes, as well as the degree of these oscillations, may alter considerably in response to climate change (Cavelan et al., 2022). The interaction between seawater and groundwater, as well as the significance of this interaction in the management of pollutants, has been a cause of intense research in the field of coastal hydrogeology as a result of greater attention being paid to environmental concerns in groundwater (X. Huang et al., 2021). A thorough assessment of solute transport characteristics is crucial for the proper evaluation and remediation of groundwater in coastal areas, particularly when dealing with certain light non-aqueous phase liquids (LNAPLs). It is necessary to examine the impacts of different tides on these characteristics to gain a comprehensive understanding of the situation (X.

Huang et al., 2021). When a contaminant is released, it moves downward through the unsaturated zone (vadose zone) to the water table and then to the saturated zone. The movement of these contaminants is controlled by a set of physical, chemical, and biotic processes. Most petroleum products are less dense than water and have low solubility. When reaches groundwater, they tend to form a separate light non-aqueous phase liquids (LNAPLs) which continues to dissolve into groundwater for years, thus becoming a continuous source of groundwater pollution (Zanello et al., 2021).

1.1 Research objectives

Petroleum hydrocarbons are considered the most potential pollutants to the environment. Water table fluctuations are known as a key process in enhancing the movement of contaminants, thus increasing dissolution, desorption, and degradation. understanding the effect of and characteristics of the contaminants and the hydrogeochemical changes in the system is essential.

In this study three experiments were performed. The main purpose was to better understand the effect of water table fluctuations in the hydrogeochemical functioning of soil by comparing soil hydrogeochemical parameters under two different water table regimes: stable and fluctuating. The three experiments as following:

1- The effect of seawater intrusion (low and high salinity) and water table fluctuation on petroleum hydrocarbon degradation using Benzene and Toluene as contaminates in soil.
2- The effect of water table fluctuations, temperature, soil layering on petroleum hydrocarbon degradation using Benzene, Toluene, ethylbenzene, xylene (BTEX) as contaminates.
3- The source zone petroleum hydrocarbon degradation under aerobic and anaerobic conditions under stable and fluctuation water table using Toluene and Naphthalene as contaminates in homogenized contaminated soil.

1.2 Outline of the thesis

This thesis consists of eight chapters as follows:

1. Chapter 2 consists of a comprehensive literature review of the topic and the parameters used to quantify the results.
2. Chapter 3 consists of the material, equipment, and the analysis used in the three experiments discussed in this thesis.
3. Chapter 4 consists of an experiment explaining the synergic impact of water table fluctuation and hydrogeochemical properties under two salinities on benzene and toluene under completely anaerobic conditions.
4. Chapter 5 consists of an experiment explaining the statistical analysis of the effect of water table fluctuation, soil layering, and temperature on soil hydrogeochemical properties and the correlation of BTEX and soil hydrogeochemical properties.
5. Chapter 6 consists of an experiment explaining the impact of water table fluctuation under aerobic and anaerobic column experiment.
6. Chapter 7 describes the summary and conclusion of the results.
7. Chapter 8 gives some recommendations for future work.

CHAPTER 2 LITERATURE REVIEW

This chapter provides an introduction to the topic. Starting from the review of groundwater contamination and the presence of non-aqueous phase liquids (LNAPLs), and their degradation in groundwater. Furthermore, the chapter explores the impact of water table fluctuation on the migration and distribution of petroleum contaminants and hydrogeochemistry of soil and groundwater.

2.1 Groundwater Contamination and Non-aqueous phase liquids

Groundwater is a sustainable source of usable, fresh, and clean water especially in places where surface water is not available. In the last decade, authorities prioritized the preservation of this valuable source of water. United nation 2021 report stated that per capita water consumption continues to increase due to the economic growth and development (Water, 2021). Currently, 69% of the world water use are for agriculture and livestock and this percent may reach 95% in developing countries (Water, 2021). A future report concludes that by 2030, the world will be facing a 40% global deficit. The seasonal variations in water resources are expected to worsen due to the impact of climate change (Cavelan et al., 2022; Water, 2021). The assessment of groundwater quality requires testing several parameters, which can be costly due to sampling, analysis, and drilling requirements. Eleven parameters are to be tested for a typical groundwater quality, these parameters include temperature, EC, pH, major cations (Na+, K+, Mg^{2+}, Ca^{2+}) and four major anions (CL^-, HCO_3^-, SO_4^{2-}, NO_3^-) (Ahmad et al., 2020; Appelo and Postma, 1993). Rainwater infiltration, evapotranspiration, and vegetations uptake cause variation in groundwater chemistry particularly in the unsaturated zone (Appelo and Postma, 1993; Dobson et al., 2007). In arid and semi-arid regions, evaporation is high which cause ion salts to collect in soil profile.

Over pumping of groundwater due to the increasing population, unplanned industrial growth, and leakage of petroleum products cause significant amounts of pollution

especially in coastal areas (Ahmad et al., 2020; X. Huang et al., 2021). Low groundwater quality occur due to a combination of climate change and heavy human use (He and Wu, 2019). When groundwater level is decrease, saltwater forced inland and upward, potentially contaminating fresh water sources. Unlike the surface water, groundwater pollution is unseen, hard to be treated, and usually irreversible (Erdogan et al., 2020; X. Huang et al., 2021). The contamination of groundwater in coastal areas has received increase attentions in recent years (X. Huang et al., 2021).

Petroleum products are the most dangerous source of contamination (Alazaiza et al., 2020). Environmental protection agency (EPA) reported 70,000 cases of underground storage tank leakage in the USA alone (Alazaiza et al., 2020). The remediation of petroleum hydrocarbon source zones is crucial for mitigating the dangers presented by subsurface hydrocarbon pollution. Unfortunately, commonly utilized methods like hydraulic recovery are only successful for the mobile component, leaving considerable volumes of residual contaminants in source zones (Irianni-Renno et al., 2016).

The natural attenuations processes comprise a range of in situ physical, chemical, and biological mechanisms that may function without human intervention to lower the concentrations of pollutants in soil and groundwater under favorable circumstances. Sorption, dispersion, advection, dilution, volatilization, biodegradation, and chemical or biological stabilization, transformation, or elimination of pollutants are examples of in situ processes (Clement et al., 2000; Marić et al., 2020).

The success of groundwater remediation can be determined by a number of environmental and site factors, in particular, the availability of nutrients and oxygen, soil moisture, pH, temperature, redox potential, and site specific properties (Cavelan et al., 2022; N.J. Sihota et al., 2016; Yadav and Hassanizadeh, 2011).

One of the very influential factors are the temperature, it directly affects the pollutants

chemistry, and the physiology and diversity of the microbial community. Temperature also affects hydrocarbon solubility, viscosity and volatility (Cavelan et al., 2022). In general, low temperature decreases the rate of hydrocarbon biodegradation. Biodegradation of contaminated semi-arid and arid coastal locations is most likely to be successful if soil moisture and temperature fluctuations and groundwater table dynamics are taken into account (McAlexander and Sihota, 2019; Yadav and Hassanizadeh, 2011). The integrated influences of these variables often result in complex and dynamic flow and transport. The total water potential which reflects the energy state of the water is greatly affected by the moisture content of the soil (Yadav and Hassanizadeh, 2011). Solute transport and soil microbial mechanisms that degrade organic contaminants are directly affected by water and air distribution in the soil. Oxygen and water are necessary for the soil bacteria to accomplish the breakdown. While the breakdown of nutrients and byproducts is regulated by soil water/air ratio, so are the diffusion rates of these nutrients and byproducts throughout the process. Because of the low soil moisture content, the air-filled porosity is larger, which should facilitate oxygen mass transfer to the microbial population that degrades LNAPLs (Yadav and Hassanizadeh, 2011). Holman and Tsang, (1995) reported that biodegradation may continue at its greatest pace with a water concentration of 50% to 70% of field capacity.

Some hydrocarbons exist in an immiscible phase when in contact with water and/or air, known as a nonaqueous phase liquid (NAPL) (Al-raoush, 2009; Langevoort, 2009). The nonaqueous are classified into light nonaqueous phase liquids (LNAPLs), or dense nonaqueous phase liquids (DNAPLs). The LNAPLs has densities lighter than water, while the DNAPLs has densities greater than water (Alazaiza et al., 2020; Newell et al., 1995). NAPLs are often a complicated combination of several hundred constituents

with varying chemical characteristics (Cavelan et al., 2022). An example for LNAPLs includes toluene, benzene, xylene, and ethyl benzene (BTEX), while, DNAPLs includes chlorinated solvents such as tetrachloroethylene (PCE) and trichloroethylene (TCE) (Alazaiza et al., 2020; Newell et al., 1995).

The LNAPLs infiltrates into the unsaturated soil and migrates in both vertical and lateral directions under the influence of gravity (Alazaiza et al., 2020; Mercer et al., 1990). It moves until it reaches the water table and stays at the top. when leaving the unsaturated zone, LNAPLs leave behind trapped residuals or sorbed to soil grains (Cavelan et al., 2022; Soga et al., 2004; Zanello et al., 2021). On the contrary, DNAPLs migrate into the unsaturated zone and travel through porous media to the saturated zone (Alazaiza et al., 2020; Huling et al., 1991; Newell et al., 1995).

Heterogeneity of soil media may drive the lateral migration of both LNAPLs and DNAPLs in the unsaturated zone (Guarnaccia et al., 1997). In their pathway, some stay in the complex void space, discontinued and immobilized by capillary forces, and become long-term source of groundwater contamination (Al-raoush, 2009; Alazaiza et al., 2020; Cavelan et al., 2022; Mercer et al., 1990). The migration of NAPLs in the subsurface is affected by several factors some are related to the NAPLs characteristics such as its properties (density, viscosity, immiscibility), saturation, capillary pressure, wettability, polar nature of the NAPLs (Alazaiza et al., 2020), the volume released, and the time and duration. Other factors related to the area where its released such as: infiltration; the properties of the media; and subsurface flow conditions (Alazaiza et al., 2020; Mercer et al., 1990).

During groundwater recharge or fluctuation, the residual NAPLs dissolved its soluble constituents which result in an aqueous-phase contaminant plume (Cavelan et al., 2022; Newell et al., 1995). After the process of infiltration, the gravitational forces and

hydraulic gradients will result in NAPLs drains from the pore space. During their migration the NAPLs leave immobile, residual along the migration path. Similarly, the saturated zone also contains multiple distributions of preferential pathways from cracks, fractures, joints, etc., thus NAPLs follow these pathways. To handle residual LNAPLs existing after active remediation and/or lengthy periods of natural depletion, new technologies and/or techniques are required (Irianni-Renno et al., 2016).

When LNAPLs is dissolving, convection and diffusion are the primary means of transporting it through the subsurface. The dissolved LNAPLs are conveyed by convective transport in the aqueous phase when water flows owing to a pressure gradient. It is also possible for soil gas to migrate by convective transport as a consequence of several processes, such as temperature variations, water table fluctuations, and air sparging (Yadav and Hassanizadeh, 2011). The evapotranspiration induced vertical movement of soil water may also cause upward movement of dissolved LNAPLs. The dissolution of LNAPLs in the saturated zone is thought to be the primary impediment for the contaminant transport process. In the unsaturated component, diffusion via the gas phase is by far the most common mode of transport (Yadav and Hassanizadeh, 2011). The most common physical processes for cleaning up LNAPLs spills include containment, mechanical removal, water flushing, and sediment displacement. (Yadav and Hassanizadeh, 2011). Chemical dispersants are less often utilized in others due to doubts about their effectiveness and worries about their potential for long-term environmental harm. The procedures outlined above are frequently the primary response option for LNAPLs spills, however, accomplish full cleaning is difficult. Secondary treatments include carbon adsorption and electro remediation as well as filtration and adsorption, as well as chemical oxidation and photo-catalysis (Yadav and Hassanizadeh, 2011). Compared to the above-mentioned

approaches, bioremediation is one of the most promising choices for a subsequent treatment option, as it is more cost-effective and less disruptive to the contaminated location.

2.1.1 Total petroleum hydrocarbons degradation (aerobic/anaerobic)

The biodegradation process in the presence of oxygen (O_2) is referred to as "aerobic" or "oxidizing," and it is characterized by low electron availability, while the lack of O_2 is referred to as "anaerobic" or "reducing," and it is characterized by electron availability (Abramowicz, 1990; Doktorgrades, 2017). When O_2 levels in the soil fall, obligatory and facultative anaerobe bacteria begin to use other electron acceptors.

NAPLs can be degraded by aerobic or anaerobic conditions. LNAPLs may either be partly oxidized to less complex by-products or completely oxidized/mineralized to carbon dioxide (CO_2) and water (H_2O) in aerobic conditions, where oxygen is the major electron acceptor. Techniques such as air sparging, bioventing, and the delivery of oxygen-releasing chemicals such as hydrogen peroxide (H_2O_2) and magnesium peroxide (MgO_2) are employed to compensate for the oxygen needed in saturated zones for the aerobic degradation of LNAPLs.

Benzene, toluene, ethylbenzene, and the xylene isomers (BTEX) make up the majority soluble gasoline when it is exposed to water (Kim et al., 2008; Zanello et al., 2021). The degradation of LNAPLs is affected by natural characteristics of soil microorganisms. Microbial communities, biodegradation of hydrocarbon components, and redox conditions, electron acceptor availability, and LNAPLs composition are all complicated and vary greatly with depth (Cavelan et al., 2022; Garg et al., 2017). Biodegradation is the process by which chemical compounds are broken down by microorganisms which break down hydrocarbons into water and carbon dioxide as a result of their biological activity (Hatipoğlu-Bağci and Motz, 2019). The

biodegradation process normally follows a redox sequence: aerobic, anaerobic, fermentation, or methanogenesis (Cavelan et al., 2022; Garg et al., 2017; P. K. Gupta et al., 2019). There is no doubt that microorganisms and the processes governing bacterial activity are substantial contributors to LNAPLs natural attenuation rates.

The original and old process of biodegradation was based on the electron acceptor evidence, where all of them has to be removed from the system before the methanogenesis occurred (Garg et al., 2017). As a results of petroleum hydrocarbon degradation, by-products gases such as methane (CH_4) and carbon dioxide (CO_2) are expected to be released (N.J. Sihota et al., 2016; Van De Ven et al., 2021). The direct outgases due to the aerobic biodegradation process occur nearby the entrapped oil in pore space (Garg et al., 2017; Gieg et al., 2014). Whereas the gasses produced due to the anaerobic biodegradation and methanogenesis described by Amos et al., (2005). The amount of by-products gases (CO_2 and CH_4) is dependent on the existing condition of the process. For example, the abundance of oxygen in the system would inhibit or oxidize CH_4 resulting in higher CO_2 in the system compared to CH_4 (Van De Ven et al., 2021). CO_2 and CH_4 has lower solubility in water, so they will diffuse into the surface (Van De Ven et al., 2021).

Recently, the NSZD is been quantifies by measuring surface effluxes (CO_2 and CH_4) (Sihota et al., 2011; Van De Ven et al., 2021), considering the subsurface heterogeneity and dynamics. These factors are ranging from temperature changes, moisture content, ebullition events, barometric pumping, and water table fluctuations. These factors can greatly impact the surface efflux, thus the NSZD actual estimation (Van De Ven et al., 2021). It was reported by N.J. Sihota et al., 2016 that the rate of NSZD varied seasonally, for instance when soil temperature increased and water table dropped, the biodegradation rate increased due to the enhance of microbial metabolic activities.

The degradation of LNAPLs at the pore level produces biogenic gases, these gases may change the geophysical characteristics of the aquifer (Atekwana and Atekwana, 2010). It will dissolve in pore water or accumulate as gas bubble in the unsaturated zone, when its concentration may exceed solubility causing exsolution (Van De Ven et al., 2021). some research has suggested that the aerobic degradation occur in sites with new contaminants release.

In recent years, the term methanogenesis appeared as a part of complex, multi phases process. In this process, the bacteria in the subsystem works cooperatively to degrade the product contaminant and by-products as well (Garg et al., 2017). The methanogenesis occur in the saturated zone and the bottom of the unsaturated zone, where the direct outgassing is noticed. Garg et al., (2017) in his review paper, compared the outgassing production from different methanogenesis systems. He found that the anaerobic degradation rate from natural porous media is much lower than the anaerobic digesters and landfills. This can give an indication that other factors play a role in controlling anaerobic degradation. some of these factors can be very significant such as temperature, which known for shifting the microbial communities resulting in higher biogas production (Garg et al., 2017; Zeman et al., 2014). Another important factor is pH and alkalinity during the biodegradation process. PH is controlled by two parts of the process, carbon dioxide produced during biodegradation and volatile fatty acids and lactate produced during fermentation. The availability of electron acceptors controls methanogenesis, oxygen at low concentrations inhibits it and other electron acceptors is an alternative biodegradation pathway. The availability of certain nutrients such as phosphorus (P) can also affects the biodegradation rate and methanogenesis (Gray et al., 2010). Water table fluctuations plays major role in LNAPLs degradation, but some researchers suggested that the absence of oxygen in saturated zone and above source

zone may inhibit the process, but on the other hand the fluctuations is beneficial mechanism to clean the accumulated byproducts. Dissolve Oxygen (DO)enter the subsurface by diffusing from air through the unsaturated or by infiltrated water (Williams and Oostrom, 2000).

2.2 Water Table Fluctuations, its enhancement on TPHs and soil hydrogeochemistry

The Fluctuations in the water table have a substantial impact on the biological and geochemical functioning of soils. It discloses crucial hydrogeological elements of an aquifer, such as the recharge rate and hydraulic conductivity. A side from that, information on the temporal and geographical distribution of groundwater level is critical in several aspects of hydrogeology, including free phase nonaqueous phase migration and solute transport, groundwater vulnerability, and groundwater induced flooding (Jeong and Park, 2017).

This variation in groundwater table and capillary fringe occurs over shorter time due to change in nearby water bodies or longer due to the change in recharge rate versus withdrawal rates (Alazaiza et al., 2020; Dobson et al., 2007; Williams and Oostrom, 2000). The fluctuation in groundwater elevation is a reason for the entrapment air which affects the hydraulic properties of the unsaturated zone as well as the biogeochemical status of the underlying groundwater. The dynamic of WTF improves atmospheric oxygen saturation in groundwater (Haberer et al., 2012), as a result, redox condition, soil water content, and matric potential exhibit both temporal and spatial gradients. (Rezanezhad et al., 2014; Zhang and Furman, 2021; Tian et al., 2021).

Many studies revealed that the chemical dynamics of the variable saturation vadose zone outweigh those of the saturated one. Biodegradation activities may take place in the capillary fringe because of the presence of both water and air (Ronen et al., 2000; Zhang and Furman, 2021). Moreover, As a result of the change in the water table,

NAPLs residue in the zone of fluctuation water table represent a risk in both the air (vapor) and water phases (Sookhak Lari et al., 2018).

The understanding of such processes in the vadose zone has comprehensive implications for a wide number of environmental issues, including groundwater pollution, soil fertility, biodiversity, (sub)-surface storage, resource exploration and climate. In the context of this project, groundwater contamination by hydrocarbon, it is critically important to understanding such process especially, the oxygen supply, soil moisture, pH, nutrients, temperature, and redox potential. Due to water table fluctuation, the subsurface environment is exposed to various events. Dilution of pollutants in the plume area which occur as a results of WTF may also boost biodegradation rates of organic compounds (Rees et al., 2007).

It is possible for entrapped air in unconfined aquifers to provide anoxic water with a large quantity of O_2. The availability of oxygen near the water table can promote the proliferation of aerobic bacteria, facilitating the degradation of groundwater pollutants in that particular zone (Haberer et al., 2012). Understanding hydraulic and mass transport dynamics is crucial to accurately assess the impact of oxygen supply on aquifer redox conditions and biogeochemical activities. Additionally, comprehending how fluctuating water tables influence pollutant spreading, degradation rates, and other key redox processes is critical for effective contamination control (Haberer et al., 2012).

The fluctuations of groundwater table impacts the movement and spatial distribution of NAPLs within the aquifer specially in the vertical direction (Alazaiza et al., 2020; Dobson et al., 2007; J. Lee et al., 2001; Van De Ven et al., 2021). Regardless of the significance of geological heterogeneity, the complexity of LNAPLs movement in pore spaces is the most significant source of challenges in LNAPLs remediation, and these complexities are emphasized by changes in the water table (Teramoto et al., 2020). The

changes in the water table has both short-term and long-term consequences on the contaminated subsurface system (Van De Ven et al., 2021).

When NAPLs spills occurred, only a small percentage of LNAPLs is mobile and can be recovered, but a considerable proportion of LNAPLs stays immobile as residual making recovery difficult. After experiencing water table variations caused by alternating wet and dry seasons, field researchers noticed more complicated situations as consequence to water table fluctuations (Teramoto et al., 2020). When it comes to the fluctuating water table in subsurface contamination with NAPLs, two different scenarios will be expected in the saturated and unsaturated zones. when water table falls, NAPLs migrate downwards with water leaving entrapped residual in the unsaturated zone which eventually decrease NAPLs saturation and decrease the mobile LNAPLs (Alazaiza et al., 2020; Blodau & Moore, 2003; Cavelan et al., 2022; Dobson et al., 2007; J. Lee et al., 2001; Reddi et al., 1998; Sookhak Lari et al., 2018; Teramoto et al., 2020). Moving water table downward will allow the soil gas to be released from water phase and accumulate which in the long-term, will results in the increase of the gas-water interfacial area, in addition to that, it will allow more oxygen to enter the smear zone. These two reasons create greater chance for aerobic bacteria to be enhanced (Van De Ven et al., 2021). Entrapped NAPLs might gains mobility and accumulate at the top of the water table when it falls from a region that was previously polluted (Teramoto et al., 2020). Alternatively, in the saturated zone, the fall of the water table increase NAPLs extent in the vertical direction and thus increase the smear zone (Dobson et al., 2007; Van De Ven et al., 2021).

On the other side, When the water table rise, two scenarios are possible. Water table moving up to the same previous location, and the mobile LNAPLs will rise with it into zones with past residuals LNAPLs, water imbibes and completely submerges the smear

zone. The water table moves to a new uncontaminated zone and create a new smear zone (Van De Ven et al., 2021).

Furthermore, when water level rises, LNAPLs move upward with water table resulting in LNAPLs redistribution upward in the unsaturated zone and leaving LNAPLs and air below the water table. The entrapped LNAPLs with air in the saturated zone leads to a decline of mobile, free phase LNAPLs (Dobson et al., 2007) in the aquifer which reduce the possibility of LNAPLs migration downward, enhances the dissolution and biodegradation. Because of the trapping of this LNAPLs in the form of discontinuous blobs at a decreased saturation, it is possible that the overall LNAPL/water interfacial area increases (Dobson et al., 2007).

The presence of LNAPLs in a zone subject to seasonal variations in water table will develop a zone characterized with high residual phase concentration called the smear zone (Cavelan et al., 2022; Kehew and Lynch, 2011). The interaction of retained hydrocarbon with water results in the partial dissolution of its components, which are mostly a set of aromatic organic chemical compounds (BTEX), In addition to being extremely mobile, the dissolved phase is also responsible for the transmission of contaminants across great distances from their source (Zanello et al., 2021).

It is necessary to determine the extent of the contaminated area in order to identify an appropriate remediation method for a NAPL-contaminated site. It is usually believed that such knowledge can only be gathered by lengthy fieldwork that is both costly and time demanding. Soil water content, heterogeneity, and geochemical features of porous media, as well as fluid movement all play a role in the process of dissolution mass transfer from NALP and immobilized hydrocarbons (Zanello et al., 2021). Study of dissolved BTEX from residual phase and involvement of numerous parameters including soil heterogeneity, depth of water table, water flow and biodegradation rate

are important for the USZ depletion (Zanello et al., 2021). One of the very important parameters that influence contaminant adsorption to soil is particle size distribution. The smallest particle sizes have the greatest surface area and, as a result, may retain more organic and inorganic substances (Zanello et al., 2021). Alternatively, Sandy sediments have lesser retention capacities, which results in contaminants moving farther in the unsaturated zone under these circumstances.

To determine the impact of water table fluctuation on LNAPLs behavior in porous surfaces, a number of researchers have conducted numerical and laboratory-scale experimental experiments (Alazaiza et al., 2020; Dobson et al., 2007; Gatsios et al., 2018; P. K. Gupta et al., 2019; J. Y. Lee et al., 2001; Qi et al., 2020; Reddi et al., 1998; Rühle et al., 2015; Sinke et al., 1998; Teramoto et al., 2020; Teramoto and Chang, 2017; Van De Ven et al., 2021; Werner and Höhener, 2002; Xia et al., 2020; Yang et al., 2017; J. F. Zhou et al., 2014; Zhu and Sun, 2016). The examination of pollutant movement in the subsurface often relies on in-direct measurement of system characteristics or on direct measurement at just a few specific places.

Sinke et al. (1998) studied the effect of WTF on toluene and 4-nitrobenzoate fate and transport. The system received electron donors (acetate and formate) and electron acceptors (CO_2/ O_2/ N_2). The experiment operated as 4-month saturation phase, followed by a 3-month WTF phase and another five months of operation in a fully saturated state. In the experiment, it was found that WTF's redox conditions were not in equilibrium but were susceptible to spatial and temporal alteration.

J. Y. Lee et al., (2001) investigated the distribution of PHCs in a highly contaminated sand aquifer in Korea. The aquifer was subject to an average of 2 m water table fluctuations per year. The investigation revealed that water levels and hydrogeological conditions play a significant role in distributing contaminants in the subsurface. Around

the source zone, a highly reduced zone was developed. The results of the geochemical, redox sensitive parameters, and concentrations of the contaminants support the occurring of the natural attenuation in some of the monitoring wells and biodegradation in others. Dobson et al., (2007) performed an experiment with two model, one model was stable and the second one subject to water fluctuating condition. The experiment confirms that dissolution and biodegradation of LNAPLs components happened simultaneously, making separation difficult. Differing amounts of biodegradation and dissolved LNAPLs components in the model aquifers indicated differences in dissolution. The water-table fluctuation increased LNAPLs component dissolution. This matches prior results for entrapped vs pooled NAPL dissolution. Dobson et al., (2007) suggested that the water table fluctuation increased microbial activity compared with non-fluctuated model as measured by spatial distribution of electron acceptors and mass balances. Because the increased microbial activity corresponded with higher dissolved LNAPLs-component concentrations, it was plausible to believe that increased LNAPLs-component biodegradation was the cause. Rühle et al., (2015) performed experiment and one-dimensional flow modelling on water table dynamics. The results showed no differences in the geochemistry between the stable and the fluctuating water table columns, while microbial activity had differed between the two columns. Variations in water content, fluxes, or velocities may have caused the observed community shifts in the dynamic column's fluctuation zone. The microbial community structure is known to be strongly influenced by water saturation (Rühle et al., 2015).

In a column experiment by Alazaiza et al., (2020) using simplified image analysis method (SIAM), the effects of water table fluctuation on LNAPLs migration and redistribution in porous media were explored for various LNAPLs volumes and water table fluctuation sequences. The results reveal that water variation has a significant

impact on LNAPLs and soil water saturation. Van De Ven et al., (2021) analyzed gas release from the smear zone and the mobile LNAPLs thickness due to fluctuated water table. Teramoto et al., (2020) notices that During an imbibition cycle, the wetting phase penetrates the pores and entraps NAPLs. As a result of this entrapment, the LNAPLs lose mobility, reducing or eliminating the floating phase in the monitoring wells. During dry seasons, the water table drops, allowing NAPLs to acquire mobility. The free LNAPLs migrates to monitoring wells, increasing the thickness of the floating phase. Teramoto et al., (2020) observed that the recorded floating phase thickness is often lower during times of rising water levels and gradually rises during periods of low water levels. To assess the risk of groundwater contamination associated with BTEX dissolution from residual phase associated with water table proximity, Zanello et al., (2021) carried out a numerical stimulation of sixty scenarios. These scenarios are related to soil characteristics, water table proximity to ground surface, as well as the physicochemical characteristics of BTEX. Zanello et al., (2021) found that each BTEX compound's mobility is tightly linked to its physicochemical features and soil properties, and Pollutant retention is influenced by the type of soil and its composition. When BTEX reached the capillary fringe, however, the vertical transport velocity was significantly lowered. As BTEX water diffusivity is lower than air diffusivity, its mobility was significantly decreased under humidity conditions near saturation. The compounds having the greatest mobility in the dissolved phase for the three different soil types were benzene and toluene. He found that close to the source zone, xylene and ethylbenzene tended to accumulate. Coarse-grained soils, on average, have a lesser potential for pollutants to adsorb than fine-grained soils, and BTEX mobility was highly restricted in silt loam and clay soils where the hydraulic conductivity is low, and the organic matter level is moderate to high. In loamy sand soil, BTEX leached to the

aquifer could be high because of quick percolation of water, the poor sorption capacity, and the short transit time of dissolved phase. In this work, Zanello et al., (2021) confirm that BTEX movement is heavily influenced by biodegradation and sorption mechanisms. When compound concentrations surpass the hazardous range for microorganisms, however, biodegradation may be slowed. In the same context, Yang et al., (2017) investigated the effect of three geological materials and WTF on toluene attenuation process excluding the biological effect. According to Yang et al., (2017), WTF has a considerable impact on the behavior of toluene in porous media settings. Toluene migration is mostly impacted by adsorption, flushing which occur at an early stage, and dissolution during the WTF period. Flushing intensity is linked to water release rate during WTF, whereas dissolution is linked to medium porosity, exhibiting an opposite effect from surface area which had the greatest influence on adsorption of toluene.

Van De Ven et al., (2021) used surface efflux of CO_2 and CH_4 to quantify the degradation of LNAPLs due to the WTF. CO_2 and CH_4 effluxes from the experiment increased greatly when the water table was decreased because anaerobically generated gas collected below the water table was released. When the water table was raised and the smear zone submergence, the CO_2 and CH_4 effluxes decreased, indicating that pollutant degradation rates were reduced. The results of the research concluded that WTF and the redistribution of pollutants impact surface effluxes, as well as short and long term contaminant degradation rates (Van De Ven et al., 2021). It is concluded that when the water table fluctuates, NAPLs redistributed, and this has long-term effects on soil gas chemistry and gas effluxes.

2.2.1 Soil and Groundwater hydrogeochemistry

The subsurface water composition changes with time, mostly owing to recharging with

precipitation, irrigation water, or fluctuations in the water table. Groundwater whose chemical composition has been altered as a result of contact with solid and gaseous substances. Berkowitz et al., (2007) stated that the characteristics of the subsurface water can be summarized as following:

- The acidity–alkalinity of the groundwater is determined by pH which is altered by the filtrating rainwater water (it is normally acidic; irrigation and effluents are neutral or alkaline) and governed by the environmental system.
- Salinity of the system is determined by the Total dissolved solids (TDS) or electrical conductivity (EC). Anions include Cl^-, SO_4^{2-}, and NO_3^-, whereas cations include Ca^{2+}, Mg^{2+}, Na^+, and K^+.
- The GW may include trace components of natural or manmade origin. Inorganic trace elements include alkali and cationic materials, transition metals, and heavy metals. Trace element distribution between solid and liquid phases occurs mostly through adsorption.
- Organic ligands produce complexation of inorganic trace elements, affecting their concentration in subsurface solution. The type and qualities of subsurface colloids, the chemical and physical properties of organic molecules, and the nature of the environmental system govern the presence of organic trace chemicals.

For a given medium the porosity and moisture content and the ratio of gas to water determine the volume of the subsurface gas phase. Subsurface gas may aid the movement of organic in vapor or dissolved constitute in water; it can also influence microbiological activity and hence define chemical permanence primarily in a near-surface environment. The subsurface gas phase is a major conduit for subsurface contamination, notably by volatile hazardous compounds, because of the gaseous

transit via pores. When chemicals are released into the ground, they might either be adsorbents or dissolved in subsurface water. In the vicinity of the water table (capillary fringe), the presence of gaseous phases may be particularly important for the geochemical transformation of contaminants (Berkowitz et al., 2007).

A well-aerated soil has an O_2 concentration of around 20%, and a CO_2 concentration of 1% to 2%. CO_2 concentrations of up to 10% have been seen in clay-dominated materials with high water content (Berkowitz et al., 2007).

According to the findings of a number of studies, the introduction of petroleum hydrocarbons into aquifers can result in increased levels of microbiological activity as well as detectable shifts in the hydrochemistry of ground water (Marić et al., 2020). Following are the parameters that discussed in this study:

2.2.1.1 Oxidation-Reduction Potential (ORP)/ Redox Potential (Eh)

Redox mechanisms is known as the potential for electrons to be transferred from reduced condition (electron donors) to oxidized condition (electron acceptor) and ORP or E_h is a measure of the reduction's intensity, or the corresponding electromotive force of the processes (Zhang and Furman, 2021). The most significant chemical change in soils is the commencement of reduction (Doktorgrades, 2017). Many biogeochemical processes in surface settings are regulated by reduction, which is the gain of an electron (e^-), and oxidation, which is the loss of an electron. Furthermore, as indicated by equation (1), reduction-oxidation (redox) processes usually occur concurrently and include the transfer of electrons and protons (H+) between the involved redox couples.

$$O_x + mH^+ + ne^- \quad \leftrightarrow \quad Red \qquad Eq\ 1$$

where Ox represents the oxidized species, m and n represent the number of H+ and e^- participating in the reaction, and Red represents the reduced species (Doktorgrades, 2017; Reddy and DeLaune, 2008).

The redox classifications by E_h include oxidizing (> 400 mV), mildly reducing (200–400 mV), moderately reducing (-100-200 mV), and strongly reducing situations (< -100) (Reddy and DeLaune, 2008; Zhang and Furman, 2021). ORP is performed by using a potentiometric measurement, an inert metal electrode measures the potential (or inclination) of a medium to transmit electrons and compares it to a reference electrode submerged in the same medium (Environmental, 2005).

Redox mechanisms drive the biogeochemical cycles of several main and trace elements include the cycles of carbon (C), nitrogen (N), sulfur (S), iron (Fe), and manganese (Mn). Reduction and oxidation processes have a direct impact of the bioavailability, toxicity, and mobility of such elements in the environment (Borch et al., 2010; Zhang and Furman, 2021). Understanding the biogeochemical processes at environmental redox interfaces is thus critical for forecasting and maintaining water quality and ecosystem health (Borch et al., 2010; Zhang and Furman, 2021). Subjected to their redox state, redox-sensitive species have varied reactivity, mobility, and toxicity properties (Zhang and Furman, 2021).

The key factors influencing carbon cycling at typical temperatures and pressures are pH and ORP (Sale et al., 2021). Because of the bicarbonate buffering involved with carbon dioxide generation, the pH values in most LNAPLs systems are near neutral (pH 7), thus ORP is considered the key master variable for biogeochemical activities in soil-groundwater systems (Sale et al., 2021). Liu et al., (2009) stated that the synergistic action of Temperature, DO, pH, and Salinity influences ORP, with no one factor playing a dominant role. Redox in soil and groundwater can be spatially and temporally varying in places such as shallow aquifers, contaminant plumes, lakes, and estuaries due to the critical play of hydrology in these areas and the dynamics of nutrients distribution, the metabolism of microorganisms, and the change of chemicals (Borch

et al., 2010; Zhang and Furman, 2021). Infiltration, precipitation, fertilization, floods, as well as evaporation and groundwater table fluctuations may cause soil redox to fluctuate strongly over time (Zhang and Furman, 2021).

The fate and transport of many metals are heavily influenced by redox and pH, which regulate sorption to the soil's mineral and organic phases as well as bioavailability. Soil redox fluctuation has a big impact on iron (Fe) compounds as a terminal electron acceptor in the absence of oxygen. Fe3+ accepts oxidation electrons from microorganisms through the metabolic decomposition of organic matter. Once the soil regains its aeration, the Fe^{2+} released during the reduction of Fe3+ is quickly oxidized, resulting in precipitation as Fe oxide when for example water table drops. Mn is another important redox-active metal in the soil and groundwater system. After dissolving to create mobile Mn^{2+}, it is oxidized and fixed to solid Mn-oxide in its oxidized state. In the soil aquifer treatment system, Oren et al. (2007) investigated the biogeochemical mechanisms responsible for Mn mobilization, adsorption, and precipitation.

Groundwater remediation of organic pollutants, microbes, and redox processes are all linked, as Tandon and Singh (2016) shown in an earlier review (Zhang and Furman, 2021). The most studied organic chemicals are benzene, toluene, ethylbenzene, and xylene (BTEX compounds), although the principle applies to nearly every hydrocarbon. As a result, E_h may be used to gauge the progress of remediation of the polluted soil as well as the overall health of the soil (Zhang and Furman, 2021).

Chemical and biogeochemical gradients describe the closeness of aerobic and anaerobic microsites, such as the capillary fringe, and the interfacial conditions associated with these systems. Under these circumstances, it is inevitable that E_h gradients will occur (Zhang and Furman, 2021). Moreover, soil microbial community structure and activity are strongly influenced by spatial and temporal redox zonation (Crawford et al., 2000;

A. xia Zhou et al., 2015).

Chemical composition, microbiological activity, and the reduction potentials of critical redox partners all influence the sequence in which redox reactions occur along redox gradients (Zhang and Furman, 2021).

2.2.1.2 Electrical Conductivity (EC)

Electrical conductivity is a measure of the ionic strength and ionic mineralization of groundwater (Marić et al., 2020; Naudet et al., 2004). Research suggests that LNAPLs biodegradation might significantly affect resistivity and ground penetrating radar (GPR) readings by changing biogeochemical characteristics (Cassidy et al., 2001). Biosurfactants and acids are two of the most common products of LNAPLs biodegradation. By raising the concentration of dissolved solids (DS), these compounds immediately increase conductivity; nevertheless, they also promote mineral dissolution. Knight, (2001) reported that bacterial activity raises the electrical conductivity of the area surrounding the contamination.

2.2.1.3 pH

Vincent et al., (2011) reported that Biodegradation rate was faster between pH 6.7-9.6 and increased hydrocarbon degraders, but this growth was considerably inhibited as the pH rose. Yang et al., (2017) suggested that pH is one of the hydro chemical parameters that mostly affect toluene attenuations. In addition to that, Rezanezhad et al., (2014) reported that water table fluctuations has cyclic effect on pH values, as pH rises slightly with groundwater levels rise and decrease during dry periods.

2.2.1.4 Dissolve Inorganic carbon

Natural groundwater in aquifers typically contains dissolved inorganic carbon (DIC), which is a combination of carbon released during the decomposition of organic matter, the dissolution of calcite and other carbonate minerals present in the aquifer, and the diffusion of atmospheric CO_2 (Porowska, 2015).

CHAPTER 3 MATERIAL AND METHODS

In this chapter, a comprehensive overview of the field sampling, soil preparation, the analysis, and the columns setup are provided. It investigates into detail the synthetic groundwater preparation, the materials employed for the columns and connections, the design setup for the columns, and the analytical method that was used for the three experiments.

3.1 Field sampling and soil analysis

Soil samples for all experiments were collected from the eastern coastline of Qatar (25°34'26.4"N 51°29'15.7"E) (Figure A 1). The site was selected because of its proximity to the Al-Shaheen oil field, where a continuous interaction between groundwater and seawater and tidal movements occurs (Ngueleu et al., 2018, 2019). Basic soil analyses such as grain size distribution, hydrometer testing, and hydraulic conductivity were performed. Analysis of particle size distribution (ASTM D 422) indicated that 80% of the soil was silty and poorly graded sand. The particle density of the soil was 2.72 kg L^{-1}. The organic matter in the soil was negligible (Ngueleu et al., 2018; Shafieiyoun, et al., 2020).

Soil samples were collected between 10-50 cm below the ground surface. The samples were kept saturated with groundwater to preserve the soil's natural conditions. The soil was subsequently packed into the columns incrementally in 5 cm layers and compacted gently. Soil scarification was used to maintain hydraulic continuity prior to the installation of a new layer of soil (Lewis and Sjöstrom, 2010; Unold et al., 2009). Groundwater pH, electrical conductivity, and major cations and anions were measured using methods described in Ngueleu et al., (2019).

Using amber bottles, the synthetic groundwater was initially prepared as follows: First, Millipore water has been treated with argon (Ar) gas to remove any trace amounts of dissolved oxygen (O_2) from the water. The groundwater that is used into the columns

is a synthetic influent solution that has been prepared based on the analysis of groundwater samples collected at the sampling site (Ngueleu et al., 2019; Shafieiyoun, Al-Raoush, Ismail, et al., 2020) analysis of the groundwater at the location. The synthetic influent solution was prepared by mixing Milli-Q water with background nutrients found in (Table 1)

Table 1: Synthetic Groundwater properties

Parameter	**Value**
pH	~7.5
Temperature	22±2 °C
$MgCl_2$	89 mg L^{-1}
KCl	24 mg L^{-1}
$CaCl_2.H_2O$	245 mg L^{-1}
$NaCl_2$	1300 mg L^{-1} (~ 4000 μS cm^{-1})
DO	< 0.8 mg L^{-1}

3.2 Experimental setup of columns

Figure 1 shows a schematic diagram of the experimental setup. Each setup consisted of a pair of soil columns and an equilibrium column made of Teflon and Acrylic, respectively. Each column had a length of 60 cm, an inner diameter of 7.5 cm and a wall thickness of 0.6 cm.

The columns' tops and bottoms were sealed by caps and connected by three steel rods secured by bolts. A filter membrane (bubbling pressure of 600 mbar) was used to cover the top and bottom of the columns (Soil Measurement Systems, LLC, USA). The top and bottom caps had openings to supply and drain water from/to the columns. Water was supplied to the soil columns by connecting the soil column from the bottom to an equilibrium column by PVC 2-way valves connected by 15 cm of chemically resistant blue polyurethane tubing (Ark-Plas Products Inc, USA). The equilibrium column controls the level of water in the soil column. The top of each soil and equilibrium column was connected to a Tedlar bag, partially filled with argon gas, to prevent oxygen

penetration into the columns. The system was completely sealed and operated under an anoxic condition where water in storage Tedlar bags was purged by argon gas to reach dissolved oxygen (DO) < 0.8 mg L^{-1}.

Each soil column is equipped with 4 ports (1/800 NPT compression fittings) along its sides at 10, 20, 30, and 50 cm below the top of the column. The 20 cm port was tightened and fitted with Teflon septa and used only for injection of NAPLs. The other three ports have filtration screens to prevent soil washout. All ports were fitted with 1/8 -27 NPT thread with 7/16" Hex to classic series Barb, 1/8" ID tubing, and white Nylon, and connected with 10 cm of chemically resistant polyurethane tubing for collecting aqueous samples. A 9-channel pump (Tower II pump, CAT. M. Zipperer, GmbH, Germany) was used to control water level fluctuation by pumping water to the Tedlar bag linked to the equilibrium columns and served as a water reservoir. Each channel of the pump was operated individually with the design flow rate.

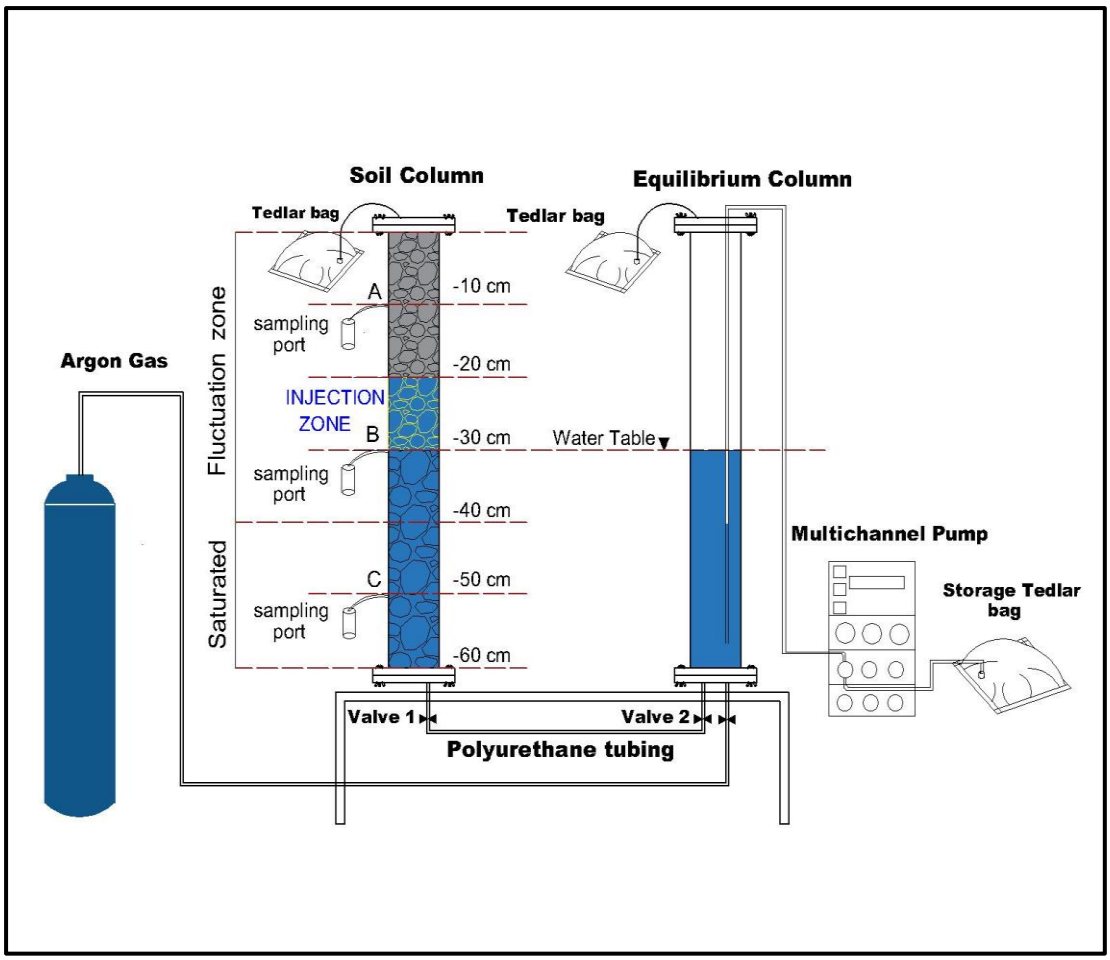

Figure 1: Schematic diagram of the experimental set-up. Depth A (-10 cm), depth B (-30 cm), and depth C (-50 cm) from the top of the column.

3.3 Analytical methods

Aqueous samples were collected for the measurements of concentrations of the contaminants (BTEX). In addition, ion chemistry (IC), dissolved inorganic carbon (DIC), dissolved oxygen (DO), redox potential (ORP), pH, and Electrical Conductivity (EC) were measured.

Eh, pH, DO, and EC were measured using an Orion™ Versa Star Pro™ Benchtop Meter (Thermo Scientific) immediately after collecting the aqueous samples to prevent the effects of degassing or reactions caused by oxygen ingress.

For the concentrations of anions and cations, Ion Chromatography (850 Professional IC (Metrohm)) with two conductivity detectors (anions and cations) was used. The

injection volume for anions of interest was 20 μL, and for the cations the injection volume was 10 μL. The column used was (Metrosep A Supp 5 - 150/4.0). The mobile phase included 1 mmol L^{-1} sodium hydrogen carbonate, 3.2 mmol L^{-1} sodium carbonate, ultra-pure water for washing, and 100 mL MH2SO4 for regeneration. 5 L ultrapure water, 0.58 g pipecolinic acid, 0.875 ml citric acid, were used as cations eluent. MagIC Net was used to process ion chromatography data.

Gas Chromatography - Flame Ionization Detector (GC-FID) (Clarus 680, Perkin Elmer, USA) was used for the measurements of organic concentrations from aqueous samples. Total organic carbon and total inorganic carbon (DIC/DOC) concentrations were measured using a total organic carbon analyser (SKALAR, Formacs HT/TN TOC/TN Analyzer, Netherland). Before the analysis, each sample was filtered by Polysulfide filters with 0.2-m pore size (Whatman, UK). The sample was examined three times, and the average was calculated.At the end of the experiment, all soil columns were fully drained and disassembled to measure the final concentrations of the contaminants in the soil by gas chromatography (GC-MS). Soil samples were obtained from the top of the soil columns using a hand hammer, and the column was divided into several layers with a thickness of 10 cm. A total of 15 g of homogenized soil was collected in three separate vials from each part.

The GC-MS analysis of organic concentrations was performed in Agilent 6890N GC system (Agilent Technologies, Palo Alto, CA, USA) with DB-5MS capillary column (30 m x 0.25 mm, 0.25 m film thickness; Agilent, Santa Clara, USA) fitted with Agilent 5975B mass selective detector in electron impact mode (ionization energy set at 70 Ev). Helium flowed at 1 mL/min. The oven was heated to 45 °C for 2 minutes, then 80 °C at 20 °C/min, then 250 °C at 25 °C/min. 1.0 L was injected splitless. Both the injector and detector were adjusted to 250 °C. Source, quadrupole, and MS interface

temperatures were 230, 150, and 250 °C. BTEX was detected using SIM at m/z 78, 91, 91, and 106 to selectively identify and quantify benzene, toluene, ethylbenzene, and xylene.

Trace elements such as Si, Fe, Mg, and S were measured using (Energy Dispersive-X-Ray Fluorescence spectrometry, ED-XRF (S2 PUMA analyzer, Bruker, Germany)). Two samples were collected from the soil before the start of the experiment, and at the end, each column was sliced into 6 parts, and three samples (10 grams each) from each slice were collected and analyzed.

The supplementary materials in Appendix A contains a comprehensive list of all the equipment used for the analysis in this study.

CHAPTER 4 THE SYNERGIC IMPACT OF WATER TABLE FLUCTUATION AND SALINITY ON LNAPLS DISTRIBUTION AND HYDROGEOCHEMICAL PROPERTIES IN THE SMEAR ZONE UNDER COMPLETELY ANAEROBIC CONDITIONS

In this chapter, a column experiment was conducted using soil samples collected from Simaisma Beach. Four columns were utilized to investigate the impact of stable water levels versus water table fluctuations on the movement of toluene and benzene within the columns, as well as the associated hydrogeochemical properties of the soil. Two different salinity levels were employed to represent brackish and seawater conditions, which are representative of the sampling location.

4.1 Introduction

Soil and groundwater contamination due to non-aqueous phase liquids (NAPLs) is considered a major environmental issue around the world where it adversely impact groundwater quality, making it inadequate for human consumption and irrigation (Alazaiza et al., 2019; Chen et al., 2020; Huang et al., 2021; Alazaiza et al., 2021). NAPLs have the potential to remain in the subsurface for many years as a continuous source of groundwater contamination (Al-Raoush, 2009; Kehew and Lynch, 2011; Al-Raoush, 2014; Ning et al., 2018). NAPLs are categorized into: light non-aqueous phase liquids (LNAPLs) with a density less than that of water and dense non-aqueous phase liquids (DNAPLs) with a density higher than that of water. The most common examples of LNAPLs are hydrocarbon fuel components, such as benzene, toluene, and xylene (Cavelan et al., 2022). LNAPLs have been the focus of many studies due to their toxicity and longevity in the environment and the subsequent impact on human health. Due to their complex interactions with geoenvironmental conditions, management and remediation activities of LNAPL-impacted sites are challenging in nature (Ebrahimi et al., 2019). LNAPLs travels downward through the unsaturated zone under the influence

of gravity until it reaches the water table, it spreads laterally while floating on the water's surface (Dobson et al., 2007; Jeong and Charbeneau, 2014). On the other hand, DNAPL migrates downward through the vadose zone and continues its migration in the saturated zone under the influence of gravity until a low permeability barrier layer is encountered (Zheng et al., 2015). Water table level in hydrogeological systems fluctuates due to groundwater withdrawal, recharge, and seasonal variations in nearby water bodies, which in turn develops unique characteristics caused by the wetting and drying cycles that lead to variations in soil water content, redox conditions, biogeochemical properties and microbial community (Haberer et al., 2012; Yang et al., 2017; Cavelan et al., 2022).

Water table fluctuations (WTF) have a significant impact on NAPL transport and spatial distribution within subsurface systems, particularly in the vertical direction (Lee et al., 2001; Alazaiza et al., 2020; Van De Ven et al., 2021). When WTF is present, mass transport of oxygen from the atmosphere to the groundwater is increased, leading to fluctuations in redox conditions (Haberer et al., 2012; Rezanezhad et al., 2014; Zhou et al., 2015; Jia et al., 2017). When the water table falls, LNAPLs migrate downwards, leaving entrapped residuals in the unsaturated zone. The residual LNAPL partitions into solid, liquid, and vapor phases depending on the geochemical conditions and properties of subsurface systems (Reddi et al., 1998; Lee et al., 2001; Kehew and Lynch, 2011; Sookhak Lari et al., 2019; Alazaiza et al., 2020; Cavelan et al., 2022). On the other hand, when the water table rises, LNAPLs move upward along the water table, which in turn induces LNAPLs redistribution upward in the unsaturated zone, leaving LNAPLs and air below the water table (Lee et al., 2001; Dobson et al., 2007). The co-existence of entrapped LNAPLs and air in the saturated zone reduces the mobile free phase LNAPLs, which limits LNAPLs downward migration and enhances the

dissolution and biodegradation of LNAPLs. Therefore, a zone of high residual phase concentration known as a smear zone could be developed due to vertical water table fluctuations in the presence of LNAPL (Kehew and Lynch, 2011; Cavelan et al., 2022). The impact of WTF on groundwater and soil contaminated with LNAPLs was monitored in the field (Teramoto and Chang, 2017; Teramoto et al., 2020), studied experimentally (Dobson et al., 2007; Yang et al., 2017; P. K. Gupta et al., 2019; Alazaiza et al., 2020; P. K. Gupta and Yadav, 2020; Van De Ven et al., 2021) and numerically (Teramoto and Chang, 2017; Sun et al., 2018; Huang et al., 2021).

Teramoto and Chang (2017) and Teramoto et al., (2020) monitored a contaminated site in Brazil and found that NAPL thickness is often lower during times of rising water levels and gradually rises during periods of low water levels. Dobson et al., (2007) found that WTF increased LNAPL dissolution and microbial activity compared with non-fluctuated model as measured by spatial distribution of electron acceptors and mass balances. Yang et al., (2017) studied the influence of three geological materials and WTF on toluene attenuation and found that the distribution of Toluene in porous media was significantly impacted by WTF. P. K. Gupta et al., (2019) assessed the fate and transport of LNAPLs under different rates of WTF. The author emphasized the relationship between biodegradation rates and initial dissolved LNAPL concentrations. Alazaiza et al., (2020) utilized a simple image analysis technique (SIAM) to monitor LNAPL volumes at WTF sequences. Their study revealed that WTF has a considerable impact on the distribution of LNAPL. Van De Ven et al., (2021) observed the changes in the smear zone and mobile LNAPL thickness as a consequence of WTF. Sun et al., (2018) demonstrated in their experimental work that WTF induces dissolution of BTEX.

Similar studied were conducted to investigate biogeochemical properties in LNAPLs

contaminated groundwater due to WTF (Lee et al., (2001); Rühle et al., (2015); and Zhou et al., (2015)). Lee et al., (2001) investigated petroleum hydrocarbons (PHCs) in a Korean sand aquifer. They found that water levels and subsurface hydrogeology affect contaminants. Rühle et al. (2015) conducted column experiments and one-dimensional flow model to investigate the dynamics of the WT. Their findings revealed variations in microbial activities between the two states. Zhou et al., (2015) investigated TPH contaminated site and found that WTF altered groundwater microbial populations.

While these studies provide valuable insights into the impact of WTF on NALP-contaminated systems, the combined effects of WTF and salinity on natural attenuation of petroleum hydrocarbons and related changes in geochemical properties under anaerobic conditions have not been fully investigated and understood. Understanding this complex synergic behavior is crucial, especially in coastline regions where high salinity and accidental spills are common.

The main objective of this study was to investigate the synergic impact of WTF and salinity on LNAPL distribution, mass removal, and changes of related geochemical properties in the smear zone under completely anaerobic reducing conditions. A series of controlled, automated soil column experiments were conducted under stable and fluctuating water table regimes for 151 days. Experiments were conducted in closed systems to limit volatilization and aeration effects and to independently control the effects of WT dynamics. Benzene and toluene were used as a source zone of LNAPLs under conditions of low and high salinity that represent brackish and seawater environments, respectively.

4.2 Experimental Setup

Four pairs of soil and equilibrium columns were used to investigate the synergic impact of WTF and salinity on the attenuation and distribution of LNAPLs in the smear zone (Figure 2). Two soil columns were allocated for stable water level conditions (labeled

as S1 and S2) whereas the other two soil columns were allocated for fluctuating water level conditions (labeled as F1 and F2). Brackish water (~ 4000 μS cm^{-1}) was used in S1 and F1 soil columns whereas high salinity water (~ 25000 μS cm^{-1}) was used in S2 and F2 soil columns.

Benzene (C_6H_6) and toluene (C_7H_8) were used as LNAPLs as these compounds can be commonly found in seawater in the vicinity of natural gas and petroleum deposits. Al-Ghouti et al., (2019) found that raw produced water in Qatar contains 21 and 3.8 mg L^{-1} of benzene and toluene, respectively. The density and solubility in water of benzene at 25 C^o were 0.874 g/cm^3 and 1800 mg L^{-1} whereas toluene is 0.867 g/cm^3 and 520 mg L^{-1}, respectively (Ruffino and Zanetti, 2009). Salinities of 4000 μS cm^{-1} and 25000 μS cm^{-1} were used to represent brackish and seawater conditions at the sampling location, respectively (Ngueleu et al., 2018, 2019). Prior to starting the experiments, soil columns were saturated with an anoxic synthetic solution with DO < 0.8 mg L^{-1} to mimic natural groundwater (Ngueleu et al., 2019). Table 1 summarizes the properties of synthetic groundwater.

Soil columns were then saturated and drained four times to develop the anaerobic conditions in the columns (i.e., to preserve reducing conditions of the natural soil). To prepare the columns for benzene and toluene injection, the water level was fixed at -25 cm (considering the top of the soil columns as reference). LNAPLs were injected with an airtight glass syringe equipped with a stainless-steel needle. At 20 cm bss, 5 ml of liquid benzene (99.9+%, Sigma-Aldrich, Canada), and 5 ml of liquid toluene (99.9+%, Sigma-Aldrich, Canada) were injected. In soil columns, water levels fluctuated between the top of the column and -40 cm. Each drainage-imbibition cycle lasted four days, allowing 6-12 hours for equilibrium. The flow rate in upward and downward directions was approximately 0.407 mL min^{-1} to mimic natural conditions in the sampled location

(Baalousha, 2016). The experiment ran for 151 days at a room temperature of (22 ± 2 ^{o} C). To ensure that oxygen (O_2) does not penetrate the system, equilibrium columns were purged with argon (Ar) gas as needed. Aqueous samples were collected from soil columns at stable conditions every 4 days from the middle of the column (i.e., port B at depth of -30 cm) and biweekly from the top of the column (i.e., port A at depth of -10 cm) and bottom of the column (i.e., port C at depth of -50 cm). Whereas, for the fluctuating columns at the time of saturation, aqueous samples were collected every 8 to 10 days from the middle of the column (depth B) and bottom of the column (depth C) and biweekly from the top of the column (depth A). At the time of drainage, aqueous samples were only collected from the bottom (depth C). Table 2 shows the experiment design.

Table 2: The experiement Design

column	**symbol**	**Salinity ($\mu S\ cm^{-1}$)**	**Porosity (%)**	**Imbibition Cycle (Days)**	**Drainage**
Stable 1	S1	4000	22	N/A	
Stable 2	S2	25000	23	N/A	
Fluctuating 1	F1	4000	24	4	
Fluctuating 2	F2	25000	26	4	

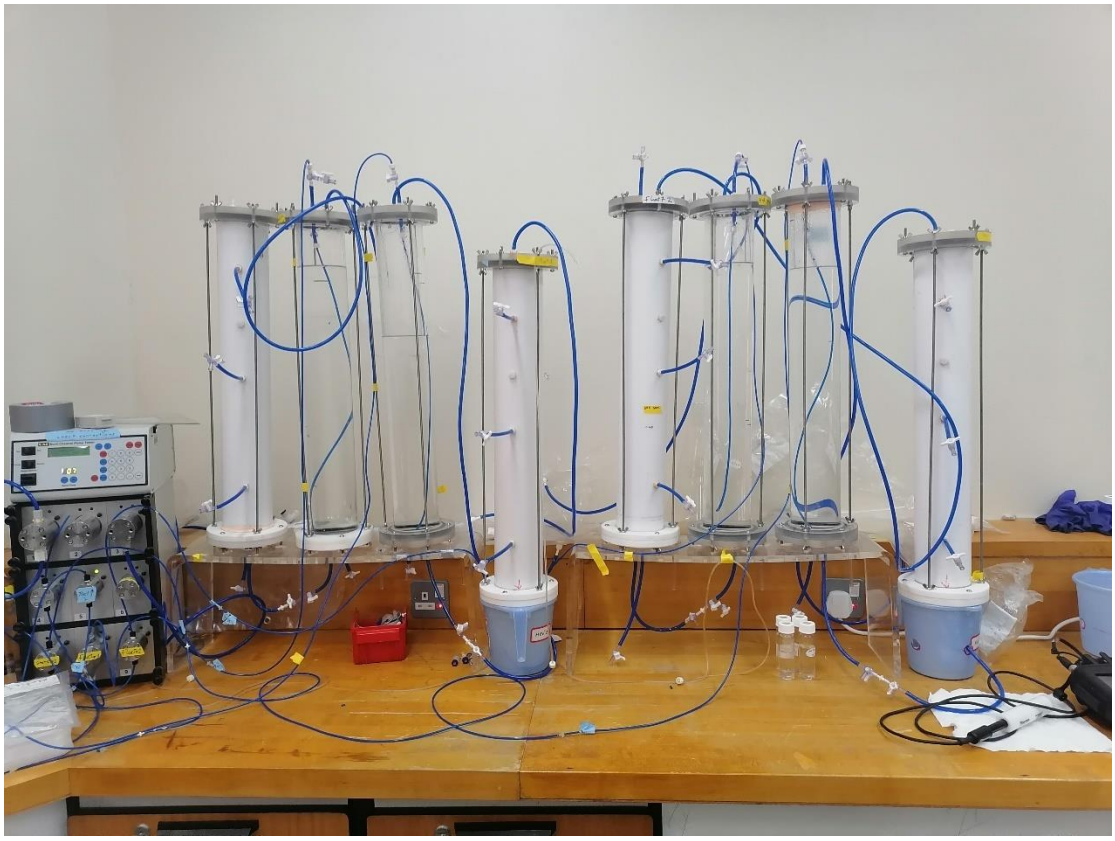

Figure 2: Experiment Setup

4.3 Results and Discussion

4.3.1 Pore water geochemistry

Prior to the start of the experiments, the porosity of the packed soil in the four soil columns was determined by the volumetric method. The porosity of the soil in the stable water level columns, S1, and S2, was 22% and 23%, respectively. Whereas the porosity of the fluctuated water level columns, F1, and F2, was 24% and 26%, respectively. Differences in the porosities between the four columns are mainly due to the manual compaction of the soil in the columns.

4.3.1.1 Water table and redox regimes

Figure 3 shows the ORP values at the middle of all soil columns. ORP indicates the ability of a given chemical to oxidize or reduce another chemical (Meng et al., 2021). Natural water chemistry is influenced by redox processes, which influence the mobility and availability of a wide range of inorganic and organic species (Ramesh Kumar and

Riyazuddin, 2012).

The influence of WTF at a given salinity can be observed by comparing stable and fluctuation columns (i.e., S and F). At low salinity conditions and in the middle of the columns (depth B), measured ORP values at the start of the experiment were +110 and +70 mV for the columns S1 and F1, respectively, whereas at the bottom (depth C), values were +140 and +60 mV, respectively. 40 and 60 days following LNAPLs injection, ORP values decreased rapidly to -100 mV and -65 mV for the middle and of the stable columns S1 and F1, while for the bottom of both S1 and F1 ORP values reached -170 mV, respectively and fluctuated in the same range until the end of the experiment. For the fluctuated low salinity conditions (i.e., F1), ORP values at the middle part (depth B), where LNAPLs were injected, and the water table fluctuates are slightly higher than the lower part (depth C).

At high salinity conditions, ORP values were +140 and +100 mV in the middle and +130 and +100 mV at the bottom of the columns S2 and F2, respectively. At 40 and 60 days after LNAPLs injection, ORP values decreased rapidly and to -130 mv and -50 mV at the middle of the columns S2 and F2, while at the bottom of both S2 and F2 decreased to -150 mV, respectively and fluctuated in the same range. Similar to the low salinity column F1, ORP values at the middle of the fluctuating column F2 are slightly higher than the lower part (depth C) at the first 60 days. Rapid decrease in ORP values occurred in the columns at 40 and 60 days which implying that anaerobic condition was developed. ORP values in the middle of the fluctuated columns is higher as compared with the bottom of the same columns F1 and F2, and with the middle of the stable columns S1 and S2, despite expectations that influent solution would significantly increase DO levels at the bottom of the column, leading to higher ORP and more oxidizing conditions at the bottom. This observation suggested that microbial activity

and anaerobic degradation were less improved in the middle of the fluctuating column. The higher ORP at the middle of the fluctuating columns could also be attributed to the effect of the presence of LNAPL as a source zone combined with the WTF that influences organic concentrations and redox conditions (Lueders, 2017; Ning et al., 2018). Moreover, during the drainage of the water table, spreading LNAPLs downward exposing the LNAPL smear zone to soil gas (Van De Ven et al., 2021). Rezanezhad et al., (2014) reported that oxidizing conditions emerged at the middle of a soil column subjected to water table fluctuations after each drainage because of oxygen penetration from the top which resulted in the increase of Eh values from -100 to +600 mV.

The influence of salinity can be observed by comparing stable columns (i.e., S1 and S2) and fluctuating columns (i.e., F1 and F2). For the stable columns, 40 and 60 days after LNAPLs injection, ORP values decreased and ranged between -100 and -130 mV at the middle and -150 mV at the bottom of both S1 and S2, respectively. Similarly, for the fluctuating columns with different salinities (i.e., F1 and F2), ORP values in the middle were ~50 and 100 mV for F1 and F2, respectively. By the third imbibition cycle, ORP values increased to ~+150 mV in both F1 and F2, then decreased to -50 mV after 60 days. The behavior of ORP at the middle and the bottom of the fluctuating columns are different, whereas in the stable columns, ORP values for the middle and the bottom are the same. The behavior in the stable columns (i.e., S1 and S2) at the middle and the bottom is similar to that of the bottom of the fluctuated columns (i.e., F1 and F2) as these conditions were under completely saturated conditions, while the middle of the fluctuating columns was subject to the fluctuating water level. These results suggested that salinity didn't affect ORP values for the middle and the bottom of stable (i.e., S1 and S2) and fluctuated columns (i.e., F1 and F2).

The results of this experiment suggested that the WTF has more profound impact on

ORP than salinity. ORP values indicate that anaerobic conditions were developed in all soil columns (Ismail et al., 2020; Shafieiyoun et al., 2020; Meng et al., 2021). In an experiment reported by Shafieiyoun et al., (2020) with the same soil samples and same flow-through reactors conditions (brackish water (~ 4000 μScm^{-1}) and high salinity (25,000 μScm−1)), after 40 days and more than 30 Pore Volumes of influent solution injection, effluent Eh values decreased to + 300 mV (equal to +100 mV ORP). Their study also confirmed that salinity does not have a major role in determining effluent Eh values when a multi-component dissolved organic phase is present, similar to our study in which two components (toluene and benzene) are partially dissolved due to water table fluctuations.

According to the classification of Reddy and DeLaune, (2008) and Zhang and Furman, (2021), soil columns were under aerobic conditions for the first 10 days, weakly reducing conditions were observed in all columns after 40 days from the start of the experiments, except at the middle of the fluctuating columns, and moderate reducing conditions were observed in all columns after 60 days. Figure 3 shows that there is no significant difference in ORP values in stable water level conditions at different salinities (i.e., S1 and S2). However, in fluctuated systems, ORP values decreased during water level rise and increased again during water level fall which is consistent with observations of Rezanezhad et al., (2014). Moreover, Vincent et al., (2011); Khan et al., (2018); and Logeshwaran et al., (2018) found that the presence of organics in the soil has an adverse effect on the development of the microbial community.

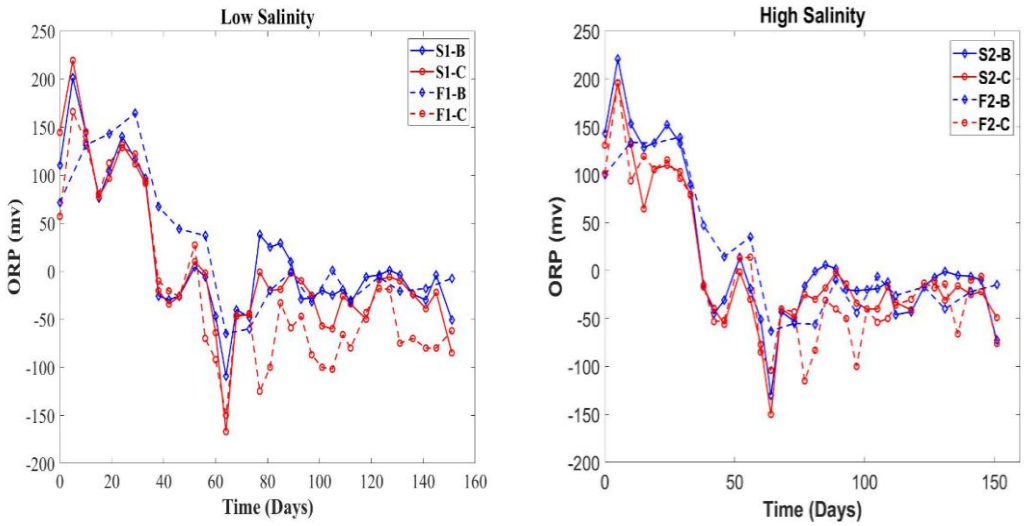

Figure 3: Oxidation-Reduction potential (ORP) at (left) depth B and C for the columns S1 and F1(for the case of low salinity columns), (right) ORP at the depth B and C for the columns S2 and F2 (for the case of high salinity columns)

4.3.1.2 Electrical Conductivity (EC)

The electrical conductivity of groundwater reflects the ionic strength of pore-water and the changes in water composition (Naudet et al., 2004; Tutmez et al., 2006). Figure 4 shows EC values measured at the middle (i.e., depth B) and the bottom (i.e., depth C) of soil columns at different experimental conditions. The influence of WTF at a given salinity was observed by comparing stable and fluctuation columns (i.e., S and F). As shown in Figure 4 (left), at low salinity conditions, the initial EC in the middle of stable and fluctuation columns was 5500 µS cm^{-1} and 4000 µS cm^{-1}, respectively. Following LNAPL injection, EC values for S1 in the middle and the bottom decreased until they reached a value of 3000 µS cm^{-1} by the end of the experiment. While for the middle of F1, EC values decreased and then increased again after 40 days. A continuous fluctuation in EC values was observed for about 60 days where it exhibited a sudden decrease. EC values fluctuated between 4500 and 3000 µS cm^{-1} until the end of the

experiment in F1 column.

The decrease in EC values in the middle of the columns S1 and F1 can be attributed to the replacement of air and pore water by LNAPLs which changes static conductivity and its relative permittivity (Lopes de Castro and Branco, 2003; Atekwana and Atekwana, 2010). Furthermore, the presence of toluene and benzene in the this section of the column and due to the their non polar nature, was expected to result in a decrease in groundwater ionic strength (Vincent et al., 2011). The EC values at S1 exhibit a significant decrease in comparison to F1. In addition, the concentration of benzene and toluene in S1 is higher than in the F1column. These differences caused by WTF which increase the dissolution and advection transport of contaminants while in S1 the only transport mechanism for contaminants is diffusion which occur at a slower rate. As a result of that higher concentration of organics are found in the middle of S1 compared with the middle of F1 by the 4^{th} imbibition cycle (see Figure 8 and Figure 9).

The increase of EC values after 60 days can be attributed to the enhancement of biodegradation due to the increase of total dissolved solids (Lopes de Castro and Branco, 2003). A decrease in EC values observed at the bottom of the column S1 and F1, can be an indication of the mobilized inorganic elements from the bottom of the columns to the middle part, in the case of S1 that occur at the time of filling the column after WT goes down due to sampling, and for F1 occur due to the fluctuation. The EC values at the bottom of F1 showed a behavior of an increase after each drainage cycle which is an indication of the mobilized inorganic elements from the middle part of the column to the bottom part (Rezanezhad et al., 2014).

In high salinity columns, the initial EC values at the middle were 31 and 23 mS cm^{-1} in S2 and F2 columns, respectively. Following LNAPL injection, EC values at the middle of S2 exhibited a slight decrease at the beginning and continued

to decrease until they reached 23 mS cm^{-1} by the 151 days. Furthermore, EC values in the F2 column decreased until they reached ~18 mS cm^{-1} after 40 days, followed by an increase to 26 mS cm^{-1} by the 151 days. The increase of EC values at 40 days is consistent with ORP values that indicated that anaerobic conditions were developed in the columns. At the bottom of the columns, the initial EC values were 32 and 21 mS cm^{-1}, for S2 and F2, respectively. In S2, EC values slightly decreased until they reached 28 mS cm^{-1} by the end of the experiment, whereas in F2, EC values increased until they reached 30 mS cm^{-1} by the end, The same explanation can be applied to account for the observed trend in the low salinity column. It is also noticed that the overall EC values in the stable columns S1 and S2 is higher than F1 and F2, this suggested that the presence of groundwater in stable condition in the S1 and S2 facilitates the dissolution of ions, resulting in higher electrical conductivity than in fluctuating columns.

The influence of salinity was observed by comparing stable columns (i.e., S1 and S2) and fluctuating columns (i.e., F1 and F2). In the middle of the stable columns, EC values of S1 were initially decreased and then a fluctuation was observed between 40 and 120 days. At high salinity conditions (S2), EC values slightly decreased throughout the entire experiment. The same finding was observed in the bottom of S1 and S2, a significant decrease occurred in EC values in S1, whereas no significant change occurred during the experiment in S2. This finding suggested that as the salinity level increases, the number of ions in the soil solution also increases, resulting in a higher electrical conductivity, while the presence of contaminants in the soil may create a hydrophobic (water-repellent) layer around soil particles, reducing the contact between water and the solid phase and reduces the contact between water and the solid phase and inhibits the movement of water and dissolved ions, which consequently lowers the

electrical conductivity of the soil.

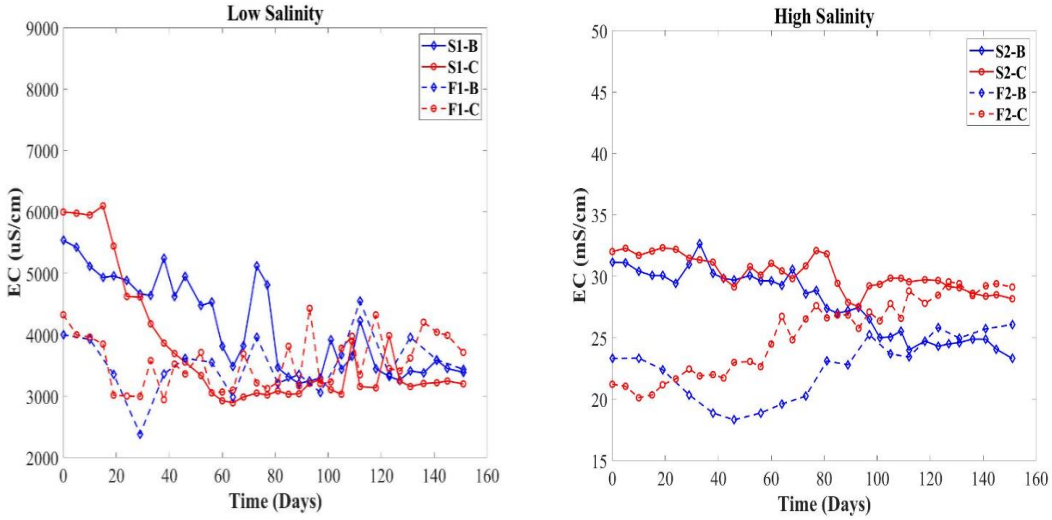

Figure 4: Electrical Conductivity (EC) concentrations at (left) at depth B and C for the columns S1 and F1(low salinity), (right) Electrical Conductivity (EC) concentrations at depth B and C for the columns S2 and F2 (high salinity)

For the fluctuating columns (i.e., F1 and F2), EC values in the middle of the columns encountered a concentration decrease after 30 days for F1, and 40 days for F2, followed by an increase for both columns. A fluctuation in EC values was observed for column F1, while a continuous increase was observed for column F2 until the end of the experiment. This finding supports the previous argument that that the presence of petroleum hydrocarbon results in the decrease in EC values, but due to the fluctuated water table which increases B&T dissolution and reduces its concentration.

For the bottom of the columns F1 and F2, EC values decreased by the third drainage cycle followed by a fluctuation in EC values in F1, and an increase for F2 which continued until the end of the experiment. The increase in EC values with each drainage cycle is more noticeable in column F1 as compared to column F2. Findings show that WTF and salinity impacted EC values in the columns. WTF enhanced the movement

of the inorganic elements along the fluctuating columns which in turn enhanced dissolution and degradation of NAPL.

4.3.1.3 pH

Figure 6 shows pH values at the middle and bottom of all soil columns. pH values ranged between 6 and 8.5 which is consistent with previous observations in similar environments as an ideal range for microbial growth and biodegradation of TPHs (Vincent et al., 2011).

The influence of WTF at a given salinity was observed by comparing stable and fluctuation columns (i.e., S and F). For the low salinity columns (i.e., S1 and F1), pH values at the middle (i.e., depth B) and the bottom (i.e., depth C) of S1 ranged between 7 and 7.5 in column S1. Whereas in F1, pH values ranged between 7 and 8 at the middle (i.e., depth B) and bottom (i.e., depth C) of the column. It can be seen that a wide range of pH values is observed in the case of water level fluctuations as opposed to stable water level which was observed also by Rezanezhad et al., (2014) By the end of the experiment, alkaline conditions were attained in F1 which can be attributed to the biodegradation process where some salts and ions were introduced in the system (Vincent et al., 2011; Shafieiyoun et al., 2020). pH values at the bottom of F1 increased with each saturation cycle and decreased with each drainage cycle. This finding can be explained as the fluctuations in the water table can affect the ion exchange capacity of the soil. As water moves through the soil profile, it can carry dissolved ions, including hydrogen ions (H^+), which increase and decrease at the bottom of the fluctuated columns due to the fluctuations.

In high salinity columns (i.e., S2 and F2), the initial pH values were 7.5 in the middle of the columns and 7 in the bottom of the columns. Throughout the S2 experiment, pH fluctuated between 7 and 7.6 in the middle of the column. Whereas in the bottom of the

columns, pH values increased and then reached 8 by the end of the experiment. pH values in the middle of F2 fluctuated between 7 and 8 whereas alkaline conditions were attained at the bottom of the column. Shafieiyoun, et al., (2020) stated that some salts associated with salinity, such carbonates and bicarbonates, have alkaline properties where these salts can dissolve in water and release hydroxides have a alkaline properties when dissolved in water will increase in pH and making groundwater more basic. Similar to the behavior of low salinity conditions, pH increased during each saturation cycle and decreased during the drainage phase. This observation is consistent with the findings of Rezanezhad et al., (2014).

The influence of salinity was observed by comparing stable and fluctuating columns. For the two stable columns S1 and S2, pH values in both columns fluctuated between 6.8 and 7.8 in the middle of columns whereas pH values show an increasing trend at the bottom of the columns. For the fluctuated columns F1 and F2, the middle of the columns has the same trend where pH values ranged between 7 and 8, whereas pH values at the bottom of the columns have the widest ranged.

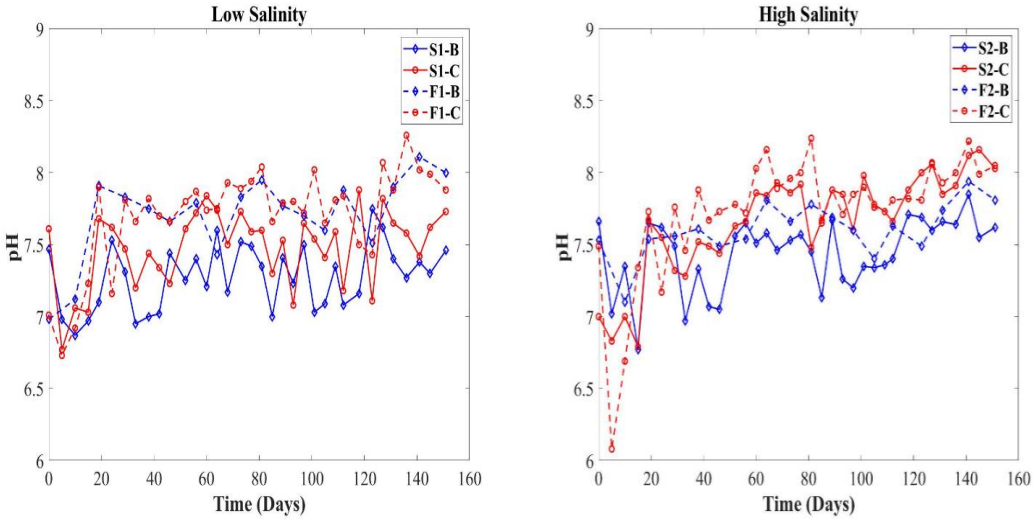

Figure 5: pH for (left) at depth B and C for the columns S1 and F1(low salinity columns), (right) pH at depth B and C for the columns S2 and F2 (high salinity)

4.3.1.4 Concentration of electron acceptors

To sustain the microorganism's living and growth, they strive for energy from the available electron donors and acceptors. Some of these microorganisms will prefer to utilize specific electrons. Because DO produces the greatest amount of energy from organic carbon oxidation of any commonly available electron acceptor, oxygen-reducing microorganisms will compete for the available electron in DO, and the reaction will continue until DO is depleted. The sequence of electron acceptor utilization is often predictable in the order of O_2> NO_3^->Mn^{4+}>Fe^{3+}>SO_4^{2-}>CO_2 (Borch et al., 2010; McMahon et al., 2011; Laverman et al., 2012; Ohio EPA, 2014). Measuring biodegradation can be determined by the removal of electron donors (i.e., benzene and toluene) or electron acceptors (i.e., nitrate and sulfate) (Chapelle et al., 1996; Borch et al., 2010; McMahon et al., 2011; Ohio EPA, 2014). Moreover, water table fluctuations can affect the availability of different electron acceptors in the soil, depending on whether the soil is saturated or unsaturated (Rezanezhad et al., 2014).

Ion chromatography (IC) was used for the measurement of cations and anions. The IC results indicated that an aqueous phase of iron (Fe), manganese (Mn), sulfur (S), and nitrogen (N) were available in the system. It was also observed that aqueous nitrate (NO_3^-) concentration was detected at the top, middle and bottom of all soil columns. During the first 30 days, the concentration of NO_3^- was in the range of 2 and 5 mg L^{-1} at the top (i.e., depth A) and the middle (i.e., depth B) of the stable columns (i.e., S1 and S2). For the fluctuating columns (i.e., F1 and F2), NO_3^- was only detected in the middle of the column in the range of 1 and 5 mg L^{-1} in the first 60 days. Detection of NO_3^- corresponds to oxygen reduction to less than o.8 mg L^{-1} and the development of the anaerobic condition as supported by ORP values given in Figure 3. The aqueous Mn concentration was detected in the middle of the columns S1 and S2 in the range of 6 and 13 µg L^{-1}, respectively until day 100. Furthermore, the aqueous Mn

concentrations for the fluctuating columns F1 and F2 were observed in the first 15 days in the middle and the bottom of the columns in the range of 1 and 23 µg L^{-1}, respectively.

For the stable columns (i.e., S1 and S2), the concentration of ferric iron was detected only in the middle and ranged between 14 and 7 µg L^{-1}. For the fluctuating water level columns (i.e., F1 and F2), the concentration in the middle was detected after 15 days and ranged between 4 and 7 µg L^{-1}, respectively. At the bottom of F1 and F2, the concentration ranged between 3 and 4 µg L^{-1}, respectively. Unlike the previously mentioned electron acceptors, the aqueous sulfate concentrations were detected in the columns at all depths in the range of 300 – 88 mg L^{-1}. Low nitrate, manganese and iron concentrations reveal that denitrification, manganese and iron reduction were not the dominant biodegradation processes, however, sulfate-reducing bacteria (SBR) are expected to be the dominant (Davis et al., 1999; Anneser et al., 2008).

As shown in Figure , the influence of WTF at a given salinity was observed by comparing stable and fluctuation columns (i.e., S and F). The initial sulfate concentrations in the middle of S1 and S2 columns were 250 and 300 mg L^{-1}, respectively. In low salinity columns (i.e., S1 and F1), the initial sulfate concentrations were 250 and 110 mg L^{-1} for S1 and F1, respectively. 10 days after the injection of LNAPLs, sulfate concentrations increased to 270 and 170 mg L^{-1}, respectively, then continued to decrease to 145 and 60 mg L^{-1}, respectively, by the end of experiment. The decrease in sulfate concentration during the experiment coupled with ORP reduction might be an indication of biodegradation of NAPL by the SBR (Anneser et al., 2008; W. H. Huang et al., 2016; Shafieiyoun, et al., 2020; Wei et al., 2018). Biodegradation is thought to be controlled by the availability of certain electron acceptors, not by thermodynamics (Meckenstock et al., 2015; M. Zhang et al., 2021).

In high salinity columns (i.e., S2 and F2), at the top of S2, the concentration of sulfate was stable for about 100 days and then decreased. For the top of F2, no observed changes in sulfate concentrations except for some decrease in concentration at 60 days. In the middle of columns S1 and F1, the initial pore water sulfate concentrations were 300 and 160 mg L^{-1}, respectively. For S2, sulfate concentration decreased to reach 160 mg L^{-1} by the end of the experiment, while for F2, 10 days following the injection of LNAPLs, sulfate concentrations increased to 170 mg L^{-1}, then decreased and reached 50 mg L^{-1} by the end of experiment. The increase in concentration that occurred at the beginning of the experiment could be a result of the movement of groundwater to the top of the column which carries sulfate ion along the column.

The influence of salinity was observed by comparing stable columns (i.e., S1 and S2) and fluctuating columns (i.e., F1 and F2). The aqueous sulfate concentrations at the top, middle and bottom of the two stable columns followed the same trend during the experiment. There was no significant concentration decrease at the top of the columns, while a the most decrease in concentration occurred in the middle, and a slight change was observed at the bottom. It was observed that concentrations at all depths in column S2 are higher than in S1.

In the fluctuating columns (i.e., F1 and F2), sulfate concentrations followed the same trend at all locations. At the top, no change in concentration was observed, whereas in the middle, sulfate concentrations decreased and values fluctuated due to the wetting and drying cycles that enhanced redox conditions (Yang et al., 2017). Sulfate concentrations at the bottom of the columns were significantly lower than those in the middle of the columns. This observation can be attributed to the dissolution of sulfate as a result of the admixing more diluted water from the equilibrium columns (Rezanezhad et al., 2014).

When the water table fluctuates, it influences the direction and rate of water flow in the subsurface. As water moves through the soil, it carries dissolved ions, including sulfate ions (SO_4^{2-}), along with it. Moreover, during periods of high-water table or saturation, water can percolate downward through the soil profile, sulfate ions can be transported vertically with the downward movement of water, reaching deeper soil layers or groundwater. Conversely, during periods of low water table, water can move upward through capillary action, commonly referred to as capillary rise. This upward movement of water can bring sulfate ions upward from deeper soil layers or groundwater toward the surface.

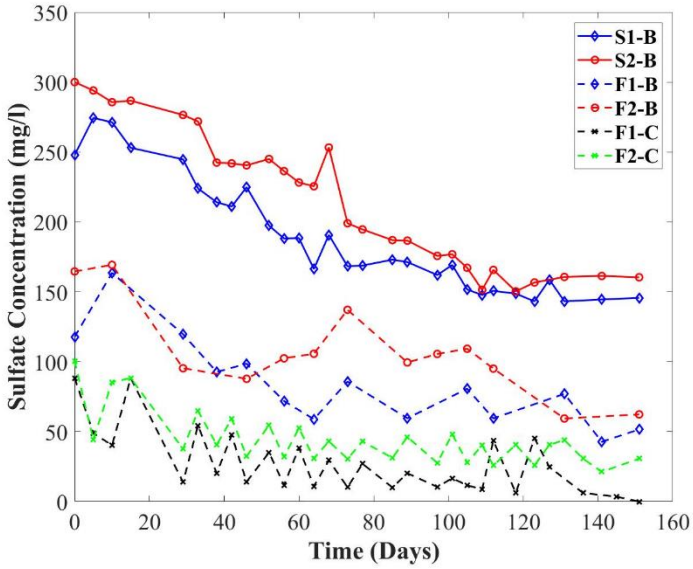

Figure 6: Dissolved sulfate concentrations at depth B of the stable columns (S1 and S2), and depth B, and C for the fluctuating columns (F1 and F2).

4.3.1.5 Dissolved Inorganic Carbon (DIC)

DIC concentration is an indicator of the mineralization of NAPL. Figure shows the

concentrations of DIC measured at the middle of soil columns at each imbibition cycle. The influence of WTF was observed by comparing the low salinity columns (i.e., S1 and F2) and the high salinity columns (i.e., S2 and F2). For the low salinity columns, the initial DIC concentrations at the middle were 19 and 16 mg L^{-1}, respectively. DIC was increased to 35 and 27 mg L^{-1} after 30 and 40 days, respectively. The increase in DIC values is consistent with the start of the reducing conditions in the columns (Figure 3). For the high salinity columns (i.e., S2 and F2), the initial DIC concentrations at the middle were 17 and 11 mg L^{-1}, respectively. However, DIC was increased to 35 and 20 mg L^{-1} for S2 and F2 after 30 and 40 days, respectively.

The influence of salinity was observed by comparing stable columns (i.e., S1 and S2) and fluctuating columns (i.e., F1 and F2). In columns S1 and S2, DIC values followed the same trend where values increased as anaerobic conditions developed in the columns. According to Wei et al., (2018), DIC is generated during biodegradation, and the carbon isotopic makeup of the DIC represents the organic carbon intake from the degraded BTX material. This is consistent with the increase in DIC concentrations occurring concurrently with the development of anaerobic conditions in all the soil columns.

DIC values in column S2 were slightly higher than S1 especially after the peak which occur at 40 days following the injection. This observation could be a result of the increase sorption in the high salinity column as stated by (Ngueleu et al., 2019).

DIC concentrations in columns F1 and F2 followed the same trend throughout the experiments where concentrations increased to 27 and 20 mg L^{-1}, respectively. At the bottom of columns, the initial DIC concentrations were 13 and 11 mg L^{-1} for F1 and F2, respectively. While at 40 days, DIC values increased to approximately 20 and 17 mg L^{-1} for F1 and F2, respectively. DIC values imply that mineralization was developed

in the middle of columns where LNAPLs were injected. In stable columns, mineralization of organics was more enhanced in S2 whereas in fluctuating columns, mineralization was more enhanced in F1. These observations are consistent with the suggestions of Kehew and Lynch, (2011), Wei et al., (2018) and Wurgaft et al., (2019).

4.3.2 Concentration of dissolved organics

Throughout the experiments, LNAPLs were under saturated conditions in the stable columns and continuously under cycles of saturated and unsaturated conditions in the fluctuating columns. This in turn led to the development of three distinct states as free, dissolved, and residual phase (Yang et al., 2017). Toluene degrades quickly under all anaerobic redox situations, whereas benzene breakdown slowly depending on the redox conditions (Ledin et al., 2011). The move of petroleum hydrocarbons in soil is influenced by various factors, including the water velocity gradient, hydraulic conductivity, intensity of evaporation and transpiration, density gradient, seasonal changes in water surface level, and diffusivity (Farahani & Mahmoudi, 2018). Which in turn enhance The decrease in the concentrations of these contaminants by the natural attenuation processes which includes volatilization, dilution and dispersion, sorption to soil particles, and biodegradation (Kehew and Lynch, 2011; Yang et al., 2017 ; Hatipoğlu-Bağci and Motz, 2019).

4.3.2.1 Concentration of dissolved and solid-phase Toluene

Dissolved toluene concentrations are presented in Figure 8 (a, b, and c). In low salinity columns (i.e., S1 and F1), the initial toluene concentrations at the top, middle and bottom were 42, 179, and 0 mg L^{-1}, and 70, 73, and 0 mg L^{-1} in S1 and F1, respectively. The concentration of toluene was the highest at the middle of the columns where the source zone of the LNAPL exists. As WT rises, it pushes toluene to the top of the column and a new smear zone was developed (Dobson et al., 2007; Van De Ven et al., 2021). At the top of the S1, no change in toluene concentration was observed during

the experiment, whereas in column F1, concentrations increased to a maximum value of 160 mg L^{-1} by the third saturation cycle. The increase in concentration in F1 resulted from the release of entrapped toluene where it was injected at (-20 cm). Thereafter, the concentration decreased until it reached 33 mg L^{-1} by the end of the experiment.

At the middle of S1, the concentration increased to a maximum value of 200 mg L^{-1} after 29 days. Whereas in F1, a maximum concentration of 160 mg L^{-1} was reached after 10 days following toluene injection (i.e., the second saturation cycle). At the bottom of S1, no toluene was detected, while toluene concentrations in F1 increased when water level rises and decreased when water level falls.

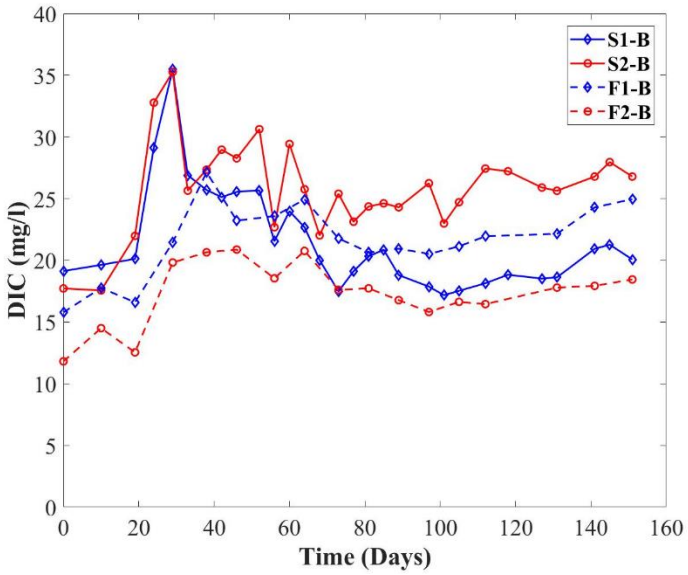

Figure 7: Dissolved inorganic carbon (DIC) concentrations at depth B for stable (S1 and S2) and fluctuation columns (F1 and F2)

In high salinity columns (i.e., S2 and F2), the initial toluene concentrations at the top, middle, and bottom of the columns were 52, 186, and 0 mg L^{-1} and 83, 105 and 0 mg L^{-1}, respectively. Similar to the low salinity columns, the concentration of toluene was the highest at the middle of the columns. At the top of column S2, no significant change was observed in toluene concentration during the experiment. In F2, toluene

concentrations increased to a maximum value of 150 mg L^{-1} by the third saturation cycle. Thereafter, the concentration decreased until it reached 42 mg L^{-1}. At the middle of S2, the concentration increased to a maximum value of 220 mg L^{-1} after 29 days, whereas in F2, a maximum concentration of 170 mg L^{-1} was reached after 10 days (i.e., the second saturation cycle). Similar to the observed in the low salinity experiments, at the bottom of S2, no toluene was detected at the bottom of the S2 whereas in the case of F2, toluene concentrations decreased when water level rise and increased when water level dropped. Since diffusion was the only mass transfer mechanism in stable columns, no toluene was observed at the bottom of these columns during the lifetime of the experiments. This is consistent with the observations of Werner and Höhener (2002).

To investigate the impact of salinity on a certain water level regime, S1 was compared to S2 and F1 was compared to F2. In stable water level conditions (i.e., S1 and S2), high toluene concentrations were observed in S2. At the top of S1 and S2, there was no significant change in concentrations in the first 100 days, followed by a small decrease for the last 50 days. Whereas in the middle of S1 and S2, toluene concentrations increased to its maximum of 200 and 220 mg L^{-1}, respectively at 29 days, then fluctuated between 200 to 150 mg L^{-1} until the end of the experiment. The slight increase in toluene concentration can be attributed to the increased dissolution of entrapped toluene due to the increase of contact time between water and toluene as water level is stable in these columns.

For the fluctuating columns (i.e., F1 and F2), toluene concentrations followed the same trend, where F2 has higher concentrations at all depths. At the top of columns, toluene concentrations in both columns increased by the third saturation cycle, then dropped, whereas in the middle of the columns, the concentrations increased to its maximum by the second saturation cycle, then decreased drastically by 40 and 60 days which

corresponds to the drastic change in ORP (Figure 3). The decrease in toluene concentration corresponds to ORP reduction and the enhancement of the anaerobic condition can be attributed to the biodegradation process. The bottom of the columns F1 and F2 had the same pattern of decreasing and increasing with the saturation and drainage cycles. It is expected that toluene was redistributed in the columns by advective mass transfer during the water table rise, while during falling water table conditions, dispersion may be reduced, leading to more localized contamination at the bottom of the column. Moreover, rising water table can lead to an increase in groundwater volume, resulting in dilution of toluene concentrations as the volume of groundwater available to dissolve and disperse toluene increases, potentially reducing the overall solubility of toluene in the groundwater. It is noticed that the toluene concentrations didn't reach its max solubility (~ 516 mg L^{-1}) which can be as a results of the limited contact time between water and toluene (P. K. Gupta et al., 2019). Moreover, biodegradation of toluene and transformation into other compounds can reduce the concentration of toluene in groundwater and prevent it from reaching its maximum solubility.

For column F1, the toluene completely depleted after 100 days from the beginning of the experiment, while for column F2, the toluene concentration reached 3 mg L^{-1} by the end of the experiment. This can be a results of increased salinity in F2 which referred to as the salting-out effect (Shafieiyoun et al., 2020)

In general, the concentration drop was observed to be higher in the columns F1 and F2 as compared to the columns S1 and S2. In terms of salinity, the decrease in toluene concentration was higher in F1 than F2, and slightly in S1 than S2. These results support the conclusion that WTF has superiority effect over salinity when it comes to dissolution and degradation of toluene.

Toluene concentrations at the top and middle of S2 are higher than S1, where high salinity reduces the dissolution of toluene. Salts in the water can interact with toluene molecules, leading to decreased interactions between toluene and water molecules and, thus, lower solubility. At the middle of S1 and F1, for S1, toluene concentration reached its maximum after 29 days, while for F1 after 10 days. Toluene concentration for S1 decreased slightly, while for F1 decreased rapidly. At the bottom of S1, toluene was not observed, while for F1, toluene concentration increased and decreased with the WTF. For the middle of S2 and F2, for S2, toluene concentration reached its maximum after 29 days, while F2 after 10 days, with rapid decrease at F2. Similar observations applied to the bottom of S2 and F2.

Upon the completion of the experiments, the solid-phase concentration of toluene in the soil was measured by GC-MS. Figure 8(d) shows toluene concentrations in the soil at different depths for all soil columns. For the low salinity columns (i.e., S1 and F1), a maximum concentration of 3 mg kg ^{1} was detected in S1 between -20 to -30 cm, whereas for the F1, the highest concentration was 1.4 mg kg^{-1} was detected between -10 to -20 cm. For the high salinity columns, (i.e., S2 and F2), a maximum toluene concertation of 18 mg kg ^{1} was observed in S2 between -20 and -30 cm, whereas in F2, a maximum concentration of 3 mg kg ^{1} was detected between -30 to - 40 cm.

Figure 8(d) shows that toluene concentrations at the source zone in the stable columns are higher than those in the fluctuating columns. In stable columns, the highest concentration of toluene was observed between -20 and -30 cm where toluene was injected, and the second highest concentrations between -10 and -20 cm. For column S1, toluene concentration at the bottom of the column was higher than S2. This can be explained by the higher salinity inhibited the dissolution of toluene and, thus the diffusion downward (Xie et al., 1997), which was discussed previously. For the

fluctuating columns (i.e., F1 and F2), the higher concentration of toluene was observed between -10 to -20 cm for column F1, and between -30 and -40 cm for column F2. However, the concentrations along the column F2 were higher than F1. It can be concluded that for columns S1 and S2, the concentration of toluene in the soil along the column is 68% higher in S2, the same goes for the columns F1 and F2, the concentration of toluene along column F2 is 48% higher than F1. Salinity influences the dissolution and natural attenuation of toluene, as it has significant effects on the solubility and mobility of organic compounds in groundwater systems. It can be summarized that the fluctuating columns have less toluene concentrations as compared to the stable columns.

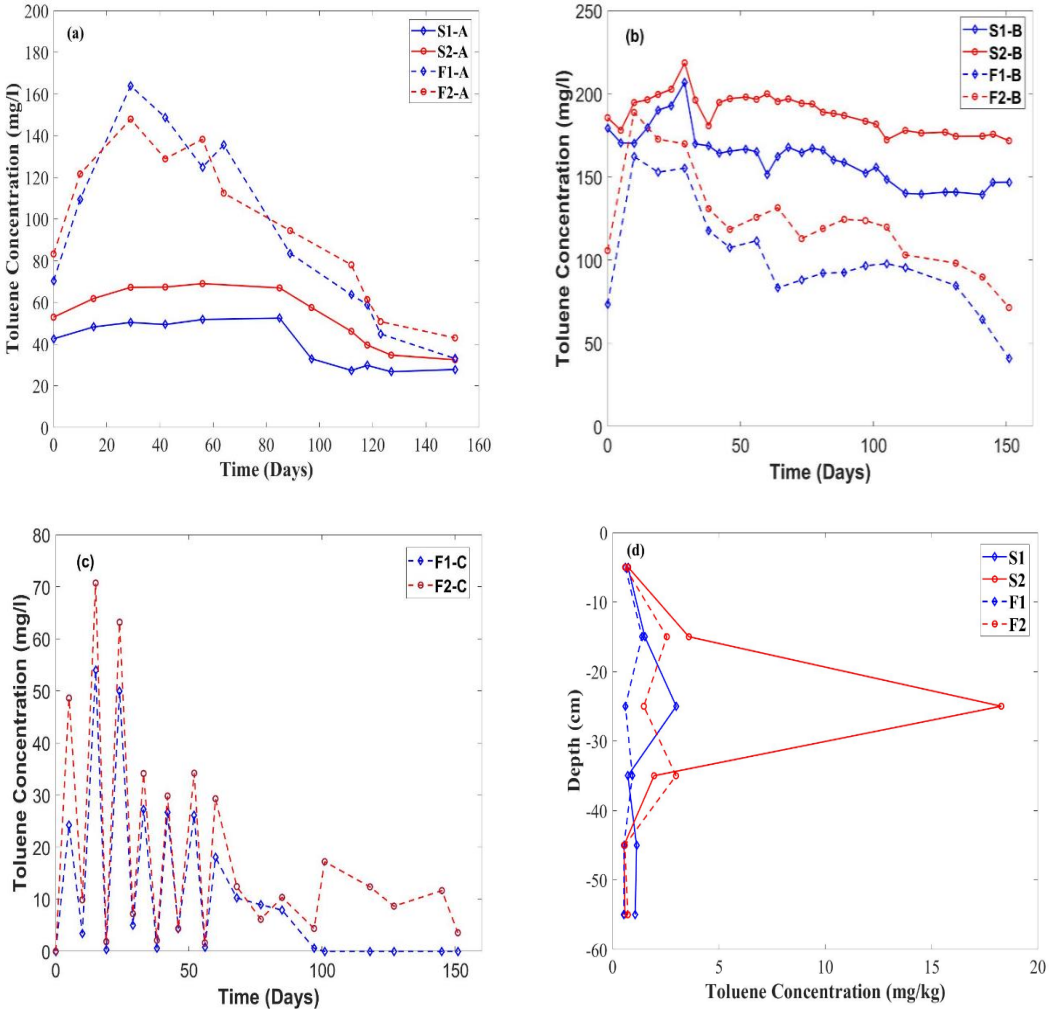

Figure 8: Toluene concentrations for (a) depth A (b) for depth B, (c) for depth C, and (d) for final soil concentrations of the columns S1, S2, F1, and F2.

4.3.2.2 Concentration of dissolved and solid-phase Benzene

Dissolved benzene concentration for all soil columns is presented in Figure 9 (a, b, and c). For the low salinity columns (i.e., S1 and F1), the initial benzene concentrations in S1 were 140, 400, and 0 mg L^{-1} at the top, middle, and bottom, respectively. While the concentrations in F1 were 190, 300, and 0 mg L^{-1} at the top, middle, and bottom, respectively. The concentration of benzene was highest at the middle of the columns, where the middle of the column is considered as a source zone of the LNAPL. At the top S1, a slight decrease was observed in benzene concentration at the first 100 days,

while after that, concentration fluctuated until the end of the experiment. For F1, benzene concentrations decreased gradually to reach 60 mg L^{-1} by end of the experiment. In the middle of S1, benzene concentration increased to a maximum value of 480 mg L^{-1} after 29 days, while for F1, it reached its maximum concentration of 430 mg L^{-1} after 10 days (i.e., the second saturation cycle). At the bottom of S1, no benzene was detected, while for F1, benzene concentrations increased when WT rises and decreased when WT moves down.

For the high salinity columns (i.e., S2 and F2), the initial benzene concentrations in S2 were 150, 400, and 0 mg L^{-1} at the top, middle, and bottom, respectively. Furthermore, the concentrations in F2 were 210, 300, and 0 mg L^{-1} at the top, middle, and bottom, respectively. At the top of the columns S2, similar to S1, slight decrease was observed in benzene concentration at the first 100 days, while after that, concentration fluctuated until the end of the experiment. For column F2, benzene concentrations decreased gradually to reach 100 mg L^{-1} by end of the experiment. In the middle of S2, benzene concentration increased to a maximum value of 500 mg L^{-1} after 29 days, while for F2, it reached its maximum concentration of 480 mg L^{-1} after 10 days following benzene injection (i.e., the second saturation cycle). At the bottom of column S2, no benzene was detected, while for F2, benzene concentrations decreased when WT rises and increased when WT moves down. Benzene is transported through a column primarily by advection and dispersion. When the water table rises, dissolved benzene is advected upward, redistributing to the top of the column. Additionally, certain disconnected benzene blobs gain mobility and move with the rising water table, reaching the top of the column. On the other hand, when water moves down, dissolved benzene moves down with the water table leaving behind discontinued blobs and moreover concentrated in the bottom part of the column.

To investigate the impact of salinity on a certain water level regime, S1 was compared to S2 and F1 was compared to F2. At the top of S1 and S2, both columns followed the same pattern with a slight increase observed in benzene concentrations in F2. It was observed that the behavior of benzene in the stable water columns was different than toluene as higher concentrations were measured at the top of the stable columns as compared to toluene. This observation can be attributed to the higher benzene solubility in water. A small decrease in benzene concentration has been observed as benzene can only be diffused down or volatilized in the upper part of the column. At the middle of S1 and S2, the concentration of benzene increases to its maximum value after 29 days following the injection. As explained before, the increase in benzene concentration can be attributed to the dissolution of the entrapped benzene. Dobson et al., (2007) stated that when LNAPLs are entrapped below the WT, an isolated blob (or ganglia) of LNAPL will increase the interfacial area between the LNAPL and water, hence, encouraging accelerated LNAPL dissolution. No benzene was observed at the bottom of the stable columns. For the fluctuated columns (i.e., F1 and F2), at the top of the columns, benzene concentrations decreased gradually. Due to the WTF between the top of the columns and -40 cm, benzene moved down during drainage cycle, thus, the concentration of benzene decreased gradually at the top of the columns and reached a concentration of 60 and 80 mg L^{-1} by the end of the experiment for F1 and F2, respectively. Benzene concentration at the middle of F1 and F2 increased to its maximum at the second imbibition cycle, as a result of increase dissolution of benzene (Dobson et al., 2007). 40 days following the injection of benzene, its concentration decreased to 65 and 100 mg L^{-1} for the columns F1 and F2, respectively. At the bottom of the columns, same observation was made, at each drainage cycle, the concentration of benzene was increased suggesting that benzene moved downward when WT moves

down. The concentration continued to fluctuate with each drainage and saturated cycle until it reached ~3 mg L^{-1} for both columns by the end of the experiment. For the stable columns (i.e., S1 and S2), benzene moved to the top of the column due to sampling and stayed there. The concentration gradually decreased throughout the experiment until 100 days, when it fluctuated till the end. The middle of the stable column (i.e., S1 and S2) has the highest benzene concentration relative to the top since it is the source zone, whereas benzene didn't move to the bottom of the column as diffusion occurred slowly. At the middle of S1 and F1, benzene concentration reached its maximum after 29 days and 10 days, respectively. No benzene has been observed at the bottom of S1, while the concentration increased and decreased with the WTF at F1. The same pattern between S2 and F2 was observed, where benzene moved up in S2 with no obvious change in concentration. For the middle of S2 and F2, benzene concentration reached its maximum after 29 days, and 10 days, respectively where the concentration at S2 decreased slightly, while for F2 decreased rapidly.

The fluctuating of the water table increases the contact between benzene and groundwater, which resulted in increased contact area providing more opportunities for the contaminants to dissolve into the groundwater. And that is case in this experiment when benzene reached its maximum concentration in the fluctuating columns (F1 and F2) after 10 days, while the stable columns (S1 and S2) reached its maximum concentration after 29 days. Moreover, it enhanced mixing between dissolved contaminants and groundwater allowing for better dissolution of benzene.

Figure 9(d) shows the concentration of benzene in the soil at different depths which was measured by GC-MS. The maximum benzene concentrations for the low salinity columns (i.e., S1 and F1), were 4 and 1.3 mg kg^{1}, respectively, between -10 to -20 cm for S1, and between -30 to -40 cm for F1. The maximum benzene concentrations for

the high salinity columns (i.e., S2 and F2), were 5 and 0.9 mg kg ^{1}, respectively, between -10 to -20 cm for S2, and between -30 to -40 cm for F2. WTFs cause desorption of benzene from soil. As the water table rises, it can displace the dissolved contaminants from the solid surfaces, making them more available for dissolution into the groundwater. The following conclusions can be drawn from a comparison of the stable and fluctuating water level columns: Firstly, the concentration of benzene and toluene for stable columns decreased slightly during the experiments, while for fluctuating columns benzene concentration decreased significantly. Secondly, the fluctuating WT within the capillary fringe resulted in the increase of the aqueous phase concentration and consequently decreases the free phase LNAPLs which resulted in more mass removal (Kemblowski and Chiang, 1990; Dobson et al., 2007). Thirdly, the low initial aqueous phase concentration for both toluene and benzene at the start of the experiment reached their maximum solubility at the source zone after 10 days for F1 and F2, and after 29 days for S1 and S2. This conclusion suggests that WTF enhance dissolution of LNAPLs, and thus the natural attenuation (Dobson et al., 2007).

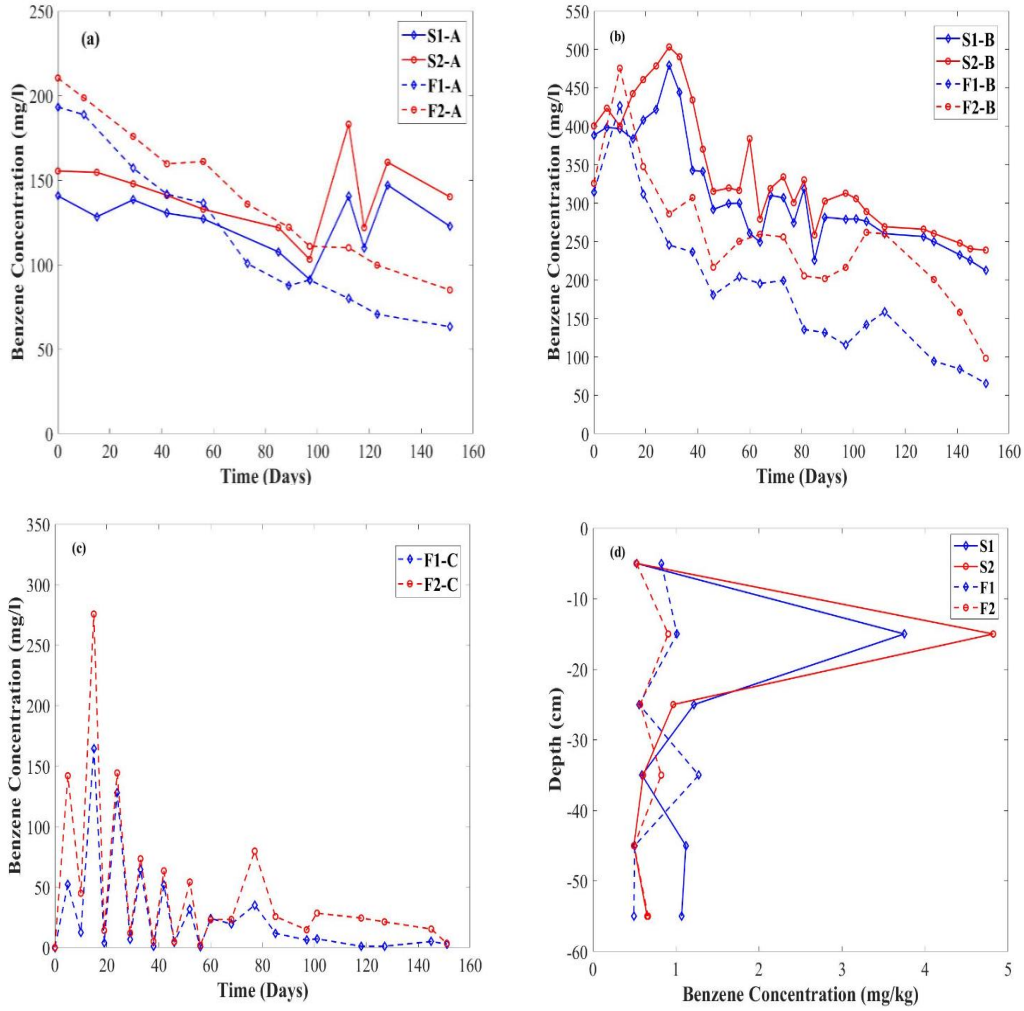

Figure 9: Benzene concentrations for (a) depth A (b) depth B, (c) depth C, and (d) the final benzene concentration of the stable and fluctuating water table columns S1, S2, F1, and F2.

4.4 Conclusion

Natural attenuation in LNAPLs contaminated groundwater is greatly affected by the movement of water table. Fluctuations of the water table within LNAPL-contaminated subsurface environments induce changes LNAPLs source zone and the geochemical properties of soil and groundwater. Results showed that redox conditions were not constant but fluctuated spatially and temporally in the soil columns. ORP values for low salinity stable column (S1) at the middle and the bottom as well as the bottom of

the fluctuating column (F1) follow the same pattern. However, the middle of the fluctuating columns in the case of the low and high salinity behaves differently. The differences in ORP behavior were due to the presence of organics and the changing WT level in this area. Furthermore, no significant change between high and low salinity columns was observed. While the EC values for S1 and S2 declined during the experiment, values for the columns F1 and F2 decreased during the first 40 days of the experiment followed by an increase. The trend of EC values differed between the stable and fluctuating columns, as well as between the low and the high salinity columns for both stable and fluctuating conditions. The differences between the stable and fluctuating columns are attributed to the movement of inorganic elements along the fluctuating column, as well as the dissolution and degradation of toluene and benzene, whereas the effect of admixing diluted water from the equilibrium column occurred at the bottom of the column in the stable column. Furthermore, salinity has influenced EC values in both the two stable columns and the two fluctuating columns. pH values in the stable columns S1 and S2 fluctuated in small range, while for the fluctuating water level columns F1 and F2, pH values covered a wide range and as the experiment progressed moved more towards alkalinity. The aqueous phase of iron, manganese, nitrogen, and nitrate were detected in the system in very low concentrations; however, sulfate was plentiful, making it the major electron acceptor. The soluble components of benzene and toluene were depleted faster in the fluctuating columns, resulting in a shorter lifespan for the source zone. The natural attenuation was also improved for the columns F1 and F2, as seen by the consumption of sulfate as compared to the columns S1 and S2. In spite of a variety of factors, including site-specific ones, results of this study showed that WTF might be used to speed up the remediation of LNAPL contaminated aquifers.

CHAPTER 5 THE CORRELATION BETWEEN BTEX ATTENUATION, AND SOIL HYDROGEOCHEMICAL PROPERTIES UNDER THE EFFECT OF WATER TABLE FLUCTUATION

In this chapter, we present a comprehensive column experiment aimed at understanding the dynamics of BTEX (benzene, toluene, ethylbenzene, and xylene) movement within natural soil samples. The experiment involved the use of five distinct soil columns, allowing us to explore the influence of various factors on BTEX transport and the associated hydrogeochemical properties of the soil. The primary objective of this study was to find a correlation between the behavior of BTEX compounds under different conditions, including stable water table conditions, water table fluctuations, the presence of soil layering, and variations in temperature.

5.1 Introduction

In many coastal areas, groundwater pollution results from the accidental spilling of petroleum products including crude oil, gasoline, and diesel fuel. This type of pollution is common (X. Huang et al., 2021; N.J. Sihota et al., 2016). Certain compounds included in LNAPL, such as benzene, for instance, are known to cause cancer in humans and have a deleterious effect on both the environment and human health (Cavelan et al., 2022; Gupta and Yadav, 2017; Sookhak Lari et al., 2018). Because of this, groundwater is inappropriate for use in agriculture as well as in the provision of drinking water (Alazaiza et al., 2021; Cavelan et al., 2022). Due to the fact that LNAPL fuels and oils are frequently a complex multi-component mixture with different physical characteristics, the process of cleaning up polluted locations may take a significant amount of time and a significant amount of money. BTEX, which stands for benzene, toluene, ethylbenzene, and xylenes, are among the hydrocarbons that are of particular concern due to their high-water solubility, which enables them to spread extensively in the subsurface environment. This is one of the reasons why BTEX is

among the hydrocarbons that are of particular concern (Chompusri et al., 2002; Brijesh K. Yadav et al., 2012).

Immediately after the discharge of LNAPLs, the mobile phase infiltrates via the soil porosity to the subsurface and accumulates at the top of the water table. By capillary pressures or by adhering to soil grains, a large portion of the pollutants may be residualized as LNAPL ganglia (Cavelan et al., 2022; Dobson et al., 2007). When the water table decreases, the mobile LNAPL goes down with it, which results in a redistribution of the LNAPL and a rearrangement of the partitioning of LNAPL components across various phases (Cavelan et al., 2022).

Over the next decade, changes in surface hydrological processes and plant cover caused by climate change will have an impact on the quantity and quality of groundwater recharge. Consequently, the levels of groundwater will be influenced by these changes. (Cavelan et al., 2022). According to the IPCC's latest report, severe weather events (heat waves, droughts, and heavy rains) are becoming more common and intense as a result of global warming. Moreover, the global mean surface temperature would rise from 1.5°C to 5.7°C by 2100 (Masson-Delmotte et al., 2021). A 1.5°C rise in mean local surface temperature should lead to a 5.7°C increase in mean shallow groundwater temperatures, which consequently affecting soil moisture content, microbial activity, and therefore LNAPL degradation and mobilization (Cavelan et al., 2022; Brijesh Kumar Yadav and Hassanizadeh, 2011).

Numerous attempts have been undertaken to evaluate remediation solutions for polluted aquifers and to better understand natural attenuation processes of hydrocarbons in both the source zone and groundwater plumes (N.J. Sihota et al., 2016). Quantification of Natural Source Zone Depletion is challenging due to factors such as subsurface geological and microbiological heterogeneity, pollutant morphology and type, and

hydrogeologic features of a site, all of which influence the amount and rate of NSZD (Sookhak Lari et al., 2018; Van De Ven et al., 2021; Zanello et al., 2021). LNAPL remobilization and degradation in polluted sites are affected by a number of mechanisms, and the relationship between them is not always clear. (Cavelan et al., 2022; Sookhak Lari et al., 2018). Understanding the mechanisms that influence LNAPL mobilization and cleanup processes has therefore been a key research objective in recent decades (Alazaiza et al., 2020; Blodau & Moore, 2003; Dobson et al., 2007; R. Ismail et al., 2020).

A few previous research suggests that the biogeochemical and microbiological dynamics of subsurface environment are altered by fluctuating redox conditions (Rezanezhad et al., 2014; Zhang and Furman, 2021). Many biogeochemical processes in surface settings are regulated by reduction, which is the process of gaining an electron (e-), while oxidation is the process of losing an electron (e-) (Doktorgrades, 2017). Furthermore, reduction-oxidation (redox) processes usually occur concurrently and include the transfer of electrons and protons (H+) between the involved redox couples (Doktorgrades, 2017; Zhang and Furman, 2021). Oxidized and reduced species in a particular system governor the measurement of Eh or ORP which is calculated based on Nernst equation (Zhang and Furman, 2021). Temperature and pH may directly impact the Eh of a system, but they can also have an indirect effect on the ratio of the activity of the dominant redox couple's reduced and oxidized species (Zhang and Furman, 2021). The concentration gradients of electron donors and acceptors are of great relevance, since they are closely connected to many biogeochemical processes' paths, rates, and products. Besides geographical gradients, water table oscillations may generate considerable temporal differences in local redox conditions (Rezanezhad et al., 2014; Zhang and Furman, 2021). Subsurface biogeochemical cycling and the fate

of contaminants and nutrients are influenced by fluctuations in soil hydrology, which occur at different durations and at varied timescales (e.g. drying-wetting cycle) (Zhang and Furman, 2021).

Natural and human-made factors both contribute to seasonal fluctuations in the nearby unsaturated and saturated zones (Meng et al., 2021). Groundwater level oscillations may become more dramatic during the next century, depending on local climatic circumstances, as a result of changes in rainfall strength and frequency, as well as increased usage of water resources (Cavelan et al., 2022; Nygren et al., 2020). This environment may have a significant influence on the mobilization of LNAPL, the duration of contamination, and the danger to downgradient receptors (Cavelan et al., 2022). Dissolution, volatilization, and transverse migration of dissolved LNAPL components are restricted in stable water table conditions due to the slow vertical dispersion and diffusion of dissolved LNAPL compounds (Cavelan et al., 2022; Dobson et al., 2007; P. K. Gupta et al., 2019). The movement of water table results in the movement and distribution of LNAPLs, particularly in the vertical direction (Alazaiza et al., 2021; Dobson et al., 2007). Moreover, groundwater table fluctuations cause entrapment air, which affects the hydraulic parameters of the unsaturated zone and the biogeochemical state of the groundwater (Haberer et al., 2012).

In addition, it is anticipated that there will be a few degrees Celsius increase in the mean temperatures of both the surface water and the groundwater in the near future (Cavelan et al., 2022). The temperature-dependent processes of mobilization and biodegradation have the ability to change the way that LNAPL elements are partitioned and released into the atmosphere and groundwater (Cavelan et al., 2022). NAPLs have the ability to either attach themselves to soil particles, evaporate into the air, or disintegrate in groundwater (Fan, 2010). Moreover, successful remediation planning is heavily reliant

on our understanding of the aquifer's structure (i.e., porosity and permeability) (Di Palma et al., 2017). Because of all these factors, a comprehensive understanding of the ways in which environmental conditions influence the path taken by a pollutant at a particular site is mandatory for the remediation process to be successful. Environmental characteristics such as temperature variances, pH fluctuations, changes in water table dynamics, and alterations in soil moisture content are often what distinguish difficult contaminated areas (Haberer et al., 2015). Seasonal shifts in shallow soil-water temperatures are anticipated for the majority of contaminated sites, and these shifts have the potential to influence the properties of hydrocarbons, as well as their rates of breakdown and mass transfer, as well as the microbial activity in soil (Brijesh K. Yadav et al., 2012). Due to a decrease in BTEX volatilization and a decrease in water solubility, low temperatures inhibit the BTEX breakdown process. On the other hand, elevated temperatures improve the solubility and bioavailability of BTEX compounds (Brijesh K. Yadav et al., 2012). When temperatures rise, the ability of soil particles to absorb organic material decreases, giving more bacteria the opportunity to decompose the substance. In addition to this, the temperature plays a role in determining the number of microbes that are responsible for hydrocarbon breakdown (Brijesh K. Yadav et al., 2012).

Several investigations, both experimental and computational, have been carried out in order to look into the impact that the dynamics of a fluctuating water table and capillary fringe (Dobson et al., 2007; P. K. Gupta et al., 2019; P. Gupta & Yadav, 2017; X. Huang et al., 2021; Teramoto & Chang, 2017; Van De Ven et al., 2021). There is a lack of research that focuses on the alteration of redox conditions and the soil hydrogeochemical properties in the presence of LNAPLs.

The primary goal of this research was to examine the effects of WTF and its intensity,

soil layering, and temperature, on the fate of LNAPL in the smear zone, under anaerobic reducing condition. Five automated controlled soil columns, one under stable conditions and four under fluctuation conditions, were employed over the period of 150 days. The use of various statistical techniques aids in the understanding of large data matrices to better explain the water quality and ecological status of the studied systems, enables the identification of potential factors/sources that influence water systems, and provides a valuable tool for reliable water resource management (Shrestha and Kazama, 2007). In this experiment, the distributions of hydrocarbon pollutants and hydrogeochemical parameters were investigated in five columns polluted with petroleum hydrocarbons (BTEX) under anaerobic conditions, and the analysis carried out using Kruskal-Wallis test for the individual parameters and Kendall correlation to find if there any connection between the hydrochemical properties and BTEX concentrations in the columns.

5.2 Experiment Setup

In a manner identical to that shown in Figure 1, five sets of columns, including one soil column and one equilibrium column, were built. One of the columns was operated under a steady state condition, and four columns were operated under transient water table condition in a range of soil surface (0 cm) to -40 cm.

Table 3 shows the specifications of each column. The stable column (S), and the Fluctuating column 1 (F1) contain homogenized soil, while the fluctuating columns 2, 3, and 4 (i.e., F2, F3, and F4) contains heterogenous soil. Moreover, the fluctuating columns 3 and 4 (i.e., F3, and F4) has higher temperature to represent groundwater temperature in the state of Qatar (Ahmad et al., 2020; Ngueleu et al., 2018).

Columns were originally filled with non-contaminated soil and injected with synthetic groundwater before adding BTEX (Benzene, Toluene, Ethylbenzene, and Xylene). The

water table in the soil columns was originally set at -25 cm below the soil surface by altering the head of water in the equilibrium column. At 5 cm above the water table (-20 cm), a total of 10 ml of BTEX were injected which contains, 2.5 ml of liquid Benzene (99.9+%, Sigma-Aldrich, Canada), 2.5 ml of liquid toluene (99.9+%, Sigma-Aldrich, Canada), 2.5 ml of Ethylbenzene (99.9+%, Sigma-Aldrich, Canada), and 2.5 ml of xylene (99.9+%, Sigma-Aldrich, Canada). The BTEX was injected in the soil to create an LNAPL pool above the water table. The water level in the equilibrium columns was used to manage the imposed water regime, and the water level in the equilibrium column was determined by pump channel.

The soil columns were saturated with anoxic synthetic groundwater prior to the commencement of the experiment. During the first 24 hours of the experiment, pump channel A was used to fill the equilibrium columns with synthetic groundwater. 2 L Tedlar bags filled with argon gas were connected to the equilibrium columns to offer hydraulic elements of water fluctuation and collect gas samples. The anaerobic conditions were achieved by continuously purging the equilibrium columns to a DO concentration < 0.8 mg L-1.

Each drainage-imbibition cycle lasted 5 days, with an average flow rate of 0.244 mL min-1 in both directions The experiment was performed for a total of 150 days.

Table 3: Water table Column's characteristics

column	symbol	Soil	Porosity (%)	temperature	Imbibition Drainage Cycle (Days)
Stable	S	homogenized	22	22±2 ℃	N/A
Fluctuating 1	F1	homogenized	22	22±2 ℃	5
Fluctuating 2	F2	layering	22	22±2 ℃	5
Fluctuating 3	F3	layering	21	32±2 ℃	5
Fluctuating 4	F4	layering	21	32±2 ℃	10

Samples were collected from the stable columns each 5 days from the middle port (-30 cm (B)) and each 10 days from the top (-10 cm (A)) and bottom ports (-50 cm(C)). Whereas effluent aqueous samples were collected from the fluctuating columns after each drainage or saturation period (5 days) from the middle and bottom for organic concentrations by Gas chromatography (GC), Ion chromatography (IC), Dissolved inorganic carbon (DIC), pH, ORP, and Electric conductivity (EC) analyses. At the beginning of sampling process, 2 ml were collected from the ports for GC analysis, followed by the measurement of DO, ORP, pH, and EC using OrionTM Versa Star ProTM Benchtop Meter (Thermo Scientific, USA) to avoid degassing or oxygen ingress reactions. 15 ml of samples were taken for DIC and IC.

5.3 Results and Discussion

5.3.1 Pore water geochemistry

Before beginning the experiments, the porosity of the packed soil samples that were placed in each of the five soil columns was evaluated by means of the volumetric method in a matter similar to section 4.3.1. The results indicated that the average porosity of the soil in the stable groundwater level column, S1, was 22%, while the average porosity of the fluctuated water level column, F1, F2, F3, and F4 are an average

porosity of 22%, 22%, 21%, and 21% respectively. It is possible that the human compaction of the soil in each column is primarily responsible for the very minor differences in porosity that can be found between the five columns. Water table and redox regimes. Figure 10 shows the oxidation reduction potential (ORP) values for all five soil columns (i.e., S, F1, F2, F3, and F4). ORP values observed at the middle and the bottom of the columns prior to the beginning of the experiment ranged between 0 and 100 mV in all soil level columns (i.e., S1, F1, F2, F3, and F4), which is considered at oxidized and weakly reduced state (Reddy and DeLaune, 2008). When BTEX injected into the columns, ORP values at the middle (depth B) of the columns fluctuated during the experiment, mostly under weakly reducing condition (Reddy and DeLaune, 2008; Zhang and Furman, 2021). It is possible that the presence of LNAPL is responsible for the impact that causes the ORP to be greater in the middle (depth B) of the fluctuating columns compared with the bottom part (depth C). This finding can be confirmed by looking at the middle of the stable column (S) compared with the fluctuating column 1 (F1), as the rise and drop of the water table in F1 distributed LNAPLs throughout the column and resulting in ORP reduction at 110, 100 days for S, and F1, respectively. Haberer et al., (2012), Rezanezhad et al., (2014), Wang et al., (2014), and Meng et al., (2021), they demonstrated that the ORP measured at a particular depth varies cyclically with the fluctuations of the water level as ORP species has the potential to migrate along with the water table (Fan, 2010).

Examine the effect of soil layering by looking at the fluctuating columns F1 and F2. The ORP reaction in column F2 was not difference from the column F1, reaching the weakly reducing condition after 120 days compared with 100 days for F1.. Comparing the fluctuations columns F2 and F3 to observe the influence of temperature, the trend of ORP values of both columns was close until at around 70 days from the beginning

of the experiment when ORP values of F3 dropped drastically at 100 days. As known from the Nernst equation, temperature has a direct effect on ORP, but in this context, the difference seems to occur later.

The influence of water fluctuation intensity is examined by comparing the fluctuated columns F3 and F4, both columns have temperature in a range of 32°, ORP values for both columns (F3 and F4) started at ~ 100 mV, but went in opposite directions, for F3 it increased, while for F4 it decreased and F4 reached the weakly reducing (200 – 400 mv) condition at 20 days. Regular purging of the columns with argon gas was conducted to eliminate oxygen (O2). The decreased Oxidation-Reduction Potential (ORP) values observed in the low-intensity water table fluctuation (WTF) column F4 provide evidence that oxygen may have infiltrated the columns, thereby increasing the ORP values. At the bottom of the columns (depth C), the ORP values exhibited fluctuation within the weakly reducing range during the first 60 days for all columns. However, in the case of the columns F3 and F4, the ORP values subsequently fluctuated within the moderately reducing condition. This suggests that circumstances conducive to anaerobic respiration have developed in each and every soil column (Ismail et al., 2020; Shafieiyoun et al., 2020; Meng et al., 2021).

Soil layers with different permeability levels influence the movement of electrons therefore affecting redox conditions. Layers with higher permeability allow for oxygen diffusion. In contrast, low permeability layers can restrict oxygen diffusion, leading to anaerobic conditions and lower ORP values. However, in the case of the columns F2, F3, and F4, the regular injection of the argon gas maintained the anoxic condition in the high permeability layer at the bottom. Furthermore, the temperature of the columns is the most influential factor affecting the ORP values. Statistical analysis of the ORP values in the five columns (i.e., S1, F1, F2, F3, and F4) is conducted by using Kruskal-

Wallis test. Kruskal-Wallis test is used as the data violated the normality test assumption. The results of the statistical test showed that the p-value for ORP values at the middle of the five columns is equal to 0.047 which is < 0.05 (significance value), which implies that there is significant difference between the ORP values, while the p-value for ORP values at the bottom of the five columns is equal to 0.0032 which is < 0.05 implies that there is statistical difference between the ORP values of these columns. Similar findings were confirmed by Haberer et al., (2012), Rezanezhad et al., (2014), Wang et al., (2014), and Meng et al., (2021), they demonstrated that the ORP measured at a particular depth varies cyclically with the fluctuations of the water level.

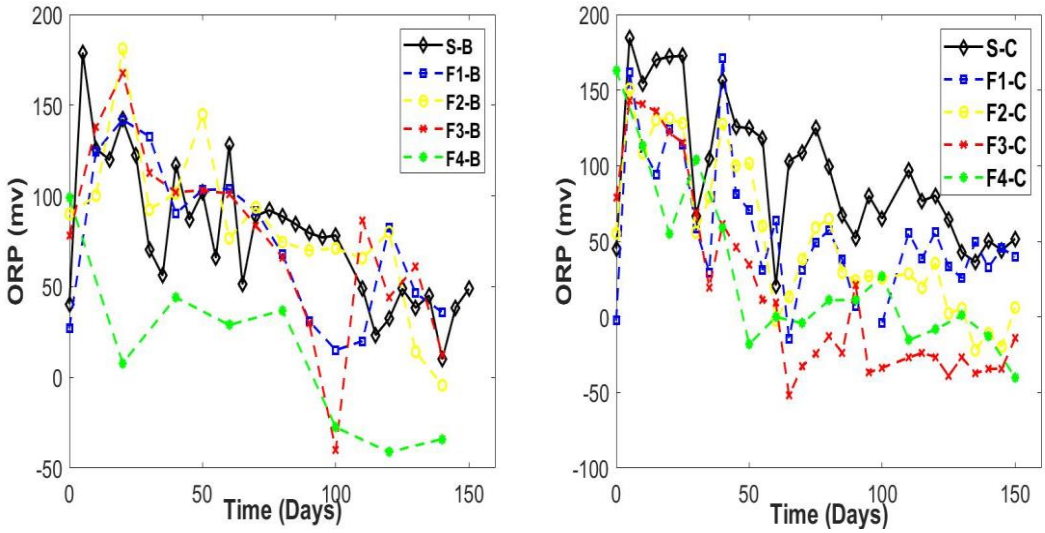

Figure 10: ORP values at (left) the middle (depth B) and (right) the bottom (depth C) of the columns S, F1, F2, F3, and F4.

5.3.2 Electrical Conductivity (EC)

The ionic strength of the pore water and the extent to which the groundwater has been ionized are both reflected in the electrical conductivity of the groundwater. The electrical conductivity (EC) values that were measured in the middle (i.e., depth B) and the bottom (i.e., depth C) of soil columns are shown in Figure 11. These values were

obtained under a variety of experimental conditions. To observe the influence of water table, stable column S was compared to the fluctuation column F1, at the middle of the columns, EC for the S was fluctuated in a lower range than F1, while F1 started at 5000 μS cm^{-1} and decreased to ~ 4000 μS cm^{-1} by the end of the experiment. There is no obvious change in EC values at the bottom (depth C) of the stable column (S), as opposed to the center, where LNAPLs are present. The fluctuations in EC values in the stable columns (S), can be a result of the movement of clean groundwater entering the column from the bottom following sampling. Comparing the fluctuating columns F1 and F2 to observe the influence of soil layering. For the middle of the columns (depth C), these two columns have an inverse effect on the EC values, as F1 started at higher concentration of 5000 μS cm^{-1} and increased, while F2 started at a lower concentration of ~3100 μS cm^{-1} and decreased. The low initial concentrations of EC at the columns F2 are the result of the lower permeable layer at this location. The permeable layer contains less water leads to lower electrical conductivity since dissolved ions in water are the main factor influencing electrical conductivity. Furthermore, this layer has higher BTEX concentrations compared with F1 which will results in lower soil dissolution and thus lower EC value (DeRyck et al., 1993; Flores Orozco et al., 2012). Comparing the fluctuations columns F2 and F3 to observe the influence of temperature, it is evident higher temperature is correlated with EC values as these two columns have similar trend but with higher values for the column F3. Atekwana and Atekwana, 2010 suggested that a rise in temperature has the potential to influence a wide range of geophysical properties which increase the bulk electrical conductivity. During the course of the experiment, that temperature maintained the EC values at a consistent level, in contrast to the EC values of the other columns (Figure 11).

The influence of intensity of the fluctuation of the water table is examined by

comparing the fluctuated columns F3 and F4, both columns have temperature in a range of 32°, EC values for both columns is higher than the rest of the water table columns (i.e., S, F1, and F2), but F4 has lower EC values compared with F3 implying that the slower water table decreased EC values. Previous research has shown that sediments impacted by hydrocarbons generally exhibit a decrease in electrical conductivity as the presence of BTEX contaminants displace pore water which led to a decrease in the measured electrical conductivity values. However, it is important to note that studies on aged hydrocarbons have revealed contrasting results. In some cases, an increase in measured electrical conductivity has been observed due to the development of porosity and mineral weathering caused by carbonic and organic acids released by bacteria due to the degradation of BTEX (Flores Orozco et al., 2012)

Utilizing these data, a statistical study of the change in EC values is carried out using the Kruskal-Wallis test. The results of the statistical analysis can be found in Figure D 2. The p-value for the EC values at the middle of all columns S1, F1, F2, F3, and F4 is found to be equal to $3.119e^{-10}$ which < 0.05 implying that there are statistical differences between EC values of these columns. Furthermore, the p-value at the middle of only fluctuating columns is $0.008 < 0.05$ confirming the differences between the columns. (E. A. Atekwana & Atekwana, 2010) reported that changes in pore fluid conductivity can be attributed to both hydrologic and microbiological processes. These processes can affect the electrical conductivity of the pore fluid in different ways. The hydrological process such as advective flow due to water table fluctuation. Furthermore, Some researchers suggested that bacterial activity causes an increase in the electrical conductivity of the region that is next to the contaminant (Knight, 2001). The ionic concentration of the pore fluid will shift due to both a reduction in the number of terminal electron acceptors and an increase in the number of redox species which

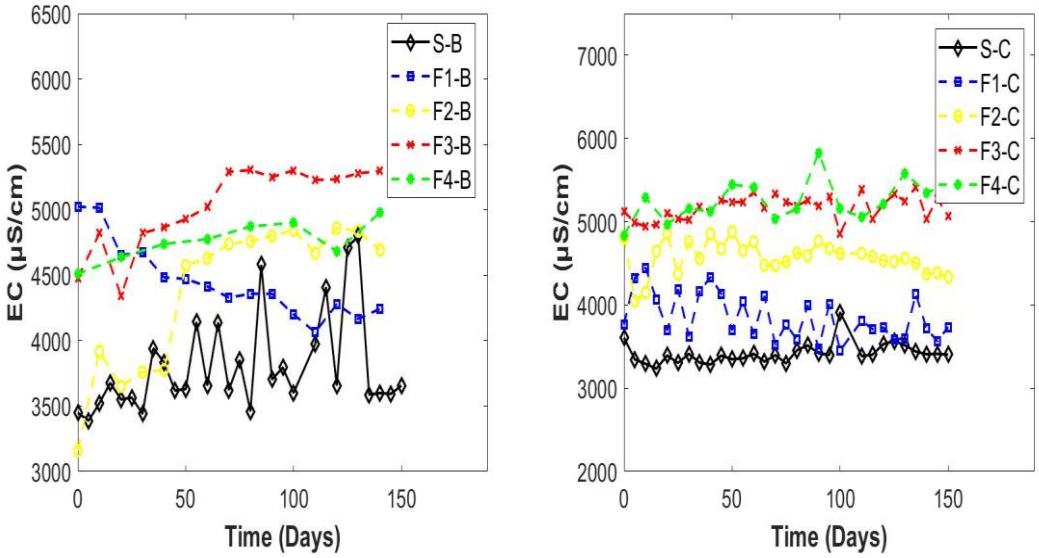

Figure 11: EC values at (left) the middle (depth B) and (right) the bottom (depth C) of the columns S1, F1, F2, F3, and F4

consequently would change EC (E. A. Atekwana and Atekwana, 2010). Cassidy et al., 2001; and Chaudhary and Vijayakumar, 2020 reported an increase in EC values due to the biodegradation process.

5.3.3 pH

Figure illustrates the pH values of all columns. The pH values at the middle (depth B) and bottom (depth C) of both the stable and fluctuated columns fluctuated between 7.2 and 8.4 throughout the duration of the experiment. A decrease in pH values occurs at the middle of the columns F1and F2 after 60 days, while for F3 it occurs after 80 days, while for F4, pH values fluctuated during the whole experiment. There have not been any differences in pH values that can be linked to any of the characteristics of these water table columns. The pH readings taken at the bottom (depth c) of the fluctuating columns (i.e., F1, F2, F3, and F4) seems to increase with saturation cycle and decrease with draining cycle, which was aligned with the observation made by (Rezanezhad et al., 2014). Another observations made by Rezanezhad et al., (2014) in his experiment

that pH values for the fluctuating water table column is broad than the stable water table column.

Kruskal Wallis statistical test was used to find if there are any statistical differences in pH values of the five columns (i.e., S1, F1, F2, F3, and F4). The results of the statistical test between the pH values at the middle (depth B) of the columns showed that P-values are equal to 0.3694 which is > 0.05 (the significant level). This result implies that there is no statistical difference in the pH values between the five columns, Thus, the data supports the conclusion that the pH values are similar across all the columns. The p-value for the statistical difference between the only fluctuating columns is equal to 0.1975 implies that there are no statistical differences between pH values.

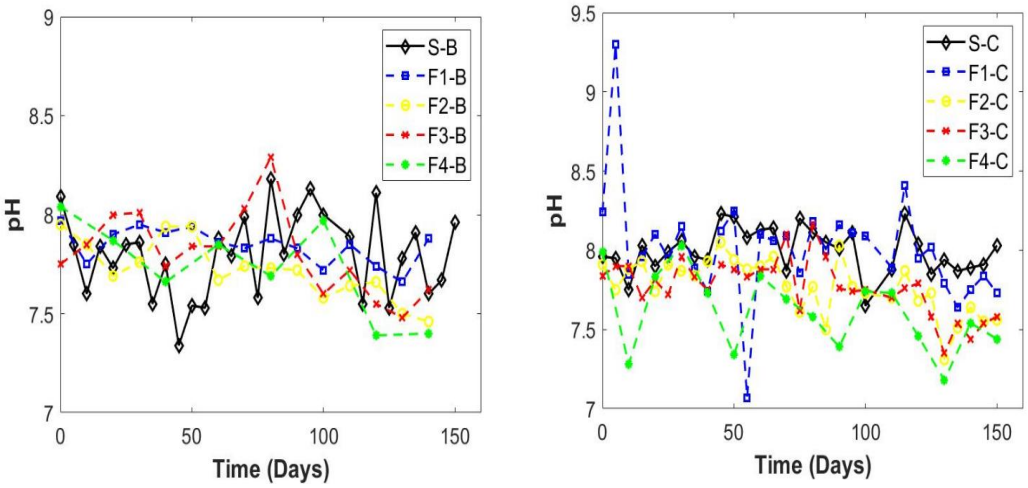

Figure 12: pH values at (left) the middle (depth B) and (right) the bottom (depth C) of the columns S1, F1, F2, F3, and F4

5.3.4 Concentration of electron acceptors

Cations and anions were measured using ion chromatography (IC). The IC results showed that the system had an aqueous phase comprising iron (Fe) and manganese (Mn) in very low concentrations, and sulfur (S) as well. The maximum iron (Fe) concentration detected in the columns as following S, F1, F2, F3, and F4 were 0.006,

0.531, 0.093, 0.013, and 0.531 mg L^{-1}, respectively. While for the manganese (Mn), it was detected in the columns as following 0.027, 0.017, 0.135, 0.893, and 0.197 mg L^{-1} for the columns S, F1, F2, F3, and F4, respectively. After 30 days from the beginning of the experiment, the concentration of iron (Fe) and manganese (Mn) were typically below detection limits. Greskowiak et al., 2005 in his work noticed that the reduction of Fe began along with Mn reduction, which can be the case here. The effect of water table regime and intensity, layering and temperature didn't have any effect on the concentrations of iron (Fe) and manganese (Mn).

Due to its high concentration in seawater, sulfate is easily accessible as a terminal electron acceptor for organic reduction in marine system (Wurgaft et al., 2019). Sulfate is a redox-defining species in the sequence of the terminal electron-accepting process (TEAP), with the reduction of sulfate taking place after the reduction of iron and before methanogenesis. Sulfate-reducing bacteria (SRB) derive their energy from the oxidation of organic molecules that are present in petroleum hydrocarbons, it is reducing sulfate (SO_4^{2-}) to hydrogen sulfide (H_2S). According to studies that were done in the past, sulfate reduction is responsible for the majority of all-natural anaerobic degradation, and it also the second most favorable electron acceptor in groundwater (Miao et al., 2012; Wei et al., 2018).

Sulfate concentrations were detected in large amounts at the middle (depth B) and the bottom (depth C) of all columns (Figure 13). The initial sulfate concentrations at the middle (depth B) of all columns are 100, 282, 134, 143, and 194 mg L^{-1} for S, F1, F2, F3, and F4, respectively. The effect of water table fluctuation is observed by comparing the columns S and F1, for the stable column (S) no change in sulfate concentration were detected during the experiment, while for the fluctuating column F1, the concentration of sulfate increased with the first imbibition cycle and then continued to decrease to

reach 50 mg L^{-1} by the end of the experiment decreased by 75% of the initial concentration. For the effect of soil layering, the fluctuating columns F1 and F2 were compared. It was observed that the peak concentration of sulfate in the column F2 was reached after the third imbibition cycle, unlike the column F1 which was reached after the second imbibition cycle. Subsequently, the concentration decreased by 75% and 34%, for F1 and F2, respectively. The presence of soil layering introduces variations in properties such as texture, porosity, and permeability within the soil profile. These variations can significantly influence the movement of water and solutes through the soil which create distinct flow pathways for water and solutes, including sulfate ions (Li et al., 2014). For column F2, due to the low permeable layer at depth B, sulfate ions may accumulate in this layer due to the leaching from the high permeability layer more rapidly.

For the effect of temperature, the fluctuating columns F2 and F3 were compared, similar to column F2, the concentration of sulfate in column F3 reached its maximum concentrations after the second imbibition cycle. The sulfate concentrations for both columns decreased by 34% and 12%, respectively of the initial concentration by the end of the experiment. Both columns have soil layering starting from a high permeable layer at the bottom of the columns to the very low permeable layer at the top of the columns. The concentration of sulfate in column F3 is slightly higher than F2 between 30 and 100 days. Temperature can have a significant impact on the redox species present in soil, including sulfate. For the effect of water table fluctuations intensity, the columns F3 and F4 were compared. The sulfate concentrations in the fluctuating column F4 increased slowly and reached a maximum after the fifth imbibition cycle and decreased by 3% by the end of the experiment. This is because slower fluctuations allow for more time for ion movement and redistribution within the soil profile, leading

to a more even distribution of ions. The increase in sulfate ions (SO_4^{-2}) observed at the middle depths is commonly attributed to the dissolution of gypsum which was also observed by (Rühle et al., 2015) as the presence of sulfate ions in groundwater has been attributed to the composition of native rock and soil, specifically limestone and gypsum (Ngueleu et al., 2019). A statistical study of the change in sulfate concentrations at the middle of the water table columns is carried out using the Kruskal-Wallis test. The results of the statistical analysis can be found in Figure A11. The p-value for the at the middle of the columns S, F1, F2, F3, and F4 is found to be equal to $1.522e^{-7}$ which < 0.05 implying that there are statistical differences between sulfate concentrations

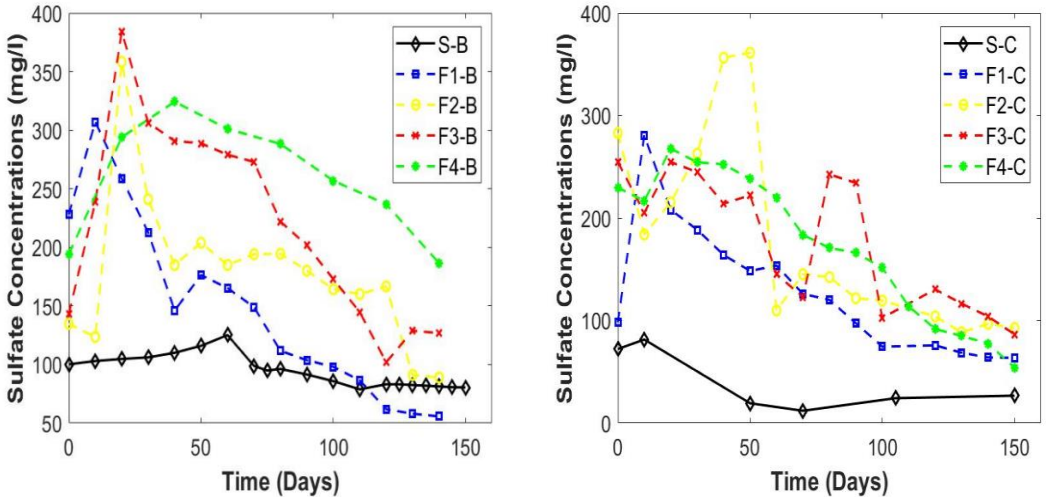

Figure 13: Sulfate concentrations at (left) the middle (depth B) and (right) the bottom (depth C) of the columns S, F1, F2, F3, and F4

during the experiment. Furthermore, the p-value at the middle of only fluctuating columns is 0.0046 < 0.05 confirming the differences in concentration between the columns.

5.3.5 Dissolved Inorganic Carbon (DIC)

The concentration of DIC can be used as a measure for determining the degree of organic carbon mineralization (Abell et al., 2009; Porowska, 2015) . The concentrations of DIC that were measured in the center of the soil columns during each imbibition

cycle are displayed in Figure 14. The initial DIC concentrations for all columns were 9.06, 30.2, 11.92, 13.32, 19.88 mg L^{-1}, for the columns S, F1, F2, F3, and F4, respectively. An increase in DIC concentrations occurred at around 100 days from the beginning of the experiment and at the same time of ORP reduction (Figure 10).

The results of the statistical analysis using the Kruskal-Wallis test can be found in Figure A12. The p-value for the statistical test at the middle of the columns S, F1, F2, F3, and F4 is found to be equal to $6.77e^{-5}$ which < 0.05 implying that there are statistical differences between DIC concentrations during the experiment between the columns. Furthermore, the p-value at the middle of only fluctuating columns is 0.0056 > 0.05 implying that there are no statistical differences between the DIC values at the middle of the fluctuating columns.

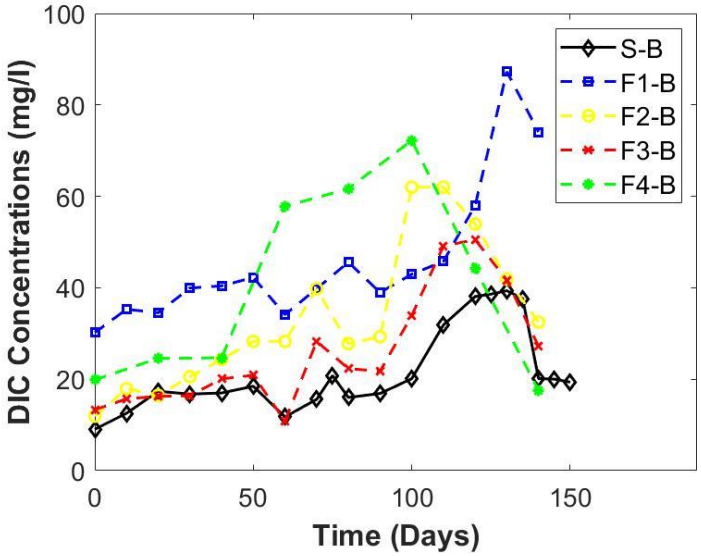

Figure 14: Dissolved Inorganic Carbon (DIC) at the middle (depth B) of the columns S, F1, F2, F3, and F4

5.3.6 Dissolve organics phase

The temporal concentrations for benzene, toluene, ethylbenzene, and xylene can be seen in supplementary material C (Figure C 1, Figure C 2, Figure C 4, and Figure C 3),

respectively. At the source zone in the middle of the columns, BTEX exhibited its highest concentrations at about 30 days following the injection in the stable column (S). On the other hand, in the fluctuating water table 1 and 2 (i.e., F1 and F2), the maximum concentration was observed at 20 days which correspond to the second imbibition cycle, while for the fluctuating columns 3 and 4 (i.e., F3 and F4), the maximum concentration was reached between 20 and 40 days, respectively, which correspond to the second and forth imbibition cycle.

It is noticed that the trend of BTEX concentrations in the fluctuating columns followed Kehew and Lynch, (2011), as they noticed that the increases and decreases in concentration follow with the longer-term shifts in the water table. This association will occur in the monitoring wells that are in the source zone. In the second type of pattern, the oscillations in the water table are not in phase with the variations in concentration, and in fact, they have an inverse correlation with the concentrations and that occur at the downgradient receptors. Cavelan et al., (2022); Dobson et al., (2007); P. K. Gupta et al., (2019) stated that the dissolution of the most soluble component accelerates the depletion of the LNAPL source zone, which reduces the time it takes for the LNAPL source zone to deplete. During the initial stages of their field monitoring Vaezihir & Molson, (2012) observed a correlation between water table fluctuations and LNAPL thickness. However, as the monitoring progressed, this relationship weakened. Despite the rise in the water table, there was no significant increase in the thickness of the LNAPL phase. As a result, the decrease in LNAPL thickness detected in the monitoring wells suggests a reduction in the overall mass of LNAPL present.

5.3.7 Correlation between the hydrogeochemical parameters of dissolved organics

For the experimental condition, LNAPLs which refer to benzene, toluene, ethylbenzene, and o-xylene were under completely saturated condition in the stable

column. Whereas the conditions of the LNAPLs in the fluctuating columns were continuously cycling between being saturated and unsaturated. The Kendall tau correlation test is used to test the correlation between the concentration of hydrogeochemical indicators (pH, ORP, EC, sulfate concentrations, and DIC) and the concentration of benzene, toluene, ethylbenzene, and o-xylene in the stable water table columns (i.e., S), fluctuating water table 1 (i.e., F1), fluctuating water table 2 (i.e., F2), fluctuating water table 3 (i.e., F3), and fluctuating water table 4 (i.e., F4). The correlation criteria are found in

Table 4. The only correlation that will be discussed in the next section is the statistically significant one, where p-value is < 0.05. In statistics, the degree to which two or more variables change in parallel is quantified by the measure of correlation. When two variables are positively correlated, their changes tend to occur simultaneously; when the correlation is negative, one variable increase while the other decreases.

5.3.7.1 Dissolved phase benzene correlation

The correlation between benzene concentrations at the middle of all columns and the hydrogeochemical indicators can be seen in Figure 15. Reporting only the statistically significant data, For the stable column (S), the concentration of benzene has strong positive correlation with sulfate concentration and positive moderate correlation with ORP, and negative moderate correlation with DIC and it is statistically significant. The positive correlation with sulfate and ORP was a result of the no change in concentration observed in the middle of the stable column for all of these parameters. For the fluctuating column 1 (F1), the correlation is moderate positive with pH and ORP, while it is strong positive correlation with EC, and sulfate concentrations. While the correlation with DIC is moderate and in the negative direction. For the fluctuating

column 2 (F2), benzene has a strong positive correlation with pH, a moderate sulfate concentration and ORP, a strong negative correlation for EC and DIC. For the fluctuating column 3 (F3), a weak positive correlation between benzene and pH, and a moderate positive correlation for sulfate concentration, and strong positive correlation for ORP. On the other hand, benzene has a negative moderate correlation with DIC, and negative strong correlation with EC. For the fluctuating column 4 (F4), benzene has moderate positive correlation with sulfate concentrations, and it is the only statistically significant.

5.3.7.2 Dissolved phase Toluene correlation

The correlation between toluene concentrations and the hydrogeochemical parameters is found in Figure . For the stable column (S), the only statically significant correlation is found to be with ORP and sulfate concentrations which is positive moderate correlation. For the fluctuating column 1 (F1), toluene has no correlation with pH, moderate with ORP, and EC, while with sulfate concentrations it is strong correlation. On the other hand, the correlation with DIC is negative moderate correlation. For the fluctuating column 2 (F2), toluene has a positive moderate correlation with pH, ORP, and sulfate concentrations, while the correlations with DIC are negative moderate and with EC it is negative strong correlation. For fluctuating column 3 (F3), the correlation is positive moderate with pH and ORP, and strong with sulfate concentrations, while the correlations with EC, and DIC is negative moderate correlation. For the fluctuating column 4 (F4), the only statistically significant is the correlation with sulfate concentration which is positive moderated correlation.

Toluene concentrations in the middle of all water table columns (S, F1, F2, F3, and F4) are positively correlated with sulfate concentrations. The association between the columns F1 and F3 and toluene is strong, whereas the correlation between columns S,

F2, and F4 is moderate. It's also important to note that ORP is moderately correlated with toluene at the columns S, F1, F2, and F3, and if we look at Figure 16, it is noticeable that ORP reduction, sulfate concentration decrease, and the decrease in toluene concentration are all correspond with each other's. DIC and toluene has a negative moderate correlation at the fluctuating columns F1, F2, and F3,

5.3.7.3 Dissolved phase Ethylbenzene correlation

The correlation between ethylbenzene concentrations and the hydrogeochemical parameters is found in Figure 17. For the stable column (S), the concentration of ethylbenzene has moderate positive correlation with sulfate concentrations and ORP and it is the only statistically significant. For the fluctuating water table column 1 (F1), ethylbenzene concentrations have positive weak correlation with pH, and ORP, and moderate with EC, while with sulfate concentrations it is strong correlation. On the other hand, the correlation with DIC is negative moderate correlation. For column F2, the correlation is positively weak with pH, ORP, and the concentrations of sulfate. On the other hand, the correlation with EC, and moderate correlation with DIC is. For column F3, the correlation is positively moderate with ORP, and sulfate concentrations, while it is strong with pH. On the other hand, the correlation is moderate with EC and DIC. For column F4, only sulfate concentration is statistically significant, and it is a strong positive correlation.

5.3.7.4 Dissolved phase xylene correlation

The correlation between xylene concentrations and the hydrogeochemical parameters is found in Figure . For the stable column (S) and the fluctuating water table column 1 (F1), the concentration of xylene has moderate positive correlation with ORP, and sulfate concentrations and it is the only statistically significant parameters. For the fluctuating water table column 2 (F2), the correlation is positive weak with sulfate concentrations and moderate with pH and ORP, while it is negatively positive with EC,

and strong with DIC. For the fluctuating water table column 3 (F3), the correlation is positive moderate with pH and ORP and strong with sulfate concentration. While the correlation is moderate with EC and DIC. For the fluctuating water table column 4 (F4), the only statistically significant correlation is with ORP and sulfate concentrations which is positive moderate correlation.

5.3.7.5 Discussion of the Correlation Results

There are two possible interpretations for the strong and moderately positive association that exists between BTEX concentration and sulfate concentration in all water table columns (S, F1, F2, F3, and F4). Starting from the stable column (S), the correlation with sulfate concentration is strong, moderate, and moderate positive with benzene, toluene, ethylbenzene, and xylene, respectively. This correlation is the result of small changes that occur in both BTEX and sulfate concentrations. It is a result of BTEX dissolution as it is the only transport mechanism for stable water table (Cavelan et al., 2022; Brijesh Kumar Yadav and Hassanizadeh, 2011). Furthermore, the movement of synthetic groundwater within the column system can contribute to the accumulation of sulfate at the middle depth (depth B) of the column. During the sampling process, synthetic groundwater from the bottom of the columns is moved to the top, which can result in the accumulation of sulfate in the middle. This movement of synthetic groundwater, combined with the dissolution of BTEX, can contribute to the observed correlation between BTEX and sulfate concentrations. This argument can be supported by a decrease in sulfate concentrations at the bottom (depth C) of the stable column (see Figure 13). In addition to this, the sulfate concentration pattern in the stable column, as well as the Ca^{2+} and Mg^{2+} concentration patterns, might provide support to this theory (Figure C 5). In a trial that was quite comparable to this one but was free of contamination, Rezanezhad et al., (2014) found that the solid-phase concentrations of

elements such as iron, manganese, and others are higher in the first 30 cm of the stable column, but decrease with increasing depth due to the movement of water from the bottom of the columns. The strong correlation with benzene concentration can be a result of its high dissolution rate and higher solubility in water (Kim et al., 2008; Njobuenwu et al., 2005), which occurs due to increase contact time. Another explanation for this correlation might be a consequence of enhanced biodegradation at this location of the column, particularly when it is accompanied with a positive correlation with ORP and a negative correlation with DIC (Figure 15, Figure 16, Figure 17, and Figure 18).

For the fluctuating columns F1, F2, F3, and F4, soil homogeneity varies over the four columns, with homogenized soil found in F1 and heterogeneous soil in F2, F3, and F4. By comparing solely homogeneous and heterogeneous soil (F1, and F2), it can be observed that homogeneity has a greater impact on the dissolution of BTEX and the flow of sulfate through the column, particularly in the layered column F2 where BTEX-injected at lower permeability soil. Johnston and Trefry, (2009) demonstrates that the layer variability has an influence on the initial vertical distribution of LNAPL, while the source zone layer does not have such a significant influence on the LNAPL recovery rate. Rather, the most influential factors are media properties around the water table that are farther from the well. On the contrary, Zanello et al.,(2021) proposed that both xylene and ethylbenzene have a tendency to be concentrated in close proximity to the source zone. Both of these factors can account for the discrepancies in correlation between the columns F1 and F2.

By increasing the temperature in the fluctuated column 3 (F3), ethylbenzene and xylene correlation become significant, implying higher groundwater temperature has an effect on hydrocarbon desorption. Shi et al., (2020) in their experiment, suggested that

temperature changes impacts Petroleum Hydrocarbon partitioning in soil pore water, which enhance the degradation. It can also alter the distribution and the diffusion rate of organic pollutants in the soil by decreasing the interfacial tensions, viscosity, and density of the LNAPL (Cavelan et al., 2022; Colombano et al., 2020; Brijesh Kumar Yadav and Hassanizadeh, 2011).

In fluctuating column 4 (F4), the magnitude of water table fluctuation is slower than the fluctuating column 3 (F3), which allows us to compare based of water fluctuation intensity. For F4, no obvious change is noticed in the correlation between BTEX and sulfate concentration. The soil texture and vertical spatial variability is significantly impact soil hydraulic characteristics and the distribution of water and contaminants throughout the soil profile (Johnston and Trefry, 2009; Li et al., 2014). When the fluctuating water table moved to the upper and lower portions of the column during the imbibition and drainage cycles, it redistributed BTEX and sulfate vertically, which explains the increase in BTEX and sulfate concentrations at the second and third imbibition cycles for the fluctuating columns (F1, F2, F3, and F4) (Supplementary Materials C). Kehew and Lynch, (2011) stated that sulfate can be carried as far as 1.75 meters below the water table.

Water table fluctuations accelerate advective transport of soil and LNAPLs gases in the USZ in the transition zone. Numerous scholars have explained how variations in groundwater level affect the vertical mobility and spatial distribution of NAPLs within an aquifer (Alazaiza et al., 2020; Dobson et al., 2007; Kehew and Lynch, 2011; Lee et al., 2001; Van De Ven et al., 2021).

Another positive moderate correlation is found between BTEX concentrations and ORP. As can be seen from the results it mostly comes with sulfate concentrations. It been seen in all columns except the fluctuating column 4 (F4). To explain ORP

correlation, look at (Figure 10), sulfate concentrations (Figure 13), and BTEX concentrations (Supplementary Materials C). At 80 days, a significant decrease in ORP is found in the middle of F1, F3, and F4, associated with decreases in sulfate and BTEX concentrations and a corresponding increase in DIC. Number of studies has linked ORP and organics degradation, where sulfate-reducing bacteria is capable of degrading LNAPLs such as BTEX (Meng et al., 2021; Shafieiyoun, Al-Raoush, Ismail, et al., 2020; Wei et al., 2018). According to Reddy and DeLaune, (2008), and Zhang and Furman, (2021) the middle of the fluctuating columns are under weakly and moderately reducing condition. On the other hand, the negative correlation with sulfate and BTEX concentration decrease can be an evidence for hydrocarbon degradation, where sulfate-reducing bacteria is capable of degrading benzene, toluene, and xylene (Wei et al., 2018). In a flow through reactor experiment, Shafieiyoun et al., (2020) found that the increase in DIC concentration is coincident with reducing condition which attributed to the mineralization of petroleum hydrocarbon.

5.4 Conclusion

The influence of water table fluctuation on Benzene, toluene, ethylbenzene, and xylene were studied under controlled experimental circumstances, as well as how it affects soil hydrogeochemical characteristics and natural attenuation. ORP values in the middle columns varied cyclically with WTF and promoting reducing conditions. In reverse, soil layering lowers the enhancement of reducing conditions as LNAPLs are present in low permeability layer, same as the slower fluctuation's intensity. while temperature increase ORP reduction. The statistical test indicated that middle and bottom ORP values are statistically different. EC values were affected greatly by fluctuation and temperature. The p-value for the statistical test is $3.119e^{-10} < 0.05$ implying that there are statistical differences between EC values of these columns. The pH for the five columns fluctuated in the same range. The statistical test for pH values at the middle of

the columns showed that P-value is 0.3694 > 0.05 which confirm that no statistical difference in the pH values between the five columns.

The influence of WTF on sulfate concentrations was found by comparing S and F1. F1 has a significant concentration decrease as compared to S, while for soil layering the decrease in F1 is greater than F2. Increasing temperature and soil layering in F3 has the opposite effect on sulfate concentration, and slow fluctuation intensity in F4 as well. The statistical test indicated that sulfate findings are significantly different (p=1.522e-7 < 0.05). A correlation between BTEX and sulfate concentrations is stable column might be due to dissolution and diffusion, whereas sulfate accumulates in the middle due to sampling. Soil homogeneity reduces the correlation between BTEX and sulfate, while temperature seems to increase even though the same layers exist. The association between BTEX and sulfate concentrations, when combined with a positive correlation with ORP and a negative correlation with DIC, may indicate an increase in biodegradation in the columns.

Table 4: Correlation values and criteria

Value	Correlation criteria
0-0.19	Very weak
0.2-0.39	weak
0.40-0.59	moderate
0.6-0.79	strong
0.8-1	Very strong

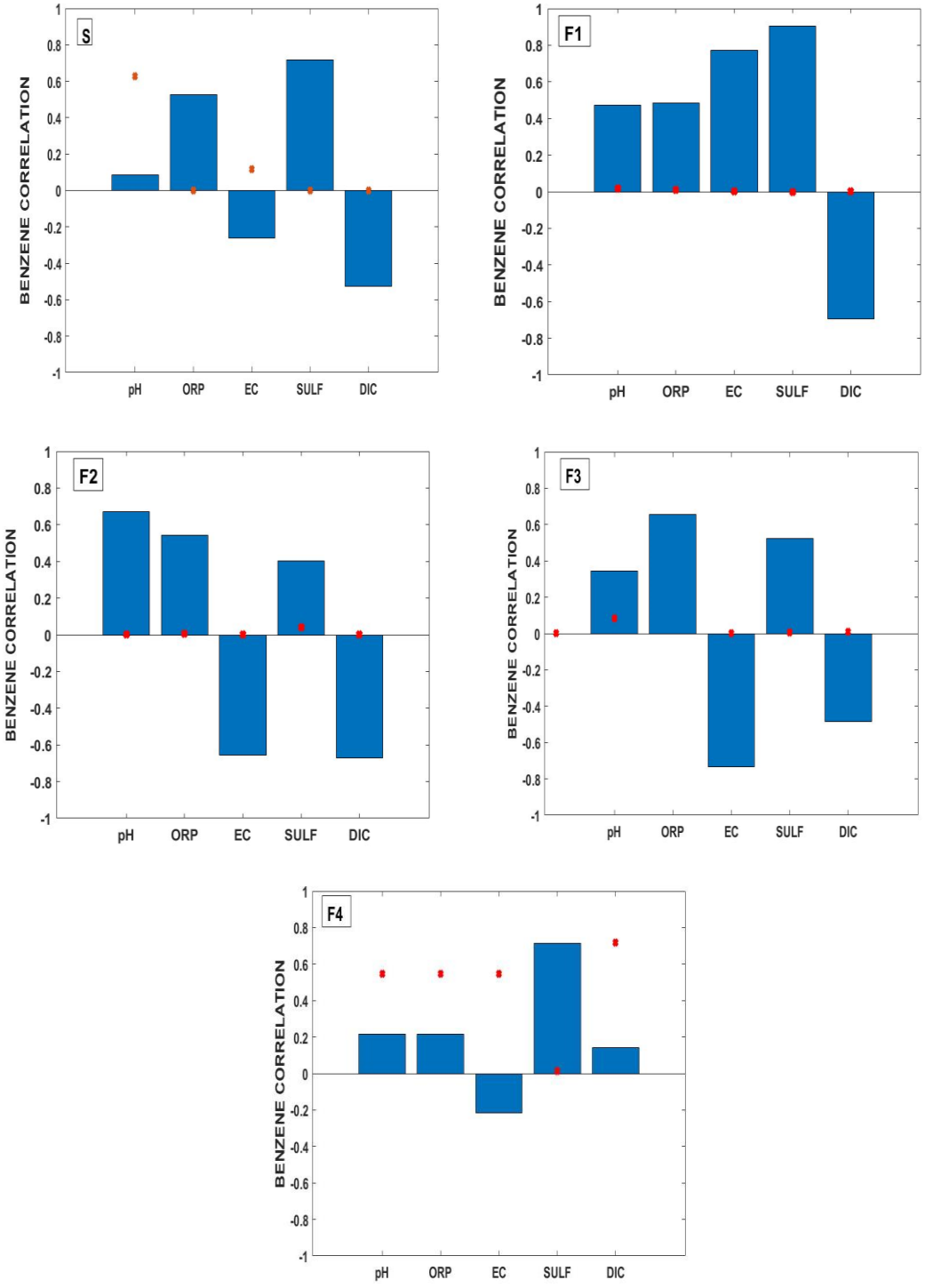

Figure 15: Benzene Correlation with pH, ORP, EC, sulfate concentrations, and DIC at the middle of the columns S, F1, F2, F3, and F4

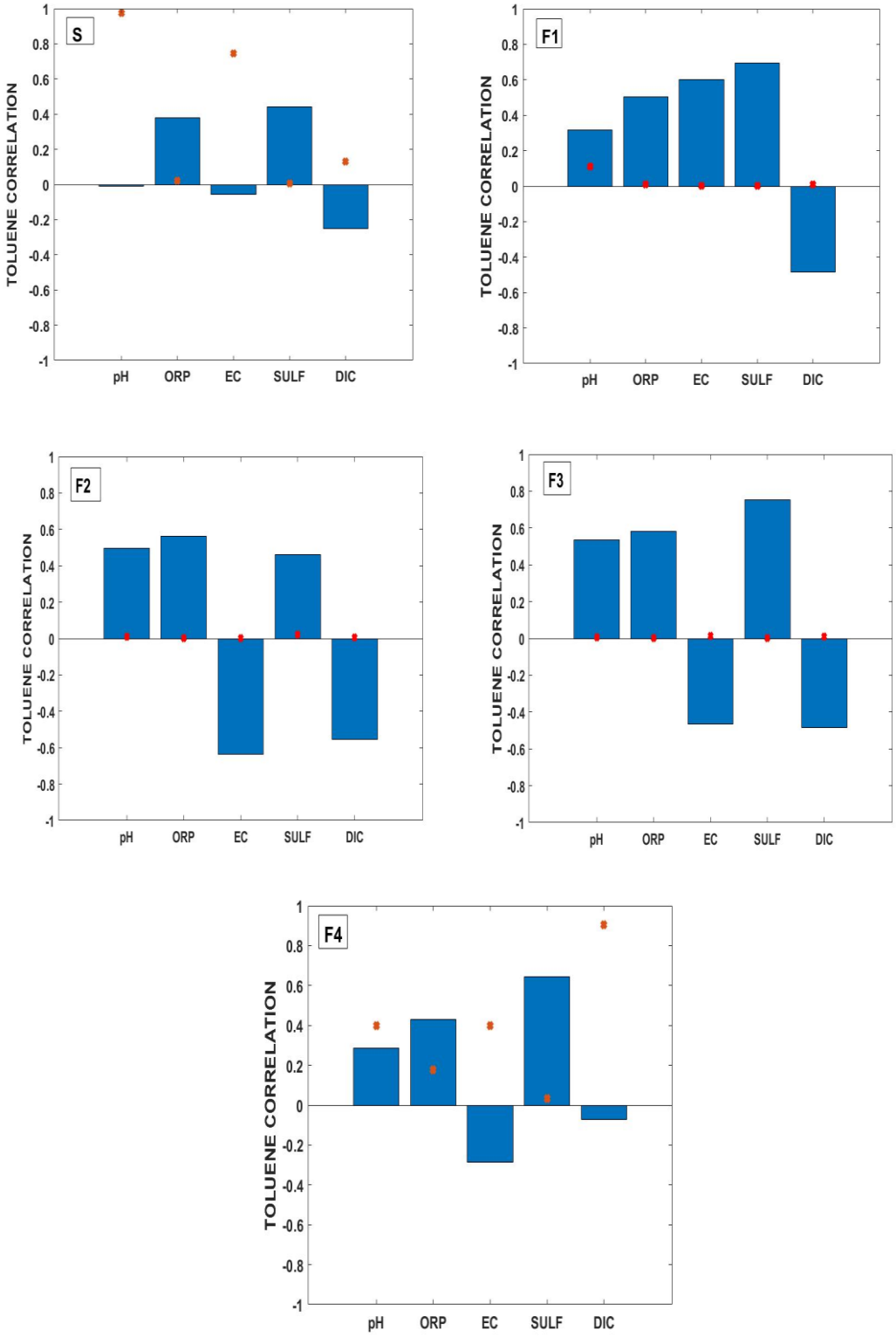

Figure 16: Toluene Correlation with pH, ORP, EC, sulfate concentrations, and DIC at the middle of the columns S, F1, F2, F3, and F4

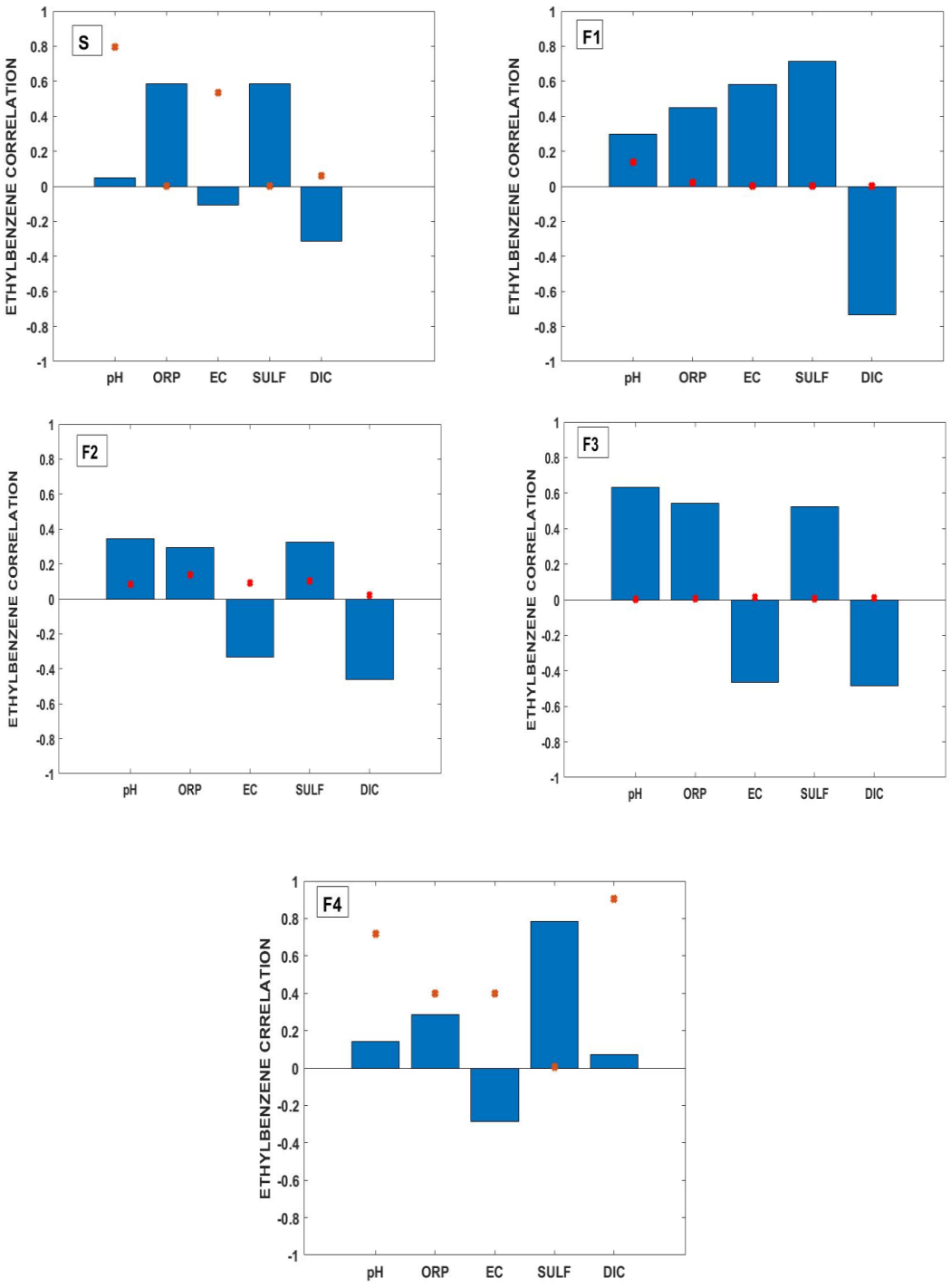

Figure 17: Ethylbenzene correlation with pH, ORP, EC, sulfate concentrations, and DIC at the middle of the columns S, F1, F2, F3, and F4

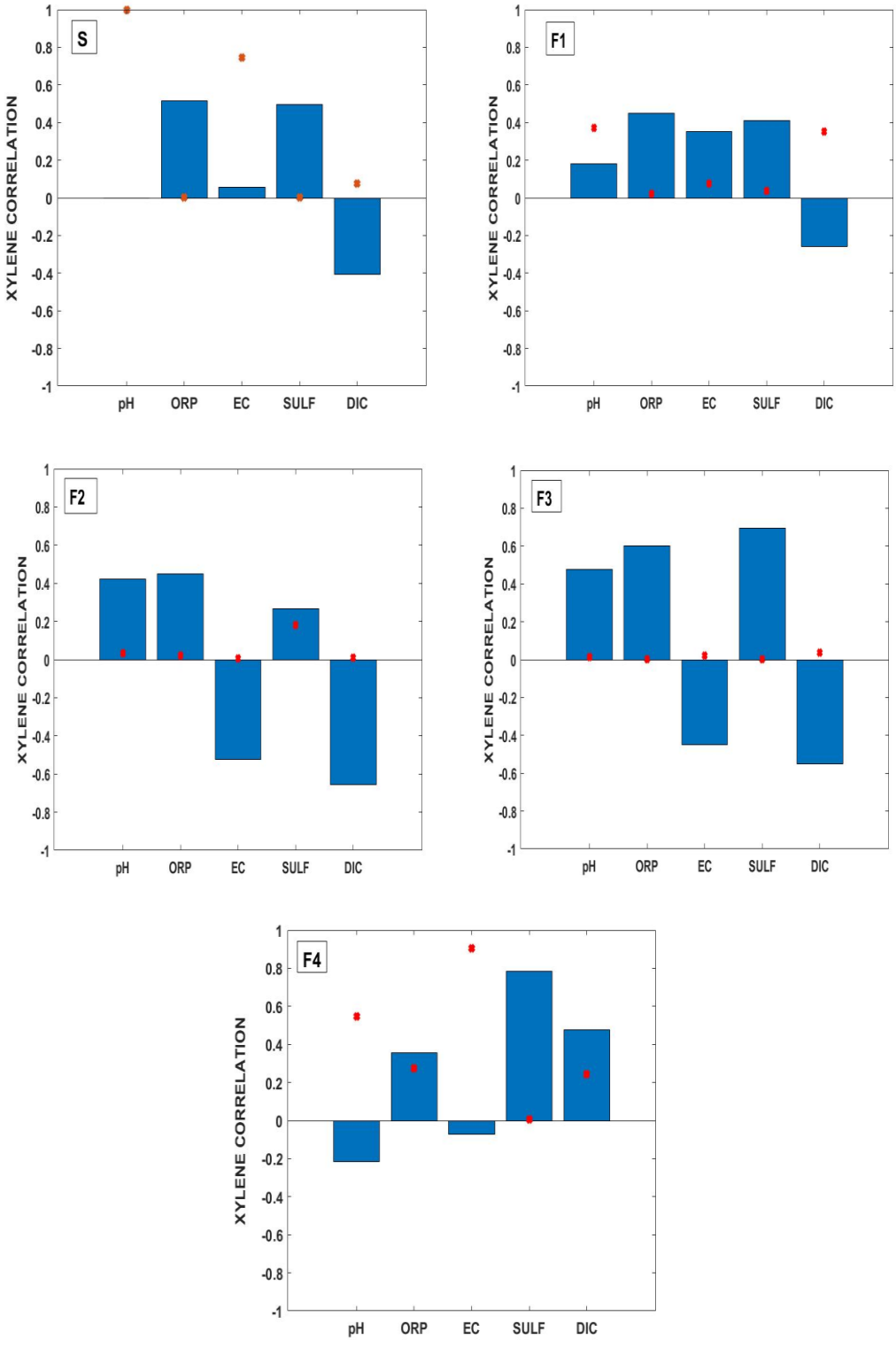

Figure 18: Xylene Correlation with pH, ORP, EC, sulfate concentrations, and DIC at the middle of the columns S, F1, F2, F3, and F4

CHAPTER 6 THE INFLUENCE OF GROUNDWATER FLUCTUATION ON THE NATURAL ATTENUATION OF HOMOGENIZED CONTAMINATED SOIL UNDER AEROBIC AND ANAEROBIC CONDITIONS

In this chapter, we present a column experiment aimed at investigating the dynamics of LNAPLs and DNAPLs in the subsurface environment. Specifically, we focused on toluene as an example of an LNAPL and naphthalene as an example of a DNAPL. The experiment aimed to understand the behavior of these contaminants and their impact on the hydrogeochemical properties of the soil under different water table regimes.

Two columns were designated as stable columns, while the other two columns were subjected to water table fluctuations. Initially, the columns were maintained under aerobic conditions and subsequently, anaerobic conditions were induced in the columns to replicate oxygen-depleted environments commonly found in contaminated subsurface zones.

6.1 Introduction

Accidental spills of petroleum products, such as crude oil, gasoline, and diesel fuel are a common source of groundwater contamination especially in coastal areas. After penetration to the ground surface, petroleum hydrocarbons form a separate non-aqueous phase liquid (NAPL) in the subsurface systems. NAPLs migrate far from their source and gradually change the composition of soil and groundwater (Dou et al., 2008). The fate of organic contaminants in the soil and groundwater has been the focus of many studies in the recent years because of their high toxicity and carcinogenicity effects (Blodau & Moore, 2003; P. K. Gupta et al., 2019; R. E. Ismail, 2019). Due to the low solubility of organic compounds, they continue to dissolve into groundwater for years as a continuous sources of groundwater contamination which can pose significant environmental problems (Newell et al., 1995).

Bioremediation has been proposed as one of the most effective and environmentally friendly techniques to clean petroleum hydrocarbon contaminants in soil and groundwater (Brown et al., 1996; Fry et al., 1997; Ngueleu et al., 2019; Ossai et al., 2020; Sookhak Lari et al., 2019). During biodegradation processes, microorganism will initially use oxygen (O_2) as an electron acceptor to oxidize organic compounds. After the depletion of oxygen, anaerobic conditions will be developed where various microorganisms use different electron acceptors such nitrate, iron, sulfate, and carbon dioxide (CO_2) to degrade organic contaminants (Huang et al., 2016; Lv et al., 2018) . During the biodegradation process, hydrocarbons can fully or partially be transformed to less complex organic compounds and/or inorganic minerals. Mineralization of organic contaminants produces H_2O and CO_2 under aerobic or CH_4 or carbonate under anaerobic conditions (Haritash and Kaushik, 2009). The biodegradation rates are affected by many factors including environmental conditions such as pH, temperature, availability of oxygen and terminal electron acceptors, type and population of microorganisms, biogeochemical redox conditions, and also the chemical structure of the hydrocarbons (Lv et al., 2018). Phelps and Young, (1999) invetigated the degradation of benzene, toluene, ethylbenzene, and xylene (BTEX) under different redox conditions. Their results indicated that while benzene was degraded just under sulfate reducing conditions, toluene was degraded under all redox conditions. In addition, the most rapid degradation rates were observed under nitrate reduction, while the most significant loss happened under sulfate reducing conditions. Jin et al., (2012) studies PAHs biodegradation from accidental oil spill in coastal area. During two years of monitoring, total PAHs, naphthalene, and phenanthrene concentration decreased drastically. The authors suggested that in addition to biodegradation, other factors contribute to the removal of naphthalene are physical transport and volatilization.

Steffen et al., 2015 were able to confirm the capability of sulfate reducing bacteria to degrade naphthalene in four different PAH contaminated anoxic aquifers.

Coastal (semi)-arid areas are characterized with extreme environment ranging from temperatures variability, high salinity, water table fluctuating, and different soil moisture content. These environmental parameters significantly affect the microbial behavior and the associated interactions with organic contaminants in the subsurface systems (Yadav and Hassanizadeh, 2011). Groundwater movement in the vadose zone is controlled by infiltration under the gravity force, seasonal variations, and redistribution by capillary rise (Bunsri et al., 1974). The fluctuation of water table is the main cause of the transport and redistribution of contaminants in the vertical direction within the vadose zone. during water table rise, the mobile free-phase NAPLs moves with water table leaving blobs trapped between soil grains. The entrapped blobs reduce the mobile free phase of NAPLs, thus reducing its migration downward. On the other hand, these blobs increase the source zone of NAPLs to groundwater and the interfacial area which enhance the dissolution and biodegradation overtime (Dobson et al.,2007; J. Lee et al. 2001.; Lenhard, 1992; Rivett et al. 2001) .

Under other condition, when water table moves down, NAPLs migrate downward leaving residual in the unsaturated zone (Dobson et al., 2007; J. Lee et al., 2001). during the rise and drawn of water table, air is trapped between soil particles which provide additional source of oxygen into the system (Dobson et al., 2007; J. Lee et al., 2001.; Lenhard, 1992).

The transition zone separating soil from water table is a dynamic part of groundwater contamination due to the concentration gradient between the unsaturated and saturated zones. The water table fluctuation and the related variations in redox conditions change the unique geochemical and mineralogical of soil and are the main drive of many

biogeochemical processes (Borch et al., 2010; Rezanezhad et al., 2014). Microbial communities in the transition zone are more diverse and flexible comparing with the one living under stable condition (Pett-Ridge and Firestone, 2005; Rezanezhad et al., 2014). In addition, the groundwater fluctuation enhances the transfer of oxygen from the atmosphere to the groundwater and result in variations in local redox conditions which utilize microbial growth and consequently will increase the rate of hydrocarbon biodegradation (Aller, 1994; Rezanezhad et al., 2014; Yadav and Hassanizadeh, 2011). Studies show that petroleum hydrocarbon leakage into groundwater results in increased microbial activity and the measurable consequence hydrochemical parameters (Marić et al., 2020). Little is done about the effect of groundwater fluctuation under the consequence of aerobic and anaerobic conditions. The reduction of dissolved oxygen gives the most energy when compared to other electron acceptors. As a result, aerobic biodegradation of petroleum hydrocarbons is the primary mechanism of hydrocarbon degradation (Marić et al., 2020). Biodegradation of petroleum hydrocarbons, on the other hand, takes place via anaerobic and methanogenic mechanisms: denitrification, reduction in manganese (IV), reduction in iron (III), reduction in sulfate, and methanogenesis.

Previous studied stated that out of all-natural anaerobic degradation, sulfate reduction accounts for most of it and it has more advantages over other processes (Miao et al., 2012; Suthersan et al. 2011; Wei et al., 2018). Sulfate has higher solubility compared to oxygen and nitrate, has prolific populations of naturally occurring microbes, persistence in the subsurface, cost effective, available and safe, and has wide range of pH (5-8) (Ayangbenro et al, 2018; Cuthbertson et al., 2010; Huang et al., 2016, Suthersan et al., 2011).The sulfate-reducing bacteria (SRB) obtain energy by oxidizing organic compounds exist in petroleum hydrocarbon while reducing sulfate (SO_4^{2-}) to

hydrogen sulfide (H_2S). In addition to the sulfate reduction, a methanogenesis may occur and is dependent on sulfate concentrations (Vroblesky et al., 1996).

Arabian gulf region is located in an arid area with high temperature and limited water resources. The soil and groundwater are characterized by high concentrations of sulfate due to the geological formation of the region (Maslehuddin, 2002). High sulfate concentration is dominant in this area due to minimal rainfall and high evaporation. Thus, sulfate reducing bacteria is expected to be dominant in this area and the decision was made to investigate its effect on biodegradation. The main objective of this study was to understand the impact of groundwater fluctuation in coastal regions on the bioremediation of petroleum hydrocarbons spilled into the (sub)-surface under the effect of sulfate and Nitrate reducing bacteria.

6.2 Experiment Setup

A schematic diagram of experiment set-up is shown in Figure 1. The setup contains two stable soil columns with one equilibrium and storage column, and two fluctuations soil columns with one equilibrium and storage column for each one. All columns are made of hard acrylic (length is 60 cm, inner diameter is 7.5 cm, wall thickness is 0.6 cm). The soil columns have 18 ports along the columns for sensors and pore water sampling. The top and bottom of the columns are closed by acrylic caps connected by steel rods and secured by bolts. The bottom of the columns is closed by a filter membrane (Soil Measurement Systems, LLC, USA, bubbling pressure: 600 mbar), and the top a nylon mesh (Soil Measurement Systems, LLC, USA, bubbling pressure: 32 mbar). The acrylic caps have an opening for connections and for supplying water to columns. The columns were covered by aluminum foil to simulate subsurface dark conditions. The equilibrium column for the stable soil columns is used for storing the water and supplying it to the equilibrium column once the water level is decreased during sampling process. The equilibrium column for the fluctuating soil columns is used to

control the water level.

6.2.1 Soil Spiking

The methane dichloromethane and the aliphatic ketone acetone are often used for the purpose of artificially contaminating soil with aromatic hydrocarbons in laboratory experiments. Two protocols of soil spiking are usually used in literature, partial treatment and full treatment protocol. The partial treatment is achieved by adding contaminant to a 25% of the soil sample and closed for specific time, so that the solvent disperses in soil. Afterward it mixed with the remaining 75% of the soil sample. The full treatment protocol is done by adding the solvent or contaminant to the whole soil sample in the flasks, closed for specific time to let it disperse, and left to evaporate for 16 hrs. (Brinch et al., 2002). In this experiment, partial contamination protocol was used. 25% g of soil is taken, cleaned from big particles and homogenized, toluene and naphthalene. Then, the soil is mixed with the contaminants with a glass spoon for five minutes. The soil mix was covered with the rest 75% of the soil and wrapped with aluminum foil and left under fume hood for 24 hrs. After 24 hrs, the soil was mixed to provide a homogenized spiked soil. During the filling process, samples (~5 g) were collected and analyzed for the initial concentration of toluene and naphthalene.

6.2.2 Column experiment

The soil columns are acrylic material and have 18 lateral ports (1/800 NPT compression fittings) spaced every 3 cm. Each one of the ports is tightened and fitted with Teflon septa except three ports are kept open for sampling at -10, -30, and -50 cm below the soil surface. These ports were fitted with 1/8 -27 NPT thread with 7/16" Hex to classic series Barb, 1/8" ID tubing, white Nylon and connected with ~10 cm of chemically resistant blue polyurethane tubing for collecting aqueous samples. On the other side of the column, RHIZON CSS 5 cm (Male luer) were installed at -10, -30, and -50 cm depths for the extraction of pore water by A vacuum pump (Soil Measurement Systems,

LLC, USA, #CL-042).

6.2.3 Water table regimes

Four soil columns were packed with synthetic contaminated soil. Naphthalene ($C_{10}H_8$, Sigma-Aldrich), and toluene (C_7H_8, Sigma-Aldrich) were used for spiking the soil as received. For the two stable columns, the water table was maintained at the top of the soil surface (no change). While for the other two columns, an oscillating water table regime was imposed (fluctuating water table). The water level fluctuated between the soil surface (0 cm) and – 40 cm, with imbibition-drainage cycle lasting for 3 days and 1 day for equilibrium. To lower and raise the water level, a pump is used to raise the water level in the equilibrium columns (Figure 1). The flow rate in both the upward and downward direction was 0.407 ml min^{-1}. The groundwater imposed in the columns is a synthetic influent solution prepared based on groundwater sample analysis from the sampling location (Table 1).

The experiment was running for 149 days at room temperature (22 ± 2 ^oC). Samples were collected at the time of high-water table from the middle (-30 cm) and bottom (-50 cm) of the soil columns using glass vials. At the time of lower water table (drainage), samples were only collected from the bottom of the soil columns.

Samples were analyzed for the concentrations of organic compounds (toluene and naphthalene), sulfate, and dissolved inorganic carbon (DIC). In addition to that redox potential (ORP), pH, dissolved oxygen (DO), and EC (Electric conductivity) were also measured.

6.3 Results and Discussion

6.3.1 Properties of groundwater and pore water geochemistry

Multiple groundwater samples were collected during soil sampling for the purpose of this study. The average EC and pH of the sampled groundwater were ~4000 µS cm^{-1} and 7.3, respectively, and can be categorized in the range of brackish water (Sardin et

al., 2009). The major anions and cations in the groundwater (Table 1) samples were added to the synthetic injected groundwater to simulate realistic subsurface conditions and account for potential depletion of any substance due to biotic/abiotic reactions as well as aqueous sampling during the experimental period.

The calculated water contents of the spiked soil after saturation were 20% of the columns' volume. During transfer of the synthetic solution from the Tedlar bags to the soil columns, DO concentration increased to ~3 mg L^{-1}. However, pore water DO concentrations at -30 and -50 cm below soil surface (bss) of all columns decreased to ~1 mg L^{-1} after 10 days indicating that due to the presence of organic contaminants, DO decreased and anaerobic condition was developed. Pore water ORP values were ~250 mV and gradually decreased to <100 mV after 65 days indicating the development of reducing conditions and enhancement of anaerobic microbial community. Shafieiyoun et al. (2020) found that sulfate reduction occurred after 40 days when ORP dropped below 100 mV in a series of anaerobic flow-through studies on soil samples taken from the same area. At the middle of the fluctuating columns (-30 cm), ORP fluctuated during the experiment, while at the bottom (-50 cm), ORP decreased during the water rise (Figure). This observation is similar the Rezanezhad et al. (2014). By addition of sodium sulfite as an important oxygen scavenger after 95 days, DO decreased very fast during water rise and ORP at both depths in all columns to -100 mV and fluctuated in the range of -50 to -100 mV until the end of experimental period.

Pore water EC values at -30 and -50 cm bss of the stable water table columns are presented in Figure 20 and Figure E 2. EC values at both depths were initially in the range of 5000 µS cm^{-1} and decreased to 3300 µS cm^{-1} at -50 cm bss after 20 days while EC reached 3500 µS cm^{-1} at -30 cm bss after 65 days followed by minor fluctuation until day 95. In general, EC values at -50 cm bss were lower than those at the middle

of the columns. This can be attributed to the less soil-water contact time at the bottom of the column compared to that at the middle. Water movement mobilized inorganic elements along the soil columns through dissolution that results in higher ionic strength and salinity in the middle and upper portions of the columns. In addition, temporal reduction of pore water EC values can be attributed to the reduction of inorganic elements in the soil due to biodegradation process, mineral precipitation under anaerobic condition, or pore water sampling. Since water should pass a shorter distance along the column to reach -50 cm bss compared to that for -30 cm bss, aqueous concentrations of inorganic elements and nutrients decreased faster at -50 cm bss and hence, EC values decreased sooner at the bottom of the column. Previous studies also identify the enrichment of inorganic elements at the upper portions of the soil due to the increase dissolution and water contact time at the bottom of the columns. Rezanezhad et al., (2014) found that as a result of the reductive dissolution of ferric iron mineral phases, significant quantities of aqueous Fe are detected below the water table in the stable column. As expected, EC values increased by introducing sodium sulfite after 95 days and eventually reached to 4200 μS cm^{-1} at both depths by the end of the experimental period. However, the increase of the EC values at -50 cm bss was more significant compared to that at -30 cm bss specifically at the beginning of sodium sulfate addition. This can be attributed to the higher concentration of sodium and sulfite ions at the bottom of the columns while their concentrations decrease along the column. Eventually, the system reached to steady state under prevailed anaerobic conditions that resulted in similar constant EC values at both depths after 140 days.

Pore water EC values at -30 and -50 cm bss of the fluctuating water table columns following each saturation period and also at -50 cm bss following each drainage period are presented in Figure 20 and Figure E 2. In general, the behavior of pore water EC

values from the fluctuating water table column are similar to that of the stable water table column. However, EC values at -50 cm increase after each drainage period specifically at the beginning of the experiment. This can be attributed to the movement of high EC pore water from the top portions of columns to the deeper parts during drainage. In addition, due to higher DO level during water rise, mineral oxidation and dissolution can occur which results in higher ionic strength and EC values in the top of columns, while anaerobic condition is prevailed during drainage and results in mineral precipitation and lower EC values. Rezanezhad et al., (2014) also identified that pore water sulfur (S) concentrations in the form of sulfate are higher at the transition zoon of the soil columns exposed to water table fluctuations where oxidizing condition is prevailed. EC values fluctuations at -50 cm bss were less pronounced after 40 days that can be attributed to the decrease of EC values at the top of the columns due to decrease of inorganic elements in the soil as a result of toluene biodegradation, mineral precipitation under anaerobic conditions, and aqueous sampling. By introducing sodium sulfite after 95 days, EC values increased and reached to 42000 µS cm^{-1} at both depths by the end of the experimental period.

Temporal changes of the pore water pH values at -30 and -50 cm bss are presented in Figure and Figure E 3. The pH values for both stable and fluctuations columns have been in the range of 7 to 8, which is appropriate for the SRB activities. The pH values at both depths of all columns were initially ~7.5 and remained almost constant in the middle of them while gradually increased to > 8 at the bottom by the end of the experimental period. While pH values at the bottom of the fluctuating water table columns were higher than those at the middle of the columns during the whole experimental period, for the stable water table columns (S1 and S2) the difference was observed just after > 60 days. The increase of pH values can be probably attributed to

the production of weaker acids during biodegradation process and soil alkalinity. However, due to transfer of buffering compounds to the middle of the columns, pH did not change. By addition of sodium sulfite to the influent solution after 95 days, pH values were disturbed at both depths of the stable water table columns while they just slightly increased in the fluctuating water table columns. This can be attributed to the dominant diffusional transport of sodium sulfite to the upper parts of the stable water table columns that results in gradual changes in different parts of the stable water table columns due to biotic and abiotic reactions of sulfite as well as enhancement of anaerobic biodegradation processes. The advective transport in the fluctuating water table columns results in faster changes throughout the soil that were not reflected by pH values. Overall, temporal-spatial results imply that combination of water table fluctuations and oscillating redox conditions enhance the mobilization of inorganic elements in the smear zone. Prevailed anaerobic and reducing conditions within the column after addition of sodium sulfite resulted in steady state condition and similar EC values at both depths indicating that lack of oscillating redox condition can significantly restrict the mobilization of inorganic element.

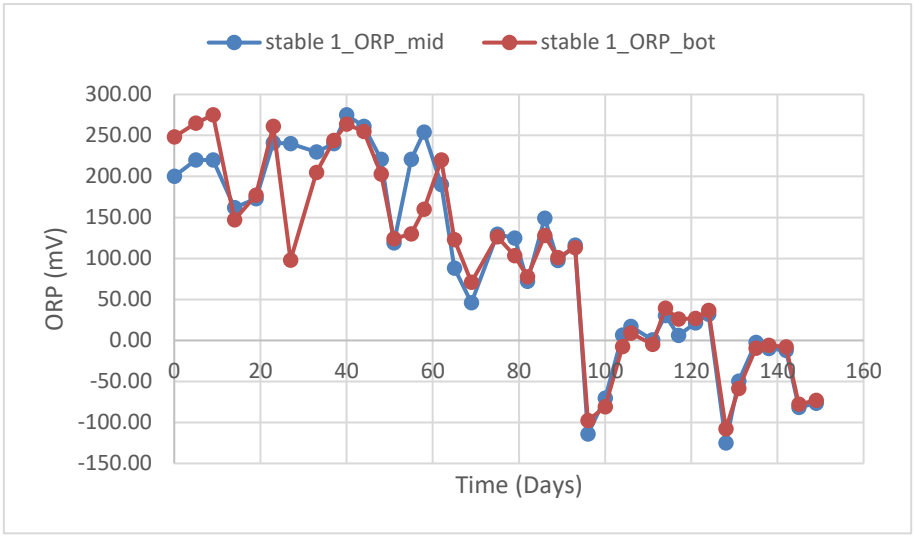

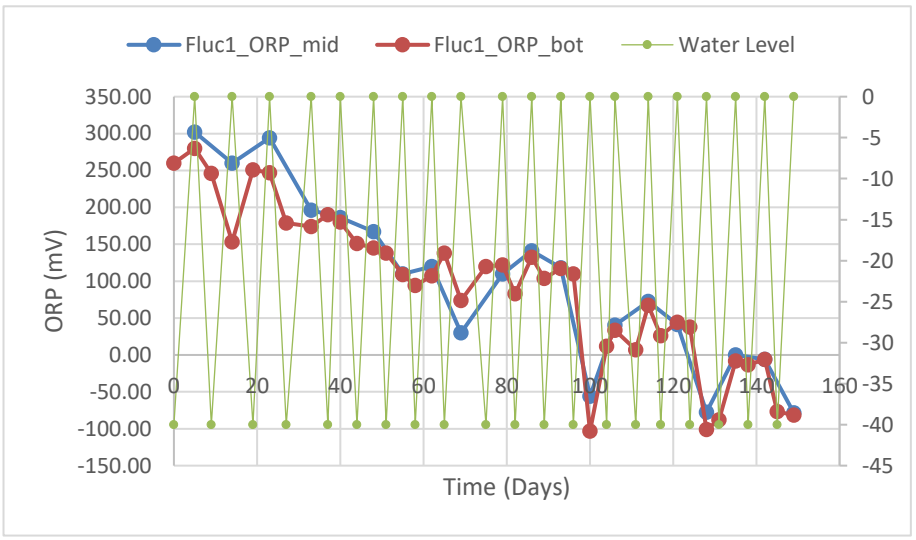

Figure 19: Oxidation reduction potential (ORP) at the middle (depth B) and the bottom (depth C) of the columns S1 and F1

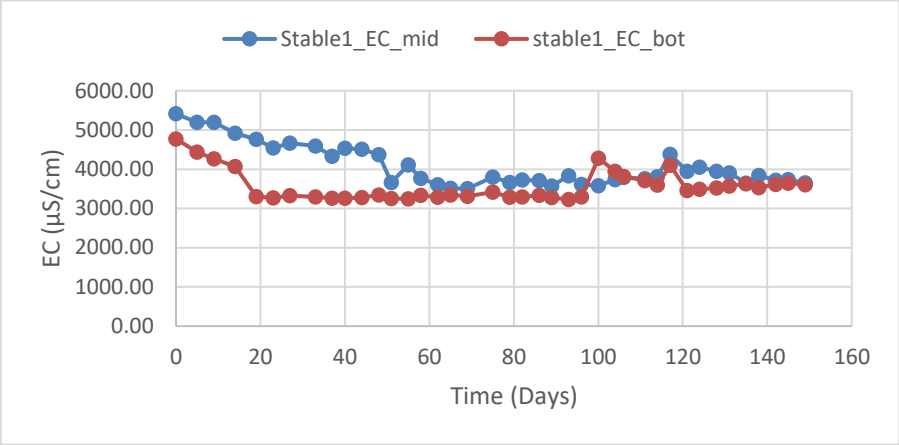

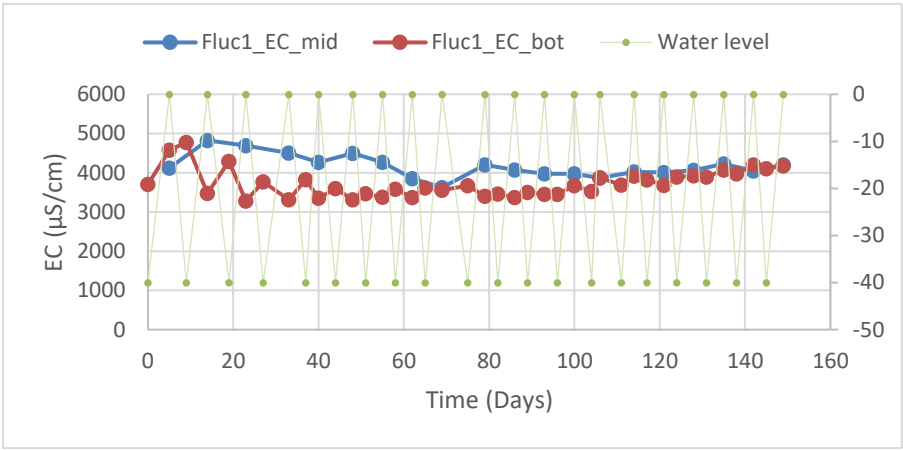

Figure 20: Electric conductivity (EC) at the middle (depth B) and the bottom (depth C) of the columns S1 and F1

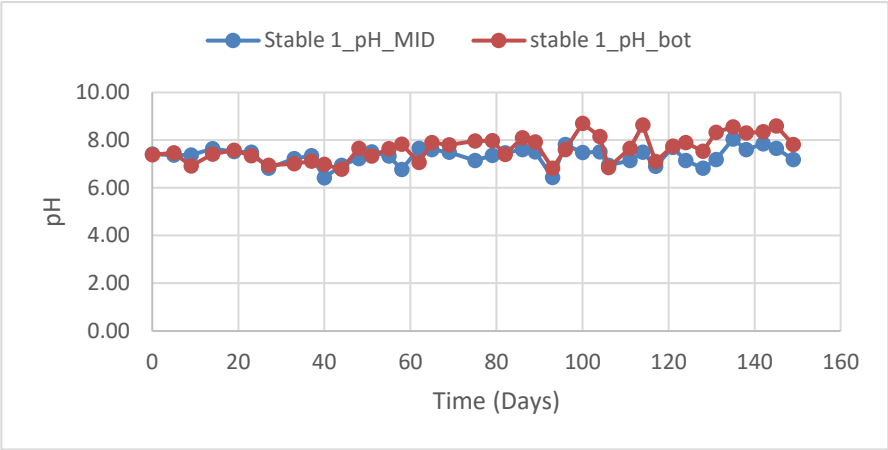

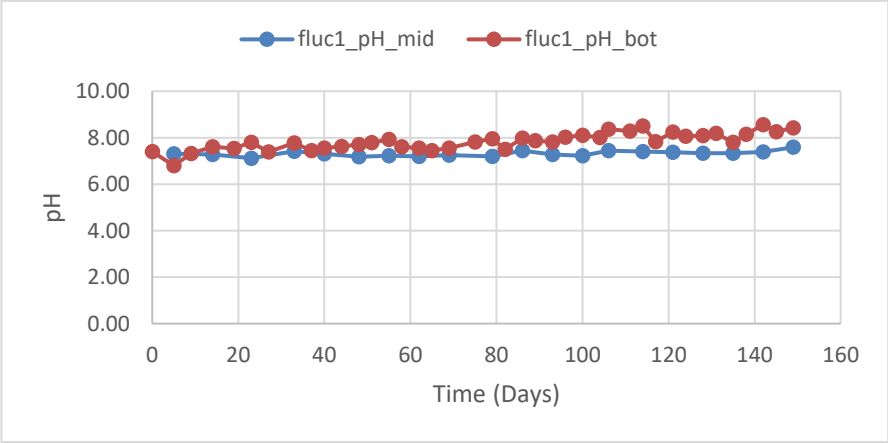

Figure 21: pH values at the middle (depth B) and the bottom (depth C) of the columns S1, and F1

6.3.2 Terminal electron acceptors and DIC

The concentrations of sulfate at the stable and fluctuating columns 1 and 2 can be seen in Figure . At the beginning of the experiment, the four columns (stable and fluctuations) were saturated and drained five times to adjust sulfate concentration. The initial sulfate concentration was in a range of 1000 mg L-1, and it was more than the ideal concentrations requirements for SRB (Shafieiyoun et al., 2020).

The state of redox conditions of the groundwater sample is determined by the major reduction/oxidation reaction. At the beginning of the experiment, and when the columns were still under aerobic condition, sulfate concentration at -30 cm was at around 450, 330 mg L^{-1} for stable 1 and 2, respectively. after 65 days, when most of DO is consumed and anaerobic condition was developed, sulfate concentration dropped

to less than 200 mg L^{-1}, and it continue to decrease after 120 days from the beginning of the experiment (Figure). The reduction in sulfate concentration in stable columns 1 and 2 is 51.4% and 59%, respectively. It is noticed that after 128 days, sulfate concentration increased, and this can be attributed to the reaction of sodium sulfite with O_2 which produces sodium sulfate.

In the case of fluctuation columns (F1 and F2), the concentration of sulfate at -50 cm follows the same pattern as stable columns. The concentration of sulfate started at 220 mg L^{-1} and increased to 320 mg L^{-1} at 35 days reaching the concentration at -30 cm and then continue to decrease until 120 days. The sudden increase of sulfate at 35 days cm can be due to the dispersion of sulfate from the bottom part of the column, and the movement of water at the time of rising groundwater. It is noticed that the concentration of sulfate at -30 cm is slightly higher than -50 cm even though it is following the same pattern. This increase in concentration can be attributed to the redistribution of nutrients, anions and cations exchange within the vadose zone due to water table fluctuations (smearing).

The consumption of sulfate is a strong indication that sulfate reducing bacteria is being developed. The anaerobic degradation under SRB can be estimated from the consumption of sulfate vs the organic mass removal (Miao et al., 2012; Shafieiyoun et al., 2020; Shafieiyoun et al., 2020). At the beginning of this experiment oxygen was the preferable electron acceptor. after the depletion of oxygen, and the availability of sulfate serving as the electron acceptor, naphthalene and toluene will be degraded be SBR (Cervantes et al., 2001; Ngueleu et al., 2019). In general, and before adding sodium sulfite, the decrease in sulfate concentrations in stable 1and 2 columns are 51% and 55% respectively, while the decrease at the middle of fluctuation columns 1 and 2 are ~45% and 42%, respectively. The concentrations of DIC can be used as an indicator

of organic carbon mineralization (Shafieiyoun et al., 2020). For stable columns, a slight decrease in dissolved inorganic carbon (DIC) was observed (Figure). At the beginning of the experiment, DIC at -30 for both columns were in a range of 44 mg L^{-1} and decreased to around ~ 20 mg L^{-1} after 60 days. The concentration of DIC continued to fluctuate in the same range until 120 days and suddenly increased, this can be attributed to the accumulation of sulfide. For the fluctuating columns, DIC at -50 cm followed the same pattern of – 30 cm of the stable columns, started at ~ 39 mg L^{-1} and fluctuated during the experiment till 120 days and suddenly increased after that. On the other hand, fluctuating columns at -30 cm started at 42 mg L^{-1} and increased slightly to 87 mg L^{-1} after 120 days.

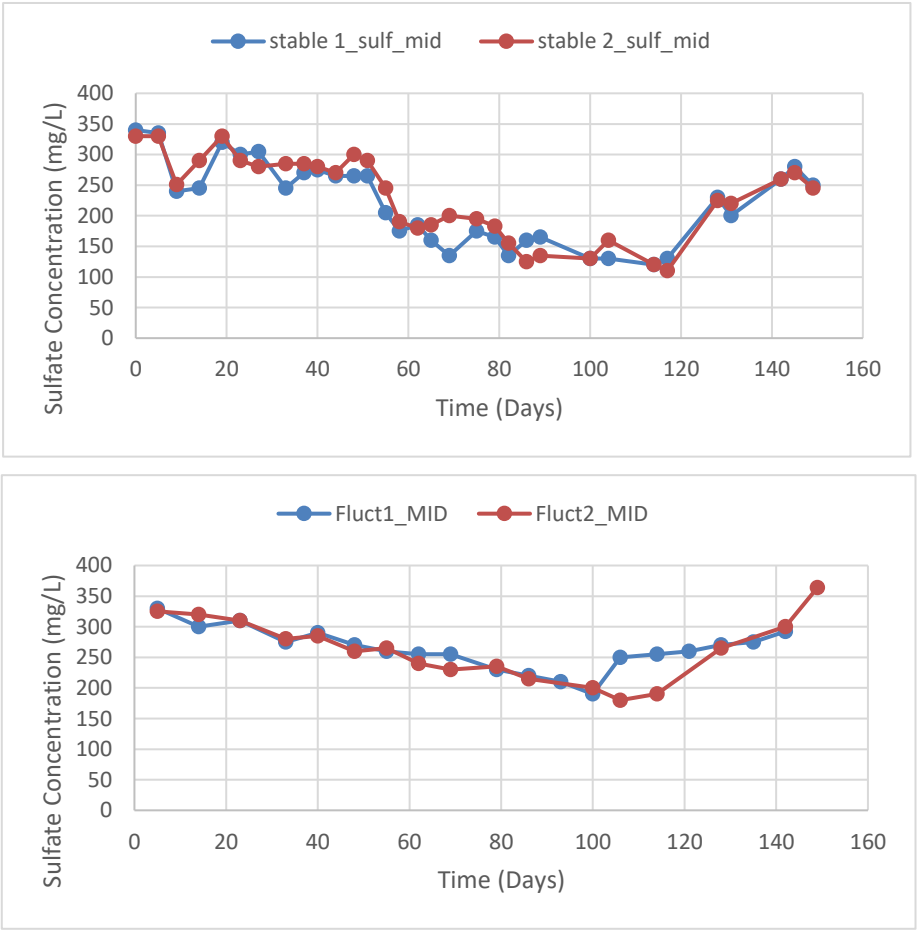

Figure 22: Dissolved sulfate concentrations at the middle (depth B) of the columns S1, S2, F1, and F2

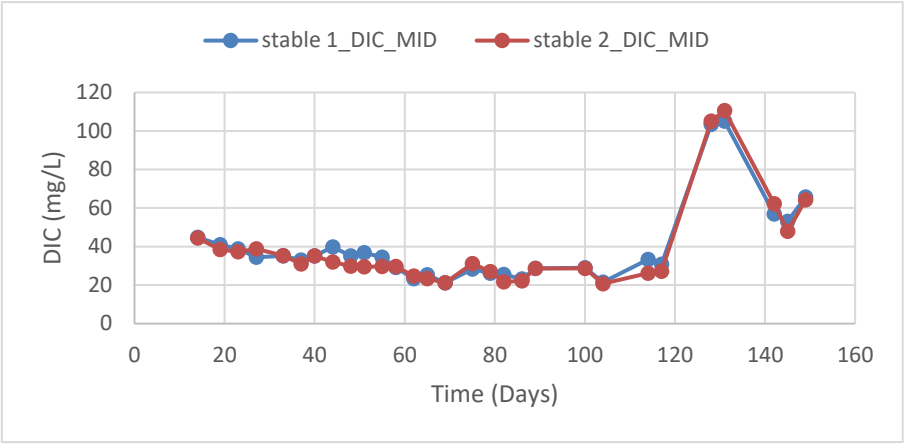

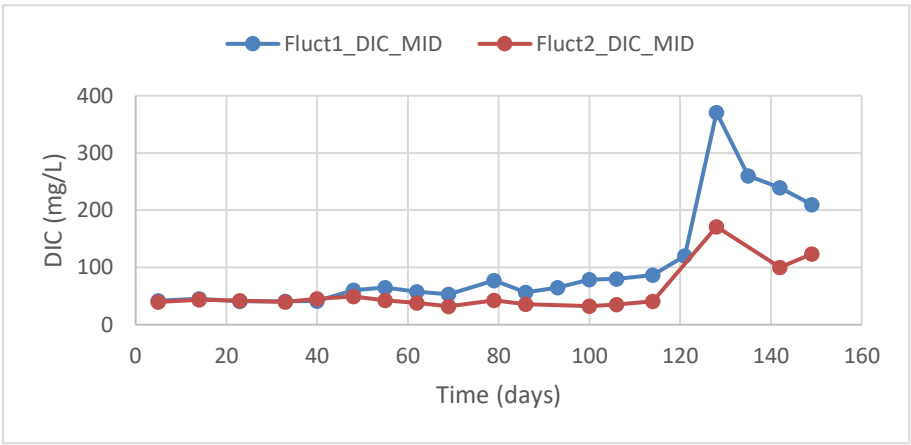

Figure 23: Dissolved inorganic carbon (DIC) at the middle (depth B) of the columns S1, S2, F1 and F2.

6.3.3 Dissolved organic phase

6.3.3.1 Dissolve Toluene phase

Figure represents temporal toluene concentrations for -30 and -50 of the stable water table columns. The initial toluene concentration at -30 was 300 mg L^{-1} for S1 and S2, it continued to fluctuate in the same range during the experiments for both columns. After 100 days, dissolved toluene concentration increased to around 400 mg L^{-1} due to the high toluene mass in the columns, so it continues to dissolve till 150 days when it started to decrease again. For the fluctuating water table columns F1 and F2, the concentration at -30 were at 200 and 300 mg L^{-1}, respectively. It is noticed that when the water table level increases, the toluene moves from bottom to the top of the columns resulting in toluene concentration increased. The toluene concentration at -50 cm for both columns started at 270 mg L^{-1} and for 100 days fluctuated between around 200 and 350 mg L^{-1}. After 100 days, the toluene concentration increased to 400 mg L^{-1} and this increased due to the movement of toluene along the column and the continuous dissolution. At 150 days, the concentration of toluene at -30 and -50 decreased to about 300 and 187 mg L^{-1} for the column F1 and 300 and 300 mg L^{-1} for F2, respectively. The increase movement of water due to the fluctuation of the water table known for increase the dissolution of organic carbon and that enhance the natural attenuations (Dobson et al., 2007).

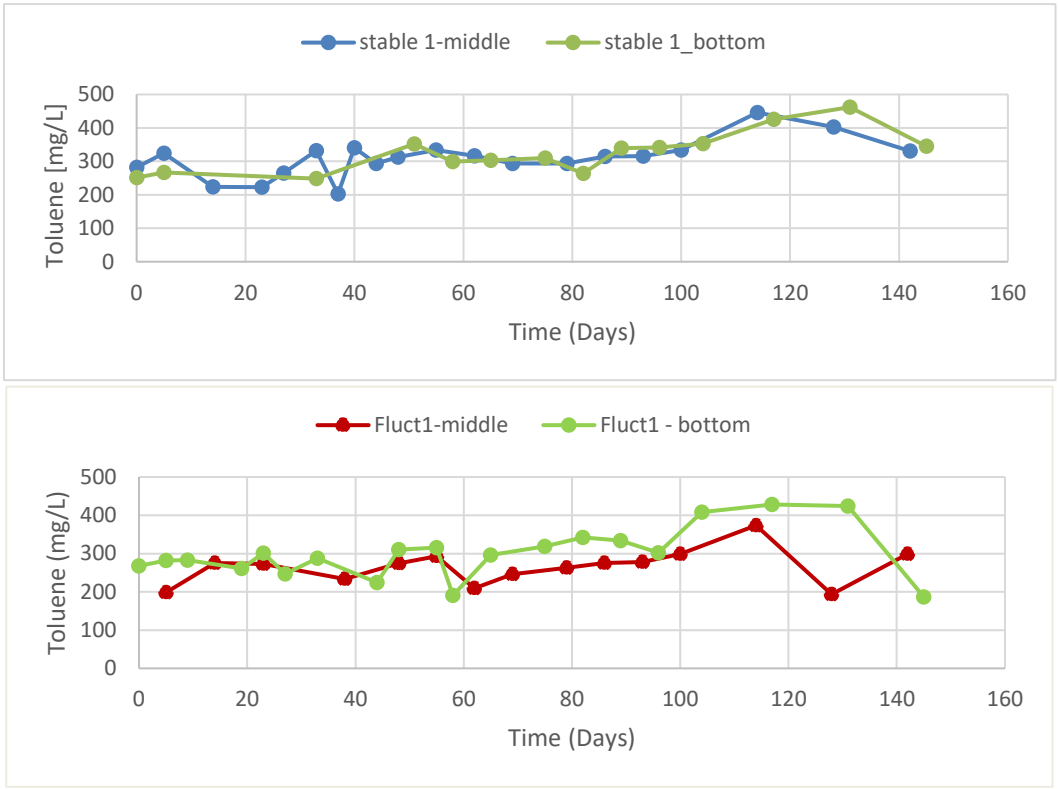

Figure 24: Toluene concentrations at the middle (depth B) and the bottom (depth C) of the columns S1 and F1

6.3.3.2 Dissolve Naphthalene

For the temporal Naphthalene concentration, the initial naphthalene concentration at -30 and-50 for stable water table 1 (S1) was 1 and 0.7 mg L^{-1}, respectively (Figure). While for the stable water table 2 (S2) at -30 and-50 started at 0.8 mg L^{-1}. After 30 days, the concentration for both columns and at both depths increased to about 1.5 mg L^{-1} due to dissolution of naphthalene. For the next 65 days of the experiment, the concentration of naphthalene decreased and fluctuated between 0.6 - 0.9 mg L^{-1}. At 100 days, dissolved naphthalene concentration at -30 cm for S1and S2 increased to around 1.55 mg L^{-1}, while for -50 cm increased to about 2 mg L^{-1}. At the end of the experiment both columns at -30 and -50 reached 0.9 mg L^{-1}. As the stable columns were always under saturated condition during the experiment, the reduction can be explained either

by the adsorption or degradation of naphthalene (Haritash and Kaushik, 2009).

The fluctuating water table column 1 (F1) at -30 and-50 cm were initially at 0.7 mg L^{-1}. After 30 days, the concentration of naphthalene at -30 and -50 cm increased to about 1 mg L^{-1}, and then decreased at both depths to the initial concentration. At 100 days, the concentration increased again to about 2 mg L^{-1} for both -30 and-50 cm and continued to fluctuate till the end of the experiment when it reached 0.7 mg L^{-1}. At the same time, the fluctuating water table column 2 at -30 and-50 cm were initially at 1 mg L^{-1}. For 100 days, the concentration at both depths fluctuated between 0.6 – 1.2 mg L^{-1}. The concentration of naphthalene at -50 cm continued to fluctuate in the same range till the end of the experiment. While at -30 cm continued to increase and reached a peak of 2.3 mg L^{-1} at 114 days and then decreased till the end of the experiment and reached 1 mg L^{-1}. It is observed that at each imbibition cycle, the concentration of Naphthalene increased slightly at F1 and F2. Many researchers tested the effect of water table fluctuations on the distribution of petroleum hydrocarbons, this distribution enhance dissolution which in effect enhance natural attenuation (Dobson et al., 2007). Ngueleu et al., (2019) performed an experiment with benzene and naphthalene, stated that the dominant process for the naphthalene degradation is sorption, while Varjani, (2017) stated that naphthalene can be degraded in most situations.

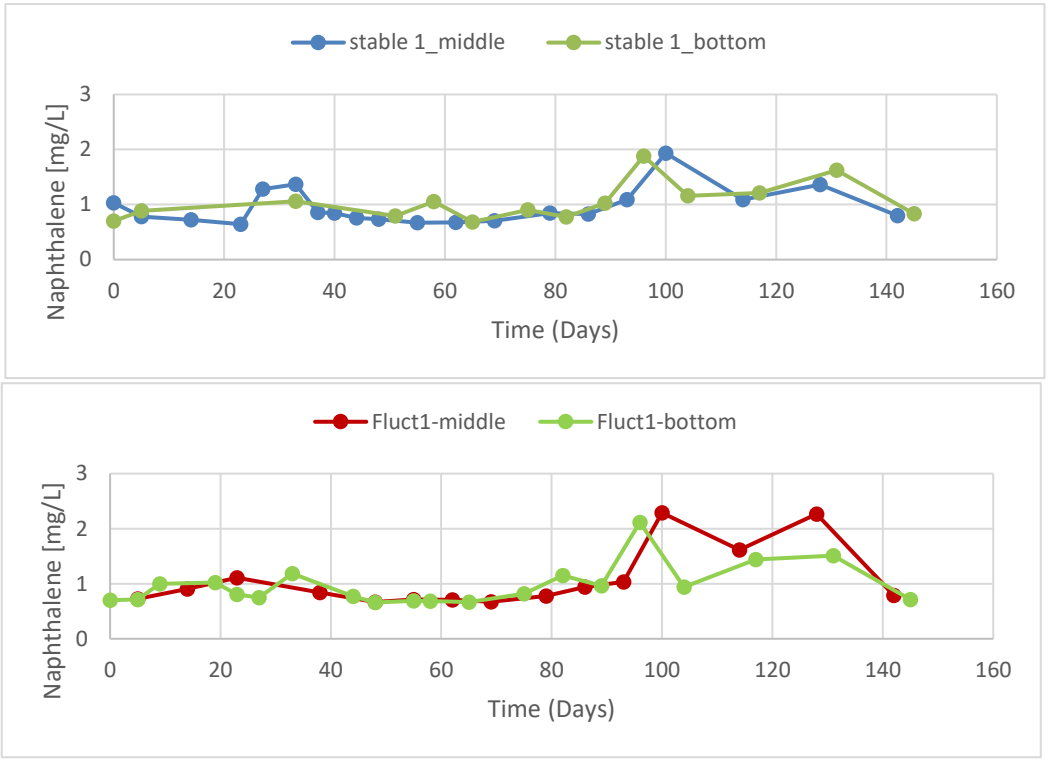

Figure 25: Naphthalene concentrations at the middle (depth B) and the bottom (depth C) of the columns S1 and F1

6.3.4 Solid Phase Geochemistry

X-ray fluorescence (XRF)XRF results for the collected soil samples provide evidence of the presence of the following major and minor elements: Ca, Sr, Si, Mg, Fe, Sc, K, Al, S, Cl, Cr, Ti, V, Mn, Co, Na, Zr, and Ni. The major elements concentrations in initial soil were as following: silicon (Si): 2.185, Magnesium (Mg): 0.945, Iron (Fe): 0.8685, Potassium (K): 0.583 and Sulfur (S): 0.313. Figure E 5 (supplementary materials) represents the final major elements concentrations values for the four water table columns. It is noticeable that there are some differences in the concentration between stable and fluctuating water table columns. In general, for Si, Mg, and Fe, the concentrations of the stable water table columns are higher than the fluctuating water table columns, therefore it is higher than the initial concentration of the homogenized soil, while the concentration in the fluctuating water table columns are lower. The

concentrations of Si, Mg, and Fe in the fluctuating water table columns are lower in the upper 40 cm of the columns and higher in the bottom part reaches the initial concentration. In the case of the stable columns, the concentrations of the elements are accumulated in the columns, while for the fluctuating ones, when water table fluctuated, the elements relocated from the upper part of the soil column to the bottom. Moreover, the possibility of the elements to be partially moved to the equilibrium columns explains the lower concentrations of these elements in the bottom part which reach the concentration of the initial homogenized soil.

6.4 Conclusion

The fluctuation of the water table has a significant impact on natural attenuation of LNAPLs in contaminated groundwater. In LNAPL-contaminated subsurface habitats, changes to the source zone and the geochemical characteristics of soil and groundwater are triggered by fluctuations in the water table. The results of this experiment had demonstrated that redox conditions in the soil columns varied temporally between the stable and fluctuated water table. As water moved through the soil, it dissolved inorganic materials, raising ionic strength and salinity in the intermediate and upper levels of the soil columns, which resulted in lower EC values at the bottom of the fluctuating columns. The values of pH at the bottom of the fluctuating water table columns were higher than those at the middle of the columns during the whole experimental period, while for the stable water table columns the difference was observed just after > 60 days. sulfate (SO_4^{2-}) is an electron acceptor whose removal rates determine the biodegradation rate. The decrease in sulfate concentration in stable columns S1 and S2 is more than the decrease in sulfate concentrations at the middle of fluctuation columns F1 and F2 during the experiment. The dissolved inorganic carbon at the stable columns decreased slightly during the experiment, encountered by sudden

increase after the addition of sodium sulfite. For the fluctuating columns F1 and F2, the DIC increased slightly during the experiment. The dissolved toluene and naphthalene concentrations at S1, S2, F1, and F2, increased slightly during the first 100 days due to the dissolution.

CHAPTER 7 SUMMARY AND CONCLUSIONS

The majority of the study on polluted soil and groundwater has been conducted on aquifers reflecting typical hydrogeological conditions in Northern America and Europe. However, in this work, we investigated the effects of water table fluctuation on the remediation of BTEX in a salty environment at a relatively medium and high groundwater temperature (22 - 32° C). This hydrological scenario is frequent in groundwater aquifers in Middle East, where water supplies are highly vulnerable to pollution due to the extensive presence of oil industries.

Water table movement affects natural attenuation of LNAPL-contaminated groundwater. It modifies the source zone and the geochemical characteristics of soil and groundwater. In this study the hydrogeochemical parameters of contaminated groundwater were evaluated as well as the concentrations of Benzene, toluene, ethylbenzene, and xylene as an example for LNAPLs and Naphthalene as an example for DNAPLs. The parameters include temperature, pH, electrical conductivity (EC), and dissolved oxygen (DO), and the concentration of major cations: calcium (Ca^{2+}), magnesium (Mg^{2+}), sodium (Na^{+}) and potassium (K^{+}), and the major anions: bicarbonate (HCO_3^{-}), sulfate (SO_4^{2-}) and chlorine (Cl^{-}).

In the study of different salinities and water table fluctuations (chapter 3), oxidation-reduction conditions in a column changed spatially and temporally, while salinity didn't affect the status of redox. Similarly, Electrical conductivity differ between stable and fluctuating columns. The difference between the stable and fluctuating columns is due to the redistribution of inorganic components and LNAPLs along the fluctuation column. Additionally, the presence of LNAPLs at the middle of the columns decrease the ionic strength thus resulting in decreased EC following the injection of the LNAPLs at the source zone. EC values increased at a later stage can be an indication of enhanced

biodegradation and increased of total dissolved solids. The pH values in the stable columns varied only slightly throughout the course of the experiment, while those in the fluctuating columns showed a much wider range and trended more toward alkalinity. Iron, manganese, nitrogen, and nitrate were found in small amounts, but sulfate was abundant, making it the dominant electron acceptor. In water table fluctuating columns, the concentrations of soluble benzene and toluene decreased by 82%, 78%, and 83%, 74% for low salinity and higher fluctuating columns, respectively. While for the low salinity and higher stable columns, the reduction was 35%, and 32%, 38%, and 37%, for benzene and toluene, respectively. The consumption of sulfate in fluctuating columns increased natural attenuation compared to the stable water table.

In another study (chapter 4), the natural attenuation of benzene, toluene, ethylbenzene, and xylene were studied to in the presence of water table fluctuations in conditions of varying soil homogeneity and temperature. Similar to the first experiment, ORP values in the middle columns varied cyclically with WTF and promoting reducing conditions in the columns. When the source zone is in a low permeable layer that would affect dissolution and thus removal of BTEX. On the other hand, slow water table fluctuation works similar to the stable column in terms of reducing BTEX concentrations. In reverse, temperature increase ORP reduction. The statistical test results showed that p-value for ORP values for the middle of all columns 0.047 which is < 0.05. EC values were affected greatly by fluctuation and temperature. The p-value for the statistical test is $3.119e^{-10} < 0.05$ implying that there are statistical differences between them. On the other hand, the statistical test for pH values at the middle of the columns showed that P-value is $0.3694 > 0.05$ which confirm that no statistical difference in the pH values between the five columns. Sulfate concentrations in fluctuated water table homogenized soil significantly lowered compared with stable water table column,

while slow fluctuating, soil heterogeneity, and temperature increased sulfate concentration. The statistical test indicated that sulfate concentrations are significantly different ($p=1.522e-7 < 0.05$).

There is correlation between sulfate concentration and BTEX in the stable column, which resulted from dissolution and diffusion downward while sulfate is accumulated at the middle of the column.

For the fluctuating columns the correlations between BTEX and sulfate concentrations soil homogeneity has a greater impact on the dissolution of BTEX and the flow of sulfate through the column, particularly in the layered column F2 where the BTEX-injected layer has a low permeability. By increasing the temperature in one of the fluctuated columns, ethylbenzene and xylene correlation become significant, implying higher groundwater temperature influences hydrocarbon desorption. Furthermore, a positive, mostly moderate, connection between BTEX concentrations and ORP is identified. The results show that it primarily comes with sulfate concentrations and negative correlation with DIC. The association between BTEX and sulfate concentrations, when combined with a positive correlation with ORP and a negative correlation with DIC, may indicate an increase in biodegradation in the columns.

In another study, homogenized contaminated soil with toluene and naphthalene. ORP, EC, and pH vary between the stable and fluctuation column as a result of fluctuated table. Due to the increased amount of toluene and naphthalene, maximum concentration reached 120 days which coincided with the reducing condition. Despite site-specific conditions, this study indicated that water table fluctuations could speed up NAPLs contaminated aquifer restoration.

CHAPTER 8 RECOMMENDATION FOR FUTURE WORK

- This work could be further enhanced by performing microbial analysis to confirm the presence of sulfate anaerobic bacteria (SRB) and the population difference between the stable and fluctuating columns and between difference depths along the soil columns.
- Measuring CO_2, bicarbonate and hydrogen sulfide (H_2S) in the stable and fluctuating columns during the experiment as evidence for BTEX biodegradation and anaerobic degradation with SBR.
- Design an experiment in which one of the columns contains a biocide to simply analyze and compare the effect of the hydraulic WTF on soil hydrogeochemistry in the presence of contaminant.
- For the experiment, the soil can be taken from different locations instead of one location, so it has different composition and properties.
- Using machine learning to create a numerical model such as adaptive neuro-fuzzy inference system (ANFIS) for the WTF effect on the hydrogeochemical properties in contaminated soil to further quantify the results of this study.

REFERENCES

Abell, J., Laverman, A. M., & Van Cappellen, P. (2009). Bioavailability of organic matter in a freshwater estuarine sediment: Long-term degradation experiments with and without nitrate supply. *Biogeochemistry*, *94*(1), 13–28. https://doi.org/10.1007/s10533-009-9296-x

Abramowicz, D. A. (1990). Aerobic and Anaerobic Biodegradation. *Biotechnology*, *10*(3), 241–251. www.polimernet.com

Ahmad, A. Y., Al-Ghouti, M. A., Khraisheh, M., & Zouari, N. (2020). Hydrogeochemical characterization and quality evaluation of groundwater suitability for domestic and agricultural uses in the state of Qatar. *Groundwater for Sustainable Development*, *11*(April), 100467. https://doi.org/10.1016/j.gsd.2020.100467

Al-amirah, A. S. (1982). *The Nowruz Oil Spill in the Arabian Gulf: Case Study of Saudi Arabia*. 16–31.

Al-Ghouti, M. A., Al-Kaabi, M. A., Ashfaq, M. Y., & Da'na, D. A. (2019). Produced water characteristics, treatment and reuse: A review. *Journal of Water Process Engineering*, *28*(September 2018), 222–239. https://doi.org/10.1016/j.jwpe.2019.02.001

Al-raoush, R. I. (2009). *Impact of Wettability on Pore-Scale Characteristics of Residual Nonaqueous Phase Liquids*. *43*(13), 4796–4801.

Al-Raoush, R. I. (2014). Experimental investigation of the influence of grain geometry on residual NAPL using synchrotron microtomography. *Journal of Contaminant Hydrology*, *159*, 1–10. https://doi.org/10.1016/j.jconhyd.2014.01.008

Alazaiza, M. Y. D., Harris, M., Copty, N. K., & Chia, M. (2021). Assessing the impact

of water infiltration on LNAPL mobilization in sand column using simplified image analysis method. *Journal of Contaminant Hydrology*, *238*(June 2020), 103769. https://doi.org/10.1016/j.jconhyd.2021.103769

Alazaiza, M. Y. D., Ngien, S. K., Copty, N., Bob, M. M., & Kamaruddin, S. A. (2019). *Assessing the influence of infiltration on the migration of light non-aqueous phase liquid in double-porosity soil media using a light transmission visualization method*. 581–593.

Alazaiza, M. Y. D., Ramli, M. H., Copty, N. K., Sheng, T. J., & Aburas, M. M. (2020). LNAPL saturation distribution under the influence of water table fluctuations using simplified image analysis method. *Bulletin of Engineering Geology and the Environment*, *79*(3), 1543–1554. https://doi.org/10.1007/s10064-019-01655-3

Aller, R. C. (1994). Bioturbation and remineralization of sedimentary organic matter: effects of redox oscillation. *Chemical Geology*, *114*(3–4), 331–345. https://doi.org/10.1016/0009-2541(94)90062-0

Amos, R. T., Mayer, K. U., Bekins, B. A., Delin, G. N., & Williams, R. L. (2005). Use of dissolved and vapor-phase gases to investigate methanogenic degradation of petroleum hydrocarbon contamination in the subsurface. *Water Resources Research*, *41*(2), 1–15. https://doi.org/10.1029/2004WR003433

Anneser, B., Einsiedl, F., Meckenstock, R. U., Richters, L., Wisotzky, F., & Griebler, C. (2008). High-resolution monitoring of biogeochemical gradients in a tar oil-contaminated aquifer. *Applied Geochemistry*, *23*(6), 1715–1730. https://doi.org/10.1016/j.apgeochem.2008.02.003

Appelo, C. A. J., & Postma, D. (1993). Geochemistry, groundwater and pollution. *Geochemistry, Groundwater and Pollution*. https://doi.org/10.1016/0016-7037(94)90585-1

Atekwana, E. A., & Atekwana, E. A. (2010). Geophysical signatures of microbial activity at hydrocarbon contaminated sites: A review. *Surveys in Geophysics*, *31*(2), 247–283. https://doi.org/10.1007/s10712-009-9089-8

Atekwana, E. A. E. A. E. A., & Atekwana, E. A. E. A. E. A. (2010). Geophysical signatures of microbial activity at hydrocarbon contaminated sites: A review. *Surveys in Geophysics*, *31*(2), 247–283. https://doi.org/10.1007/s10712-009-9089-8

Ayangbenro, A. S., Olanrewaju, O. S., & Babalola, O. O. (2018). Sulfate-reducing bacteria as an effective tool for sustainable acid mine bioremediation. *Frontiers in Microbiology*, *9*, 1986.

Baalousha, H. M. (2016). Groundwater vulnerability mapping of Qatar aquifers. *Journal of African Earth Sciences*, *124*, 75–93. https://doi.org/10.1016/j.jafrearsci.2016.09.017

Berkowitz, B., Dror, I., & Yaron, B. (2007). *Contaminant geochemistry*. Springer.

Blodau, C., & Moore, T. R. (2003). Experimental response of peatland carbon dynamics to a water table fluctuation. *Journal of Aquatic Sciences*, *65*(3), 1–15. https://doi.org/10.1016/j.jconhyd.2007.07.007

Borch, T., Kretzschmar, R., Skappler, A., Van Cappellen, P., Ginder-Vogel, M., Voegelin, A., & Campbell, K. (2010). Biogeochemical redox processes and their impact on contaminant dynamics. *Environmental Science and Technology*, *44*(1), 15–23. https://doi.org/10.1021/es9026248

Brinch, U. C., Ekelund, F., & Jacobsen, C. S. (2002). Method for spiking soil samples with organic compounds. *Applied and Environmental Microbiology*, *68*(4), 1808–1816. https://doi.org/10.1128/AEM.68.4.1808-1816.2002

Brown, R. A., Hinchee, R. E., Norris, R. D., & Wilson, J. T. (1996). Bioremediation of

petroleum hydrocarbons: A flexible, variable speed technology. *Remediation Journal*, *6*(3), 95–109.

Bunsri, T., Sivakumar, M., & Hagare, D. (1974). *Simulation of Water and Contaminant Transport Through Vadose Zone - Redistribution System*. *1*, 395–416.

Cassidy, D. P., Werkema, D. D., Sauck, W., Atekwana, E., Rossbach, S., & Duris, J. (2001). The Effects of LNAPL Biodegradation Products on Electrical Conductivity Measurements. *Journal of Environmental and Engineering Geophysics*, *6*(1), 47–52. https://doi.org/10.4133/jeeg6.1.47

Cavelan, A., Gol, F., Colombano, S., Davarzani, H., Deparis, J., & Faure, P. (2022). *Science of the Total Environment A critical review of the in fl uence of groundwater level fl uctuations and temperature on LNAPL contaminations in the context of climate change*. *806*. https://doi.org/10.1016/j.scitotenv.2021.150412

Cervantes, F. J., Dijksma, W., Duong-Dac, T., Ivanova, A., Lettinga, G., & Field, J. A. (2001). Anaerobic Mineralization of Toluene by Enriched Sediments with Quinones and Humus as Terminal Electron Acceptors. *Applied and Environmental Microbiology*, *67*(10), 4471–4478. https://doi.org/10.1128/AEM.67.10.4471-4478.2001

Chapelle, F. H., Bradley, P. M., Lovley, D. R., & Vroblesky, D. A. (1996). Measuring rates of biodegradation in a contaminated aquifer using field and laboratory methods. *Ground Water*, *34*(4), 691–698. https://doi.org/10.1111/j.1745-6584.1996.tb02057.x

Chaudhary, A. K., & Vijayakumar, R. P. (2020). Effect of chemical treatment on biological degradation of high-density polyethylene (HDPE). *Environment, Development and Sustainability*, *22*(2), 1093–1104. https://doi.org/10.1007/s10668-018-0236-6

Chen, M., Al-Maktoumi, A., Al-Mamari, H., Izady, A., Reza Nikoo, M., & Al-Busaidi, H. (2020). Oxygenation of aquifers with fluctuating water table: A laboratory and modeling study. *Journal of Hydrology*, *590*(March). https://doi.org/10.1016/j.jhydrol.2020.125261

Chompusri, S., Rivett, M. O., & Mackay, R. (2002). LNAPL redistribution on a fluctuating water table: Column experiments. *IAHS-AISH Publication*, *275*, 225–234.

Clement, T. P., Johnson, C. D., Sun, Y., Klecka, G. M., & Bartlett, C. (2000). Natural attenuation of chlorinated ethene compounds: model development and field-scale application at the Dover site. *Journal of Contaminant Hydrology*, *42*(2–4), 113–140. https://doi.org/10.1016/S0169-7722(99)00098-4

Colombano, S., Davarzani, H., Hullebusch, E. D. van, Ignatiadis, I., Huguenot, H., Zornig, C., & Guyonnet, D. (2020). In situ thermal treatments and enhancements: theory and case study. In *Environmental Soil Remediation and Rehabilitation* (pp. 149–209). Springer.

Crawford, J. J., Traina, S. J., & Tuovinen, O. H. (2000). *in Fixed-Film Sand Columns*. 624–634. https://doi.org/10.2136/sssaj2000.642624x

Cuthbertson, J. F., Kaestner, J. A., & Bruce, L. G. (2010). *Use Of High Concentration Magnesium Sulfate Solution To Remediate Petroleum Impacted Groundwater*. *12*(January).

Davis, G. B., Barber, C., Power, T. R., Thierrin, J., Patterson, B. M., Rayner, J. L., & Wu, Q. (1999). The variability and intrinsic remediation of a BTEX plume in anaerobic sulphate-rich groundwater. *Journal of Contaminant Hydrology*, *36*(3–4), 265–290. https://doi.org/10.1016/S0169-7722(98)00148-X

DeRyck, S. M., Redman, J. D., & Annan, A. P. (1993). Geophysical monitoring of a

controlled kerosene spill. *6th EEGS Symposium on the Application of Geophysics to Engineering and Environmental Problems*, cp-209.

Di Palma, P. R., Parmigiani, A., Huber, C., Guyennon, N., & Viotti, P. (2017). Pore-scale simulations of concentration tails in heterogeneous porous media. *Journal of Contaminant Hydrology*, *205*(July), 47–56. https://doi.org/10.1016/j.jconhyd.2017.08.003

Dobson, R., Schroth, M. H., & Zeyer, J. (2007). Effect of water-table fluctuation on dissolution and biodegradation of a multi-component, light nonaqueous-phase liquid. *Journal of Contaminant Hydrology*, *94*(3–4), 235–248. https://doi.org/10.1016/j.jconhyd.2007.07.007

Dobson, R., Schroth, M. H., Zeyer, J., Aller, R. C., Campbell, C. D., Chapman, S. J., Cameron, C. M., Davidson, M. S., Potts, J. M., Campbell, C. D., Chapman, S. J., Cameron, C. M., Davidson, M. S., & Potts, J. M. (1994). Effect of water-table fluctuation on dissolution and biodegradation of a multi-component, light nonaqueous-phase liquid. *Journal of Contaminant Hydrology*, *94*(3–4), 3593–3599. https://doi.org/10.1016/j.jconhyd.2007.07.007

Doktorgrades, E. (2017). *Monitoring of reducing conditions in soils and implications for biogeochemical processes*.

Dou, J., Liu, X., Hu, Z., & Deng, D. (2008). *Anaerobic BTEX biodegradation linked to nitrate and sulfate reduction*. *151*, 720–729. https://doi.org/10.1016/j.jhazmat.2007.06.043

Ebrahimi, F., Lenhard, R. J., Nakhaei, M., & Nassery, H. R. (2019). An approach to optimize the location of LNAPL recovery wells using the concept of a LNAPL specific yield. *Environmental Science and Pollution Research*, *26*(28), 28714–28724. https://doi.org/10.1007/s11356-019-06052-7

Environmental, Y. S. I. (2005). *Measuring ORP on YSI 6-Series sondes: Tips, cautions and limitations*.

Erdogan, I. G., Fosso-Kankeu, E., Ntwampe, S. K. O., Waanders, F., & Hoth, N. (2020). Seasonal variation of hydrochemical characteristics of open-pit groundwater near a closed metalliferous mine in O'Kiep, Namaqualand Region, South Africa. *Environmental Earth Sciences*, *79*(5), 1–15. https://doi.org/10.1007/s12665-020-8863-2

Fan, X. (2010). Enhancement of anaerobic biodegradation of petroleum hydrocarbons in contaminated groundwater : laboratory mesocosm studies. *Environmental Engineering*.

Farahani, M., & Mahmoudi, D. (2018). Optimization, modeling and its conformity with the reality of physico-chemical and microbial processes of petroleum hydrocarbons reduction in soil: a case study of Tehran oil refinery. *Environmental Earth Sciences*, *77*(9), 1–12. https://doi.org/10.1007/s12665-018-7512-5

Fent, K. (2004). Ecotoxicological effects at contaminated sites. *Toxicology*, *205*(3), 223–240. https://doi.org/10.1016/j.tox.2004.06.060

Flores Orozco, A., Kemna, A., Oberdörster, C., Zschornack, L., Leven, C., Dietrich, P., & Weiss, H. (2012). Delineation of subsurface hydrocarbon contamination at a former hydrogenation plant using spectral induced polarization imaging. *Journal of Contaminant Hydrology*, *136–137*, 131–144. https://doi.org/10.1016/j.jconhyd.2012.06.001

Fry, V. A., Selker, J. S., & Gorelick, S. M. (1997). Experimental investigations for trapping oxygen gas in saturated porous media for in situ bioremediation. *Water Resources Research*, *33*(12), 2687–2696. https://doi.org/10.1029/97WR02428

Garg, S., Newell, C. J., Kulkarni, P. R., King, D. C., Adamson, D. T., Renno, M. I., &

Sale, T. (2017). Overview of Natural Source Zone Depletion: Processes, Controlling Factors, and Composition Change. *Groundwater Monitoring and Remediation*, *37*(3), 62–81. https://doi.org/10.1111/gwmr.12219

Gatsios, E., García-Rincón, J., Rayner, J. L., McLaughlan, R. G., & Davis, G. B. (2018). LNAPL transmissivity as a remediation metric in complex sites under water table fluctuations. *Journal of Environmental Management*, *215*, 40–48. https://doi.org/10.1016/j.jenvman.2018.03.026

Gieg, L. M., Fowler, S. J., & Berdugo-Clavijo, C. (2014). Syntrophic biodegradation of hydrocarbon contaminants. *Current Opinion in Biotechnology*, *27*, 21–29. https://doi.org/10.1016/j.copbio.2013.09.002

Gray, N. D., Sherry, A., Hubert, C., Dolfing, J., & Head, I. M. (2010). Methanogenic degradation of petroleum hydrocarbons in subsurface environments: Remediation, heavy oil formation, and energy recovery. In *Advances in Applied Microbiology* (1st ed., Vol. 72, Issue C). Elsevier Inc. https://doi.org/10.1016/S0065-2164(10)72005-0

Greskowiak, J., Prommer, H., Massmann, G., Johnston, C. D., Nützmann, G., & Pekdeger, A. (2005). The impact of variably saturated conditions on hydrogeochemical changes during artificial recharge of groundwater. *Applied Geochemistry*, *20*(7), 1409–1426. https://doi.org/10.1016/j.apgeochem.2005.03.002

Guarnaccia, J., Pinder, G., & Fishman, M. (1997). *Project Summary NAPL : Simulator Documentation*.

Gupta, P. K., & Yadav, B. K. (2020). Three-Dimensional Laboratory Experiments on Fate and Transport of LNAPL under Varying Groundwater Flow Conditions. *Journal of Environmental Engineering*, *146*(4), 04020010.

https://doi.org/10.1061/(asce)ee.1943-7870.0001672

Gupta, P. K., Yadav, B., & Yadav, B. K. (2019). Assessment of LNAPL in Subsurface under Fluctuating Groundwater Table Using 2D Sand Tank Experiments. *Journal of Environmental Engineering*, *145*(9), 04019048. https://doi.org/10.1061/(asce)ee.1943-7870.0001560

Gupta, P., & Yadav, B. (2017). Bioremediation of Nonaqueous Phase Liquids (NAPLs)-Polluted Soil-Water Resources. *Environmental Pollutants and Their Bioremediation Approaches , July*, 241–256. https://doi.org/10.1201/9781315173351-9

Haberer, C. M., Muniruzzaman, M., Grathwohl, P., & Rolle, M. (2015). Diffusive-Dispersive and Reactive Fronts in Porous Media: Iron(II) Oxidation at the Unsaturated-Saturated Interface. *Vadose Zone Journal*, *14*(5), vzj2014.07.0091. https://doi.org/10.2136/vzj2014.07.0091

Haberer, C. M., Rolle, M., Cirpka, O. A., & Grathwohl, P. (2012). Oxygen Transfer in a Fluctuating Capillary Fringe. *Vadose Zone Journal*, *11*(3), vzj2011.0056. https://doi.org/10.2136/vzj2011.0056

Haritash, A. K., & Kaushik, C. P. (2009). Biodegradation aspects of Polycyclic Aromatic Hydrocarbons (PAHs): A review. *Journal of Hazardous Materials*, *169*(1–3), 1–15. https://doi.org/10.1016/j.jhazmat.2009.03.137

Hatipoğlu-Bağci, Z., & Motz, L. H. (2019). Methods for investigation of natural attenuation and modeling of petroleum hydrocarbon contamination in coastal aquifers. *Jeoloji Muhendisligi Dergisi*, *43*(1), 131–154. https://doi.org/10.24232/jmd.572505

He, S., & Wu, J. (2019). Hydrogeochemical Characteristics, Groundwater Quality, and Health Risks from Hexavalent Chromium and Nitrate in Groundwater of Huanhe

Formation in Wuqi County, Northwest China. *Exposure and Health*, *11*(2), 125–137. https://doi.org/10.1007/s12403-018-0289-7

Holman, H. Y., & Tsang, Y. W. (1995). *Effects of soil moisture on biodegradation of petroleum hydrocarbons*. Battelle Press, Columbus, OH (United States).

Huang, W. H., Asce, S. M., Kao, C. M., & Asce, F. (2016). Bioremediation of Petroleum-Hydrocarbon Contaminated Groundwater under Sulfate-Reducing Conditions: Effectiveness and Mechanism Study. *Journal of Environmental Engineering*, *142*(3), 04015089. https://doi.org/10.1061/(asce)ee.1943-7870.0001055

Huang, X., Liu, G., Xia, C., & Yang, M. (2021). Simulated groundwater dynamics and solute transport in a coastal phreatic aquifer subjected to different tides. *Marine Georesources and Geotechnology*, *39*(6), 719–734. https://doi.org/10.1080/1064119X.2020.1754975

Huling, S. G., Weaver, J. W., & Environmental, R. S. K. (1991). *Ground Water Issue*.

IPCC. (2014). Part A: Global and Sectoral Aspects. (Contribution of Working Group II to the Fifth Assessment Report of the Intergovernmental Panel on Climate Change). *Climate Change 2014: Impacts, Adaptation, and Vulnerability.*, 1132. https://www.ipcc.ch/pdf/assessment-report/ar5/wg2/WGIIAR5-FrontMatterA_FINAL.pdf

Irianni-Renno, M., Akhbari, D., Olson, M. R., Byrne, A. P., Lefèvre, E., Zimbron, J., Lyverse, M., Sale, T. C., & De Long, S. K. (2016). Comparison of bacterial and archaeal communities in depth-resolved zones in an LNAPL body. *Applied Microbiology and Biotechnology*, *100*(7), 3347–3360. https://doi.org/10.1007/s00253-015-7106-z

Ismail, R. E. (2019). *Groundwater pollution by petroleumderived contaminants in*

coastal semiarid environment. https://doi.org/10.5339/qfarc.2018.eepd709

Ismail, R., Shafieiyoun, S., & Al-Raoush, R. I. (2020). *Influence of Water Table Fluctuation on Natural Source Zone Depletion in Hydrocarbon Contaminated Subsurface Environments*.

Jeong, J., & Charbeneau, R. J. (2014). An analytical model for predicting LNAPL distribution and recovery from multi-layered soils. *Journal of Contaminant Hydrology*, *156*, 52–61.

Jeong, Jina, & Park, E. (2017). A shallow water table fluctuation model in response to precipitation with consideration of unsaturated gravitational flow. *Water Resources Research*, *53*(4), 3505–3512. https://doi.org/10.1002/2016WR020177

Jia, M., Bian, X., & Yuan, S. (2017). Production of hydroxyl radicals from Fe(II) oxygenation induced by groundwater table fluctuations in a sand column. *Science of the Total Environment*, *584–585*, 41–47. https://doi.org/10.1016/j.scitotenv.2017.01.142

Jin, H. M., Kim, J. M., Lee, H. J., Madsen, E. L., & Jeon, C. O. (2012). *Alteromonas As a Key Agent of Polycyclic Aromatic Hydrocarbon Biodegradation in Crude Oil-Contaminated Coastal Sediment*. https://doi.org/10.1021/es3018545

Johnston, C. D., & Trefry, M. G. (2009). Characteristics of light nonaqueous phase liquid recovery in the presence of fine-scale soil layering. *Water Resources Research*, *45*(5), 1–20. https://doi.org/10.1029/2008WR007218

Kehew, A. E., & Lynch, P. M. (2011). Concentration trends and water-level fluctuations at underground storage tank sites. *Environmental Earth Sciences*, *62*(5), 985–998. https://doi.org/10.1007/s12665-010-0583-6

Kemblowski, M. W., & Chiang, C. Y. (1990). Hydrocarbon thickness fluctuations in monitoring wells. *Groundwater*, *28*(2), 244–252.

Khan, M. A. I., Biswas, B., Smith, E., Naidu, R., & Megharaj, M. (2018). Toxicity assessment of fresh and weathered petroleum hydrocarbons in contaminated soil-a review. *Chemosphere*.

Kim, J. M., Le, N. T., Chung, B. S., Park, J. H., Bae, J. W., Madsen, E. L., & Jeon, C. O. (2008). Influence of soil components on the biodegradation of benzene, toluene, ethylbenzene, and o-, m-, and p-xylenes by the newly isolated bacterium Pseudoxanthomonas spadix BD-a59. *Applied and Environmental Microbiology*, *74*(23), 7313–7320. https://doi.org/10.1128/AEM.01695-08

Knight, R. (2001). Ground penetrating radar for environmental applications. *Annual Review of Earth and Planetary Sciences*, *29*, 229–255. https://doi.org/10.1146/annurev.earth.29.1.229

Langevoort, M. (2009). Multiphase flow and enhanced biodegradation of dense non-aqueous phase liquids (PhD Dissertation). In *Geologica Ultraiectina* (Issue 303).

Laverman, A. M., Pallud, C., Abell, J., & Cappellen, P. Van. (2012). Comparative survey of potential nitrate and sulfate reduction rates in aquatic sediments. *Geochimica et Cosmochimica Acta*, *77*, 474–488. https://doi.org/10.1016/j.gca.2011.10.033

Ledin, A., Ask, L., & Bjerg, P. L. (2011). *Quantitative determination of toluene , ethylbenzene , and xylene degradation products in contaminated groundwater by solid-phase extraction and in-vial derivatization*. *7319*. https://doi.org/10.1080/03067310500194920

Lee, B. C., Lee, J., Cheon, J., & Lee, K. (2001). Attenuation of Petroleum Hydrocarbons in Smear Zones: A Case Study. *Journal of Environmental Engineering*, *127*, 639–647.

Lee, J., Cheon, J., & Lee, K. (n.d.). *Factors affecting the distribution of hydrocarbon*

contaminants and hydrogeochemical parameters in a shallow sand aquifer. *50*, 139–158.

Lee, J., Cheon, J., Lee, K., Lee, S., & Lee, M. (2001). System Contaminated with Petroleum Hydrocarbons. *J. Environ.Qual.*, *30*(October), 1548–1563.

Lee, J. Y., Cheon, J. Y., Lee, K. K., Lee, S. Y., & Lee, M. H. (2001). Factors affecting the distribution of hydrocarbon contaminants and hydrogeochemical parameters in a shallow sand aquifer. *Journal of Contaminant Hydrology*, *50*(1–2), 139–158. https://doi.org/10.1016/S0169-7722(01)00101-2

Lenhard, R. J. (1992). Measurement and modeling of three-phase saturation-pressure hysteresis. *Journal of Contaminant Hydrology*, *9*(3), 243–269.

Lewis, J., & Sjöstrom, J. (2010). Optimizing the experimental design of soil columns in saturated and unsaturated transport experiments. *Journal of Contaminant Hydrology*, *115*(1–4), 1–13.

Li, X., Chang, S. X., & Salifu, K. F. (2014). Soil texture and layering effects on water and salt dynamics in the presence of a water table: A review. *Environmental Reviews*, *22*(1), 41–50. https://doi.org/10.1139/er-2013-0035

Liu, X., Wang, J., Zhang, D., & Li, Y. (2009). Grey relational analysis on the relation between marine environmental factors and oxidation-reduction potential. *Chinese Journal of Oceanology and Limnology*, *27*(3), 583–586. https://doi.org/10.1007/s00343-009-9152-9

Logeshwaran, P., Megharaj, M., Chadalavada, S., Bowman, M., & Naidu, R. (2018). Petroleum hydrocarbons (PH) in groundwater aquifers: An overview of environmental fate, toxicity, microbial degradation and risk-based remediation approaches. *Environmental Technology and Innovation*, *10*, 175–193. https://doi.org/10.1016/j.eti.2018.02.001

Lopes de Castro, D., & Branco, R. M. G. C. (2003). 4-D ground penetrating radar monitoring of a hydrocarbon leakage site in Fortaleza (Brazil) during its remediation process: A case history. *Journal of Applied Geophysics*, *54*(1–2), 127–144. https://doi.org/10.1016/j.jappgeo.2003.08.021

Lueders, T. (2017). The ecology of anaerobic degraders of BTEX hydrocarbons in aquifers. *FEMS Microbiology Ecology*, *93*(1), 1–13. https://doi.org/10.1093/femsec/fiw220

Lv, H., Su, X., Wang, Y., Dai, Z., & Liu, M. (2018). Chemosphere Effectiveness and mechanism of natural attenuation at a petroleum- hydrocarbon contaminated site. *Chemosphere*, *206*, 293–301. https://doi.org/10.1016/j.chemosphere.2018.04.171

Maliszewska-Kordybach, B. (1996). Polycyclic aromatic hydrocarbons in agricultural soils in Poland: preliminary proposals for criteria to evaluate the level of soil contamination. *Applied Geochemistry*, *11*(1–2), 121–127.

Marić, N., Štrbački, J., Mrazovac Kurilić, S., Beškoski, V. P., Nikić, Z., Ignjatović, S., & Malbašić, J. (2020). Hydrochemistry of groundwater contaminated by petroleum hydrocarbons: the impact of biodegradation (Vitanovac, Serbia). *Environmental Geochemistry and Health*, *42*(7), 1921–1935. https://doi.org/10.1007/s10653-019-00462-9

Maslehuddin, M. (2002). *CHARACTERISTICS OF THE ARABIAN GULF ENVIRONMENT AND ITS IMPACT ON CONCRETE DURABILITY – AN OVERVIEW*. *3*(December).

Masson-Delmotte, V., Zhai, P., Pirani, A., Connors, S. L., Péan, C., Berger, S., Caud, N., Chen, Y., Goldfarb, L., & Gomis, M. I. (2021). Climate Change 2021: The Physical Science Basis. Contribution of Working Group I to the Sixth Assessment Report of the Intergovernmental Panel on Climate Change. *IPCC: Geneva*,

Switzerland.

McAlexander, B., & Sihota, N. (2019). Influence of Ambient Temperature, Precipitation, and Groundwater Level on Natural Source Zone Depletion Rates at a Large Semiarid LNAPL Site. *Groundwater Monitoring and Remediation*, *39*(1), 54–65. https://doi.org/10.1111/gwmr.12309

McMahon, P. B., Chapelle, F. H., & Bradley, P. M. (2011). Evolution of redox processes in groundwater. *ACS Symposium Series*, *1071*(January), 581–597. https://doi.org/10.1021/bk-2011-1071.ch026

Meckenstock, R. U., Elsner, M., Griebler, C., Lueders, T., Stumpp, C., Aamand, J., Agathos, S. N., Albrechtsen, H. J., Bastiaens, L., Bjerg, P. L., Boon, N., Dejonghe, W., Huang, W. E., Schmidt, S. I., Smolders, E., Sørensen, S. R., Springael, D., Breukelen, B. M. Van, & Van Breukelen, B. M. (2015). Biodegradation: Updating the Concepts of Control for Microbial Cleanup in Contaminated Aquifers. *Environmental Science and Technology*, *49*(12), 7073–7081. https://doi.org/10.1021/acs.est.5b00715

Meng, L., Zuo, R., Wang, J. sheng, Li, Q., Du, C., Liu, X., & Chen, M. (2021). Response of the redox species and indigenous microbial community to seasonal groundwater fluctuation from a typical riverbank filtration site in Northeast China. *Ecological Engineering*, *159*(October 2020), 106099. https://doi.org/10.1016/j.ecoleng.2020.106099

Mercer, J. W., Cohen, R. M., & Va, U. S. A. (1990). Review Paper A REVIEW OF IMMISCIBLE FLUIDS IN THE SUBSURFACE : PROPERTIES , MODELS , CHARACTERIZATION AND REMEDIATION Nonaqueous phase liquids (NAPL ' s) have been discovered at numerous hazardous waste sites (e . g ., Faust , 1985 ; Mercer et al ., 19. *Journal of Contaminant Hydrology*, *6*, 107–163.

Miao, Z., Brusseau, M. L., Carroll, K. C., Carreón-Diazconti, C., & Johnson, B. (2012). Sulfate reduction in groundwater: characterization and applications for remediation. *Environmental Geochemistry and Health*, *34*(4), 539–550.

Naudet, V., Revil, A., Rizzo, E., Bottero, J. Y., & Bégassat, P. (2004). Groundwater redox conditions and conductivity in a contaminant plume from geoelectrical investigations. *Hydrology and Earth System Sciences*, *8*(1), 8–22. https://doi.org/10.5194/hess-8-8-2004

Newell, C. J., Acree, D. A., Randall, R. R., & Huling, S. G. (1995). Light Nonaqueous Phase Liquids. *Ground Water Issue*, 1–28. https://doi.org/10.1056/NEJMoa030660

Newton, J. (1990). Remediation of petroleum contaminated soils. *Pollut Eng*, *2*, 46–52.

Ngueleu, S. K., Al-Raoush, R. I., Shafieiyoun, S., Rezanezhad, F., & Van Cappellen, P. (2019). Biodegradation Kinetics of Benzene and Naphthalene in the Vadose and Saturated Zones of a (Semi)-Arid Saline Coastal Soil Environment. *Geofluids*, *2019*(December). https://doi.org/10.1155/2019/8124716

Ngueleu, S. K., Rezanezhad, F., Al-Raoush, R. I., & Van Cappellen, P. (2018). Sorption of benzene and naphthalene on (semi)-arid coastal soil as a function of salinity and temperature. *Journal of Contaminant Hydrology*, *219*(May 2019), 61–71. https://doi.org/10.1016/j.jconhyd.2018.11.001

Ning, Z., Zhang, M., He, Z., Cai, P., Guo, C., & Wang, P. (2018). Spatial pattern of bacterial community diversity formed in different groundwater field corresponding to electron donors and acceptors distributions at a petroleum-contaminated site. *Water (Switzerland)*, *10*(7), 1–14. https://doi.org/10.3390/w10070842

Njobuenwu, D. O., Amadi, S. A., & Ukpaka, P. C. (2005). Dissolution rate of BTEX

contaminants in water. *Canadian Journal of Chemical Engineering*, *83*(6), 985–989. https://doi.org/10.1002/cjce.5450830608

Nygren, M., Giese, M., Kløve, B., Haaf, E., Rossi, P. M., & Barthel, R. (2020). Changes in seasonality of groundwater level fluctuations in a temperate-cold climate transition zone. *Journal of Hydrology X*, *8*(August), 100062. https://doi.org/10.1016/j.hydroa.2020.100062

Ohio EPA. (2014). *Reduction-Oxidation (Redox) Control in Ohio's Ground Water Quality The Technical Series on Ground Water Quality*. *November*.

Ossai, I. C., Ahmed, A., Hassan, A., & Hamid, F. S. (2020). Remediation of soil and water contaminated with petroleum hydrocarbon: A review. *Environmental Technology and Innovation*, *17*, 100526. https://doi.org/10.1016/j.eti.2019.100526

Pett-Ridge, J., & Firestone, M. K. (2005). Redox fluctuation structures microbial communities in a wet tropical soil. *Appl. Environ. Microbiol.*, *71*(11), 6998–7007.

Phelps, C. D., & Young, L. Y. (1999). *Anaerobic biodegradation of BTEX and gasoline in various aquatic sediments*. 15–25.

Porowska, D. (2015). Determination of the origin of dissolved inorganic carbon in groundwater around a reclaimed landfill in Otwock using stable carbon isotopes. *Waste Management*, *39*, 216–225. https://doi.org/10.1016/j.wasman.2015.01.044

Prusty, B. A. K., Chandra, R., & Azeez, P. A. (2017). *Wetland Science: Perspectives From South Asia*. Springer.

Qi, S., Luo, J., O'Connor, D., Cao, X., & Hou, D. (2020). Influence of groundwater table fluctuation on the non-equilibrium transport of volatile organic contaminants in the vadose zone. *Journal of Hydrology*, *580*(October 2019), 124353. https://doi.org/10.1016/j.jhydrol.2019.124353

Ramesh Kumar, A., & Riyazuddin, P. (2012). Seasonal variation of redox species and redox potentials in shallow groundwater: A comparison of measured and calculated redox potentials. *Journal of Hydrology*, *444–445*, 187–198. https://doi.org/10.1016/j.jhydrol.2012.04.018

Reddi, L., Han, W., & Banks, M. K. (1998). MASS Loss FROM LNAPL POOLS UNDER FLUCTUATING WATER _ ~ H (t = O). *Journal of Environmental Engineering*, *124*(December), 1171–1177. https://doi.org/10.1061/(ASCE)0733-9372(1998)124:12(1171)

Reddy, K. R., & DeLaune, R. D. (2008). *Biogeochemistry of wetlands: science and applications*. CRC press.

Rees, H. C., Oswald, S. E., Banwart, S. A., Pickup, R. W., & Lerner, D. N. (2007). Biodegradation processes in a laboratory-scale groundwater contaminant plume assessed by fluorescence imaging and microbial analysis. *Applied and Environmental Microbiology*, *73*(12), 3865–3876. https://doi.org/10.1128/AEM.02933-06

Rezanezhad, F., Couture, R. M., Kovac, R., O'Connell, D., & Van Cappellen, P. (2014). Water table fluctuations and soil biogeochemistry: An experimental approach using an automated soil column system. *Journal of Hydrology*, *509*, 245–256. https://doi.org/10.1016/j.jhydrol.2013.11.036

Rivett, M. O., Feenstra, S., & Cherry, J. A. (2001). *A controlled field experiment on groundwater contamination by a multicomponent DNAPL : creation of the emplaced-source and overview of dissolved plume development*.

Ronen, D., Scher, H., & Blunt, M. (2000). Field observations of a capillary fringe before and after a rainy season. *Journal of Contaminant Hydrology*, *44*(2), 103–118. https://doi.org/https://doi.org/10.1016/S0169-7722(00)00096-6

Ruffino, B., & Zanetti, M. (2009). Adsorption study of several hydrophobic organic contaminants on an aquifer material. *American Journal of Environmental Sciences*, *5*(4), 507–515. https://doi.org/10.3844/ajessp.2009.507.515

Rühle, F. A., von Netzer, F., Lueders, T., & Stumpp, C. (2015). Response of Transport Parameters and Sediment Microbiota to Water Table Fluctuations in Laboratory Columns. *Vadose Zone Journal*, *14*(5), vzj2014.09.0116. https://doi.org/10.2136/vzj2014.09.0116

Sale, T., Gallo, S., Karimi, K., Irianni-renno, M., Lyverse, M., Hopkins, H., Blotevogel, J., & Burge, S. (2021). Real-time soil and groundwater monitoring via spatial and temporal resolution of biogeochemical potentials. *Journal of Hazardous Materials*, *408*(October 2020), 124403. https://doi.org/10.1016/j.jhazmat.2020.124403

Sardin, T., Dowd, S., Herman, D., & Maier, R. (2009). Chapter 6 - Aquatic Environments. In *Environmental Microbiology*. Shanghai, China: Elsevier Academic,. https://doi.org/https://doi.org/10.1016/B978-0-12-370519-8.00006-7

Shafieiyoun, S., Al-Raoush, R. I., Ismail, R. E., Ngueleu, S. K., Rezanezhad, F., & Van Cappellen, P. (2020). Effects of dissolved organic phase composition and salinity on the engineered sulfate application in a flow-through system. *Environmental Science and Pollution Research*, *27*(11), 11842–11854. https://doi.org/10.1007/s11356-020-07696-6

Shafieiyoun, S., Al-Raoush, R. I., Ngueleu, S. K., Rezanezhad, F., & Van Cappellen, P. (2020). Enhancement of Naphthalene Degradation by a Sequential Sulfate Injection Scenario in a (Semi)-Arid Coastal Soil: a Flow-Through Reactor Experiment. *Water, Air, and Soil Pollution*, *231*(8), 1–16. https://doi.org/10.1007/s11270-020-04725-5

Shi, B., Ngueleu, S. K., Rezanezhad, F., Slowinski, S., Pronk, G. J., Smeaton, C. M., Stevenson, K., Al-Raoush, R. I., & Van Cappellen, P. (2020). Sorption and desorption of the model aromatic hydrocarbons naphthalene and benzene: Effects of temperature and soil composition. *Front. Environ. Chem. 1: 581103. Doi: 10.3389/Fenvc*.

Shrestha, S., & Kazama, F. (2007). Assessment of surface water quality using multivariate statistical techniques: A case study of the Fuji river basin, Japan. *Environmental Modelling and Software*, *22*(4), 464–475. https://doi.org/10.1016/j.envsoft.2006.02.001

Sihota, N.J., Trost, J. J., Bekins, B. A., Berg, A., Delin, G. N., Mason, B., Warren, E., & Mayer, K. U. (2016). Seasonal Variability in Vadose Zone Biodegradation at a Crude Oil Pipeline Rupture Site. *Vadose Zone Journal*, *15*(5), vzj2015.09.0125. https://doi.org/10.2136/vzj2015.09.0125

Sihota, Natasha J, Singurindy, O., & Mayer, K. U. (2011). *CO 2 -Efflux Measurements for Evaluating Source Zone Natural Attenuation Rates in a Petroleum Hydrocarbon Contaminated Aquifer*. *45*(2), 482–488.

Sinke, A. J. C. C., Dury, O., & Zobrist, J. (1998). Effects of a fluctuating water table: Column study on redox dynamics and fate of some organic pollutants. *Journal of Contaminant Hydrology*, *33*(1–2), 231–246. https://doi.org/10.1016/S0169-7722(98)00072-2

Soga, K., Page, J. W. E., & Illangasekare, T. H. (2004). A review of NAPL source zone remediation efficiency and the mass flux approach. *Journal of Hazardous Materials*, *110*(1–3), 13–27. https://doi.org/10.1016/j.jhazmat.2004.02.034

Sookhak Lari, K., Davis, G. B., Rayner, J. L., Bastow, T. P., & Puzon, G. J. (2019). Natural source zone depletion of LNAPL: A critical review supporting modelling

approaches. *Water Research*, *157*(5), 630–646. https://doi.org/10.1016/j.watres.2019.04.001

Sookhak Lari, K., Johnston, C. D., Rayner, J. L., & Davis, G. B. (2018). Field-scale multi-phase LNAPL remediation: Validating a new computational framework against sequential field pilot trials. *Journal of Hazardous Materials*, *345*, 87–96. https://doi.org/10.1016/j.jhazmat.2017.11.006

Steffen, K., Herbst, F., Bahr, A., Pieper, D. H., Jehmlich, N., Seifert, J., Bergen, M. Von, Bombach, P., Richnow, H. H., & Vogt, C. (2015). *Anaerobic naphthalene degradation by sulfate- reducing Desulfobacteraceae from various anoxic*. *September 2014*, 1–13. https://doi.org/10.1093/femsec/fiv006

Suk, H., Zheng, K. W., Liao, Z. Y., Liang, C. P., Wang, S. W., & Chen, J. S. (2022). A new analytical model for transport of multiple contaminants considering remediation of both NAPL source and downgradient contaminant plume in groundwater. *Advances in Water Resources*, *167*(July), 104290. https://doi.org/10.1016/j.advwatres.2022.104290

Sun, L., Chen, Y., Jiang, L., & Cheng, Y. (2018). Numerical Simulation of the Effect about Groundwater Level Fluctuation on the Concentration of BTEX Dissolved into Source Zone. *IOP Conference Series: Earth and Environmental Science*, *111*(1). https://doi.org/10.1088/1755-1315/111/1/012017

Suthersan, S., Houston, K., Schnobrich, M., & Horst, J. (2011). Engineered anaerobic bio-oxidation systems for petroleum hydrocarbon residual source zones with soluble sulfate application. *Ground Water Monitoring and Remediation*, *31*(3), 41–46. https://doi.org/10.1111/j.1745-6592.2011.01354.x

Teramoto, E. H., & Chang, H. K. (2017). Field data and numerical simulation of btex concentration trends under water table fluctuations: Example of a jet fuel-

contaminated site in Brazil. *Journal of Contaminant Hydrology*, *198*, 37–47. https://doi.org/10.1016/j.jconhyd.2017.01.002

Teramoto, E. H., Pede, M. A. Z., & Chang, H. K. (2020). Impact of water table fluctuations on the seasonal effectiveness of the pump-and-treat remediation in wet–dry tropical regions. *Environmental Earth Sciences*, *79*(18). https://doi.org/10.1007/s12665-020-09182-1

Toxfaqs, D. R. (1999). *TOTAL PETROLEUM HYDROCARBONS (TPH)*. *August*.

Tutmez, B., Hatipoglu, Z., & Kaymak, U. (2006). Modelling electrical conductivity of groundwater using an adaptive neuro-fuzzy inference system. *Computers and Geosciences*, *32*(4), 421–433. https://doi.org/10.1016/j.cageo.2005.07.003

Unold, M., Kasteel, R., Groeneweg, J., & Vereecken, H. (2009). Transport and transformation of sulfadiazine in soil columns packed with a silty loam and a loamy sand. *Journal of Contaminant Hydrology*, *103*(1), 38–47. https://doi.org/https://doi.org/10.1016/j.jconhyd.2008.09.002

Vaezihir, A., & Molson, J. (2012). *Field-Scale Modeling of Benzene , Toluene , Ethylbenzene , and Xylenes (BTEX) Released from Multiple Source Zones*. *9868*. https://doi.org/10.1080/10889868.2012.687415

Van De Ven, C. J. C., Scully, K. H., Frame, M. A., Sihota, N. J., & Mayer, K. U. (2021). Impacts of water table fluctuations on actual and perceived natural source zone depletion rates. *Journal of Contaminant Hydrology*, *238*(July 2020), 103771. https://doi.org/10.1016/j.jconhyd.2021.103771

Varjani, S. J. (2017). Microbial degradation of petroleum hydrocarbons. *Bioresource Technology*, *223*, 277–286. https://doi.org/10.1016/j.biortech.2016.10.037

Vincent, A. O., Felix, E., Weltime, M. O., Ize-Iyamu, O. K., & Daniel, E. E. (2011). Microbial Degradation and its Kinetics on Crude Oil Polluted Soil. *Research*

Journal of Chemical Sciences Sept. Res.J.Chem.Sci, *1*(6), 8–14.

Vroblesky, D. A., Bradley, P. M., & Chapelle, F. H. (1996). Influence of electron donor on the minimum sulfate concentration required for sulfate reduction in a petroleum hydrocarbon-contaminated aquifer. *Environmental Science & Technology*, *30*(4), 1377–1381.

Wang, P., Yu, J., Pozdniakov, S. P., Grinevsky, S. O., & Liu, C. (2014). Shallow groundwater dynamics and its driving forces in extremely arid areas: A case study of the lower Heihe River in northwestern China. *Hydrological Processes*, *28*(3), 1539–1553. https://doi.org/10.1002/hyp.9682

Water, U. N. (2021). *The United Nations World Water Development Report 2021: Valuing Water*. UNESCO: Paris, France.

Weelink, S. A. B., van Eekert, M. H. A., & Stams, A. J. M. (2010). Degradation of BTEX by anaerobic bacteria: Physiology and application. *Reviews in Environmental Science and Biotechnology*, *9*(4), 359–385. https://doi.org/10.1007/s11157-010-9219-2

Wei, Y., Thomson, N. R., Aravena, R., Marchesi, M., Barker, J. F., Madsen, E. L., Kolhatkar, R., Buscheck, T., Hunkeler, D., & DeRito, C. M. (2018). Infiltration of Sulfate to Enhance Sulfate-Reducing Biodegradation of Petroleum Hydrocarbons. *Groundwater Monitoring and Remediation*, *38*(4), 73–87. https://doi.org/10.1111/gwmr.12298

Werner, D., & Höhener, P. (2002). The influence of water table fluctuations on the volatilization of contaminants from groundwater. *IAHS-AISH Publication*, *275*, 213–218.

Williams, M. D., & Oostrom, M. (2000). Oxygenation of anoxic water in a fluctuating water table system: An experimental and numerical study. *Journal of Hydrology*,

230(1–2), 70–85. https://doi.org/10.1016/S0022-1694(00)00172-4

Wurgaft, E., Findlay, A. J., Vigderovich, H., Herut, B., & Sivan, O. (2019). Sulfate reduction rates in the sediments of the Mediterranean continental shelf inferred from combined dissolved inorganic carbon and total alkalinity profiles. *Marine Chemistry*, *211*(June 2018), 64–74. https://doi.org/10.1016/j.marchem.2019.03.004

Xia, X., Cheng, L., Zhu, Y., Liu, Y., Wang, K., Ding, A., Cai, Z., Shi, H., & Zuo, L. (2020). Response of soil bacterial community and geochemical parameters to cyclic groundwater-level oscillations in laboratory columns. *Vadose Zone Journal*, *19*(1), 1–12. https://doi.org/10.1002/vzj2.20011

Xie, W. H., Shiu, W. Y., & Mackay, D. (1997). A review of the effect of salts on the solubility of organic compounds in seawater. *Marine Environmental Research*, *44*(4), 429–444. https://doi.org/10.1016/S0141-1136(97)00017-2

Yadav, Brijesh K., Shrestha, S. R., & Hassanizadeh, S. M. (2012). Biodegradation of toluene under seasonal and diurnal fluctuations of soil-water temperature. *Water, Air, and Soil Pollution*, *223*(7), 3579–3588. https://doi.org/10.1007/s11270-011-1052-x

Yadav, Brijesh Kumar, & Hassanizadeh, S. M. (2011). An overview of biodegradation of LNAPLs in coastal (Semi)-arid environment. *Water, Air, and Soil Pollution*, *220*(1–4), 225–239. https://doi.org/10.1007/s11270-011-0749-1

Yang, Y. S., Li, P., Zhang, X., Li, M., Lu, Y., Xu, B., & Yu, T. (2017). Lab-based investigation of enhanced BTEX attenuation driven by groundwater table fluctuation. *Chemosphere*, *169*, 678–684. https://doi.org/10.1016/j.chemosphere.2016.11.128

Zanello, V., Scherger, L. E., & Lexow, C. (2021). Assessment of groundwater

contamination risk by BTEX from residual fuel soil phase. *SN Applied Sciences*, *3*(3), 1–20. https://doi.org/10.1007/s42452-021-04325-w

Zeman, N. R., Irianni Renno, M., Olson, M. R., Wilson, L. P., Sale, T. C., & De Long, S. K. (2014). Temperature impacts on anaerobic biotransformation of LNAPL and concurrent shifts in microbial community structure. *Biodegradation*, *25*(4), 569–585. https://doi.org/10.1007/s10532-014-9682-5

Zhang, M., Guo, C., Shi, C., Ning, Z., & Chen, Z. (2021). A quantitative redox zonation model for developing natural attenuation-based remediation strategy in hydrocarbon-contaminated aquifers. *Journal of Cleaner Production*, *290*, 125743. https://doi.org/10.1016/j.jclepro.2020.125743

Zhang, Z., & Furman, A. (2021). Soil redox dynamics under dynamic hydrologic regimes - A review. *Science of the Total Environment*, *763*, 143026. https://doi.org/10.1016/j.scitotenv.2020.143026

Zheng, F., Gao, Y., Sun, Y., Shi, X., Xu, H., & Wu, J. (2015). Influence de la vitesse d'écoulement et de l'hétérogénéité spatiale sur la migration de phase liquide non aqueuse dense (DNAPL) en milieu poreux: aperçus des expériences en laboratoire et de modélisation numérique. *Hydrogeology Journal*, *23*(8), 1703–1718. https://doi.org/10.1007/s10040-015-1314-6

Zhou, A. xia, Zhang, Y. ling, Dong, T. zi, Lin, X. yu, & Su, X. si. (2015). Response of the microbial community to seasonal groundwater level fluctuations in petroleum hydrocarbon-contaminated groundwater. *Environmental Science and Pollution Research*, *22*(13), 10094–10106. https://doi.org/10.1007/s11356-015-4183-6

Zhou, J. F., Li, Y., Xu, J., & Kamon, M. (2014). Testing of NAPL simulator to predict migration of a light nonaqueous phase liquid (LNAPL) under water table fluctuation in a sandy medium. *Journal of Central South University*, *21*(1), 317–

325. https://doi.org/10.1007/s11771-014-1943-2

Zhou, Q. X. (1995). Ecology of combined pollution. *China Environmental Science Press, Beijing*, 127–128.

Zhu, J., & Sun, D. (2016). Significance of groundwater flux on contaminant concentration and mass discharge in the nonaqueous phase liquid (NAPL) contaminated zone. *Journal of Contaminant Hydrology*, *192*, 158–164. https://doi.org/10.1016/j.jconhyd.2016.08.002

APPENDIX A: SOIL SAMPLING AND EXPERIMENT EQUIPMENT'S

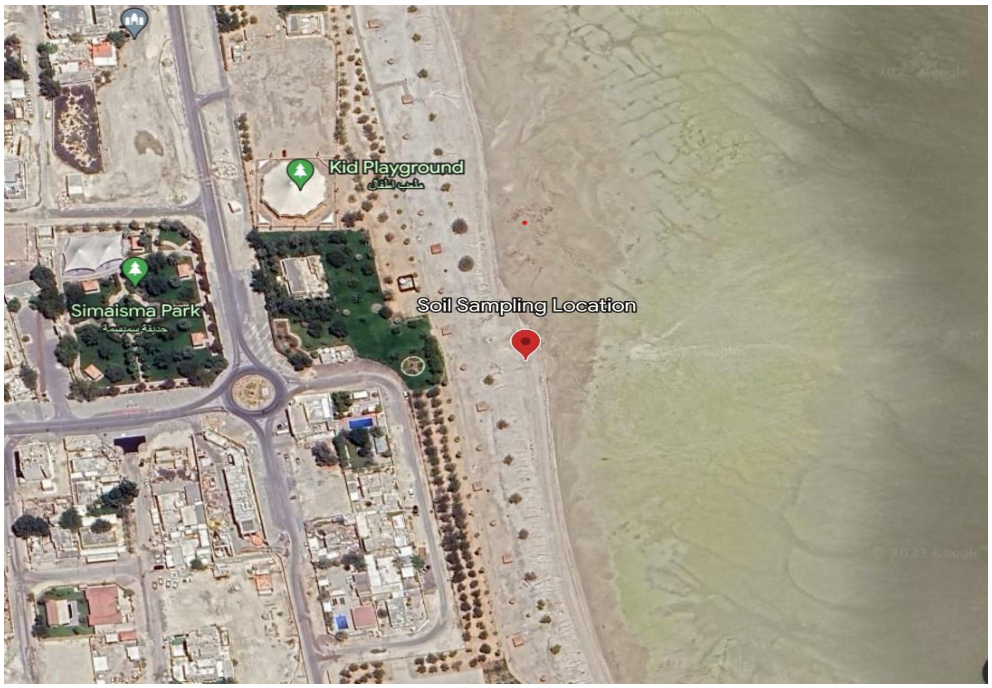

Figure A 1: The soil sampling location - simaisma beach area

Figure A 2: Orion™ Versa Star Pro™ Benchtop Meter (Thermo Scientific) sed to measure ORP, DO, pH, and EC.

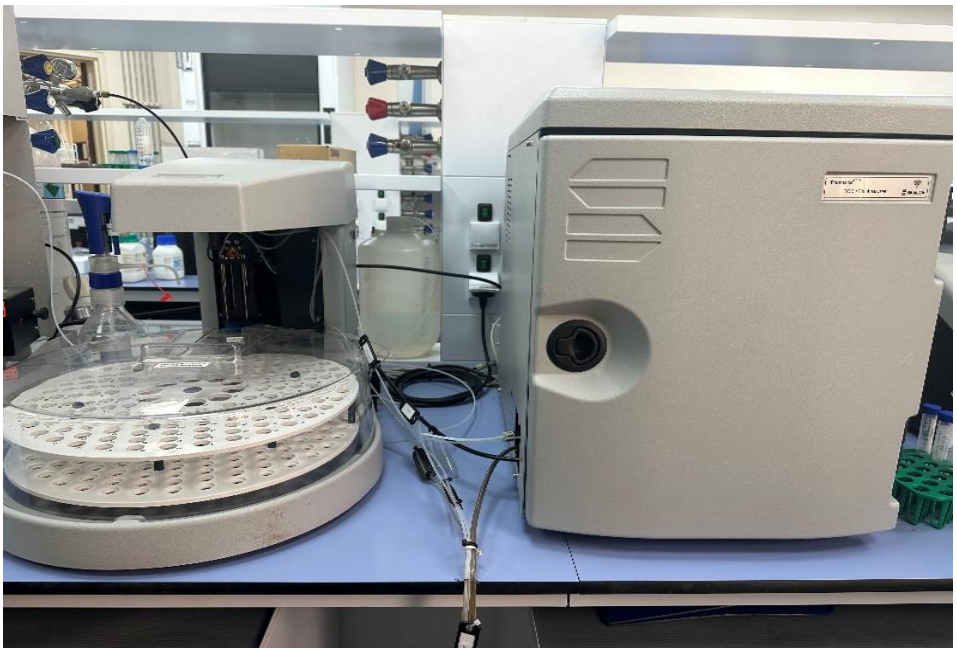

Figure A 3: Total Organic Carbon Analyzer (TOC) was used for the measurement of DIC from the pore water samples collected during the experiment.

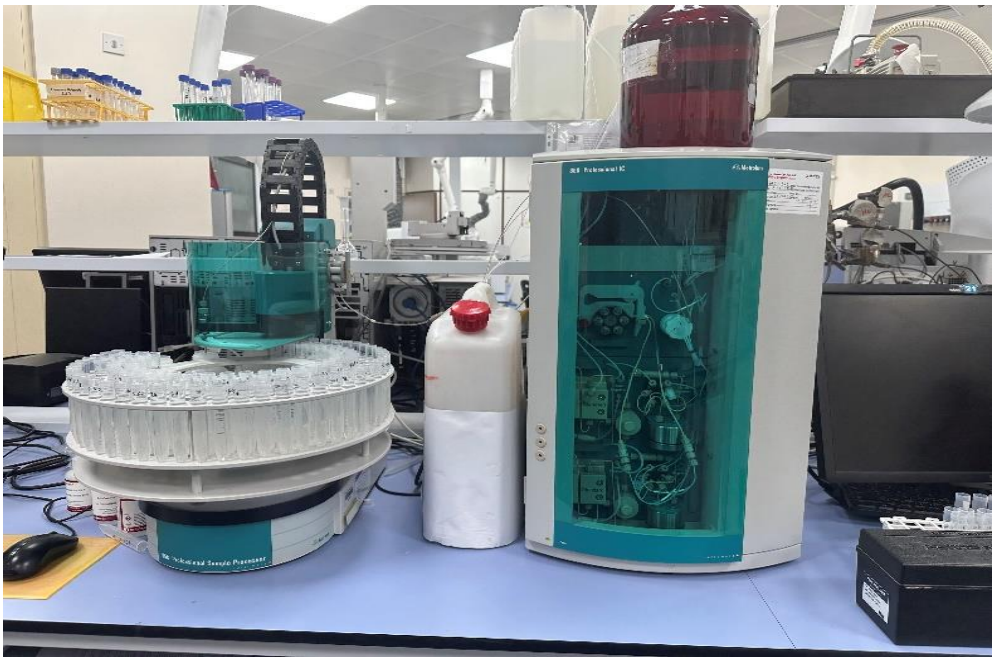

Figure A 4: 850 Professional Ion Chromatography (Metrohm)

Figure A 5: Gas Chromatography - Flame Ionization Detector (Clarus 680, Perkin Elmer, USA)

Figure A 6:Gas Chromatography – Mass spectrometry (GC-MS)

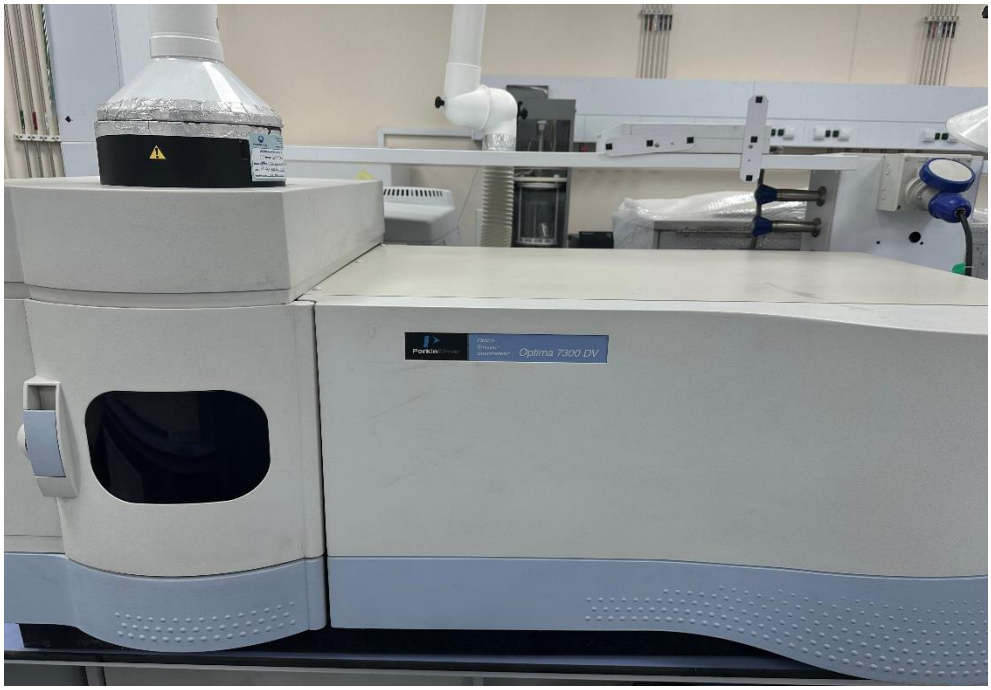

Figure A 7: Inductively Coupled Plasma Optical Emission spectroscopy (ICP-OES)

Figure A 8: X-ray fluorescence (XRF) - S2 PUMA analyzer

APPENDIX B: CALIBRATION CURVED FOR GC ANALYSIS

Example of Gas Chromatography Calibration curves:

Gas chromatography flame ionization detector (FID):

Toluene		
Time	Area under the curve	Conc (ppm)
12.864	16278.490	0.5
12.888	27157.850	1
12.89	50907.900	2
12.88	78545.990	3
12.881	102501.740	4
12.883	132125.850	5
12.883	161749.960	6

Benzene		
Time	Area under the curve	Conc (ppm)
7.994	14817.7	0.5
8.003	31220.86	1
8.005	57979.13	2
8.003	88408.53	3
8.005	114580.31	4
8.004	147626.43	5
8.008	179707.31	6

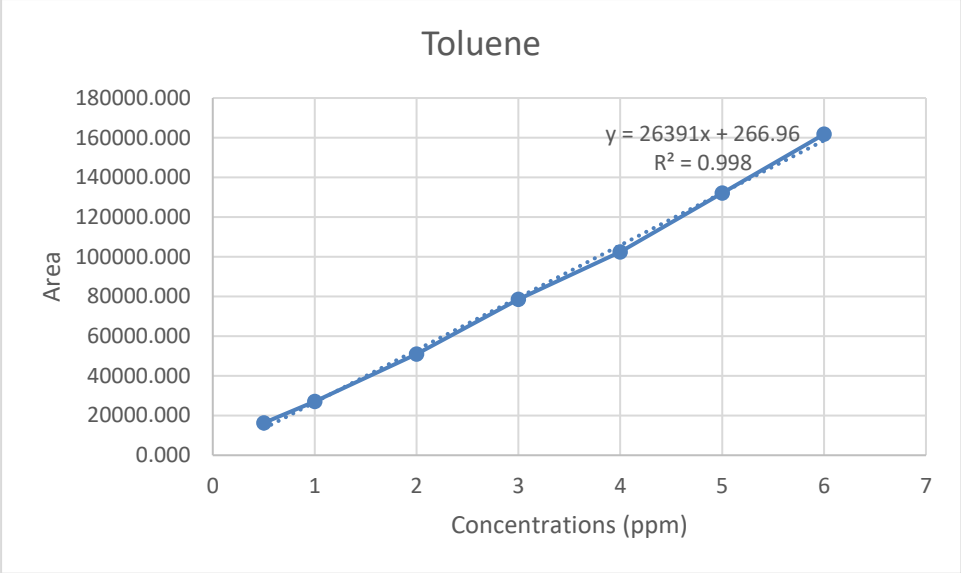

Figure B1: Toluene Calibration Curve

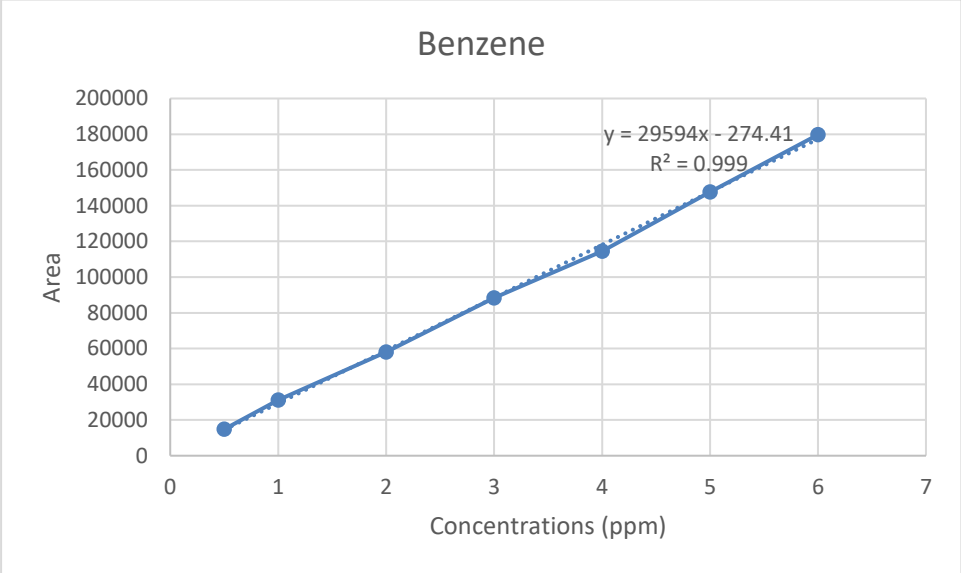

Figure B2: Benzene Calibration Curve

Gas chromatography–mass spectrometry (GC-MS)

Ethylbenzene		
Time	Area under the curve	Conc (ppm)
	25277	0.1
	92402	0.5
	125543	1
	593707	10

xylene		
Time	Area under the curve	Conc (ppm)
	27939	0.1
	125812	0.5
	173812	1
	851086	10

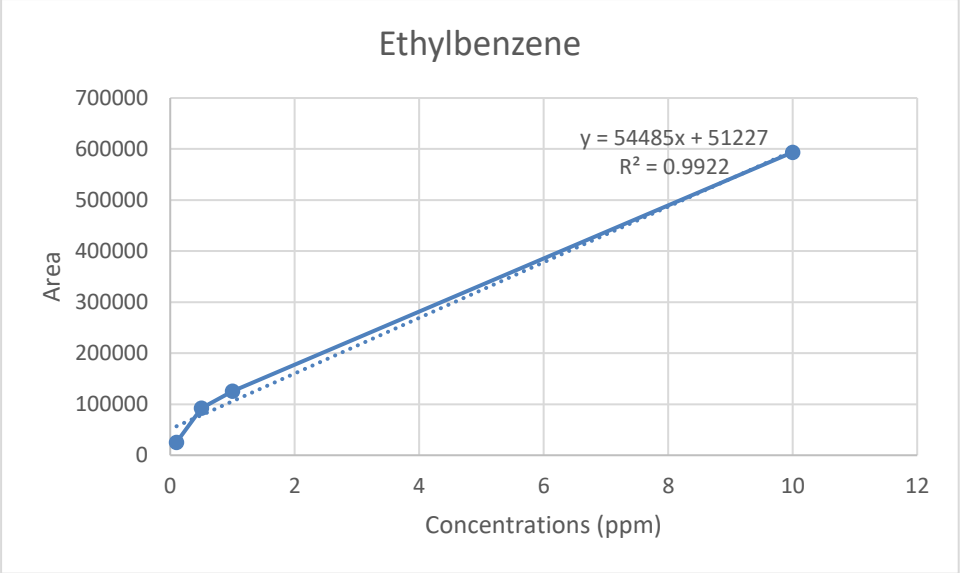

Figure B3: Ethylbenzene Calibration Curve

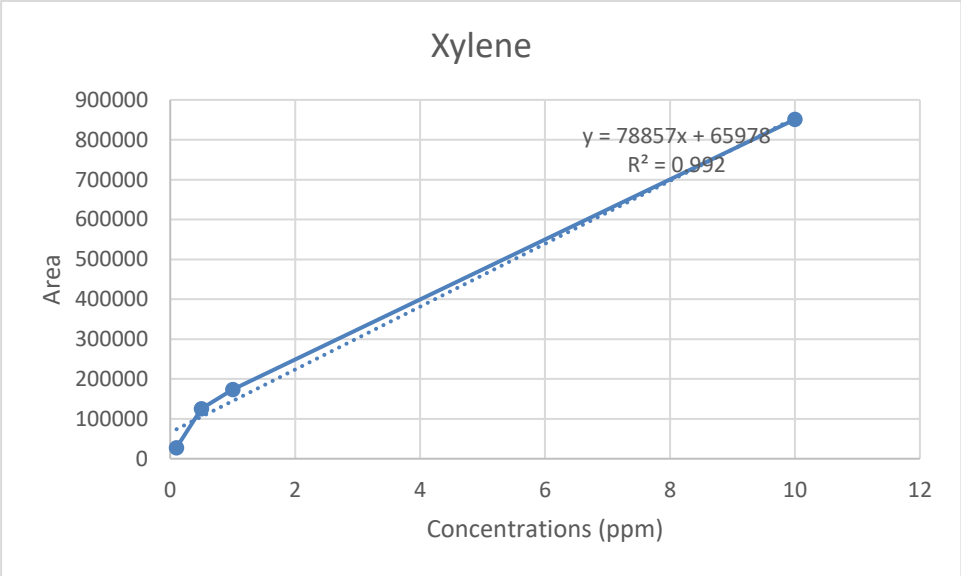

Figure B4: Xylene Calibration Curve

APPENDIX C: CHAPTER 5 FIGURES

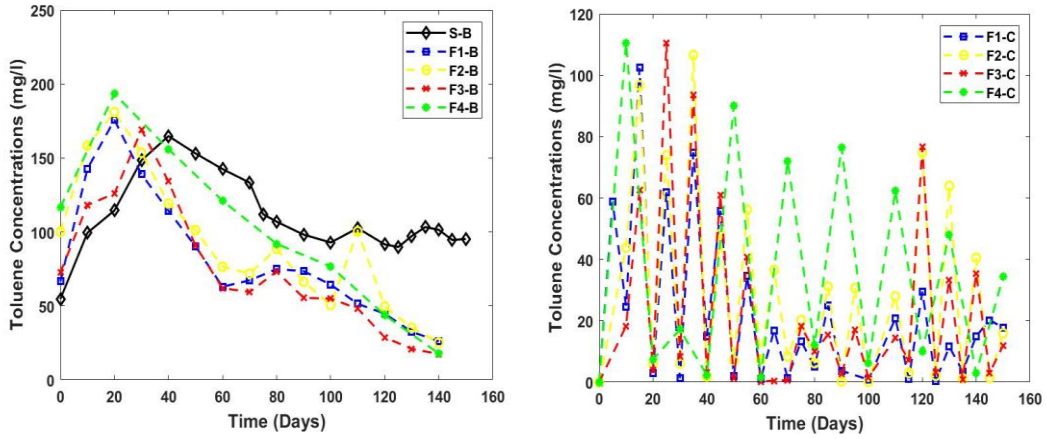

Figure C 1: Toluene Concentrations at (left) the middle (depth B) and (right) the bottom (depth C) of the columns S, F1, F2, F3, and F4

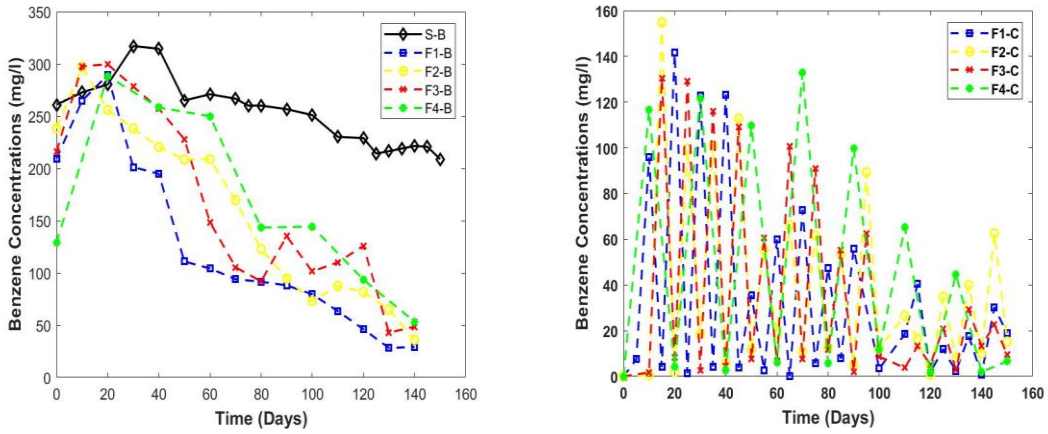

Figure C 2: Benzene concentrations at(left) the middle (depth B) and (right) the bottom (depth C) of the columns S, F1, F2, F3, and F4

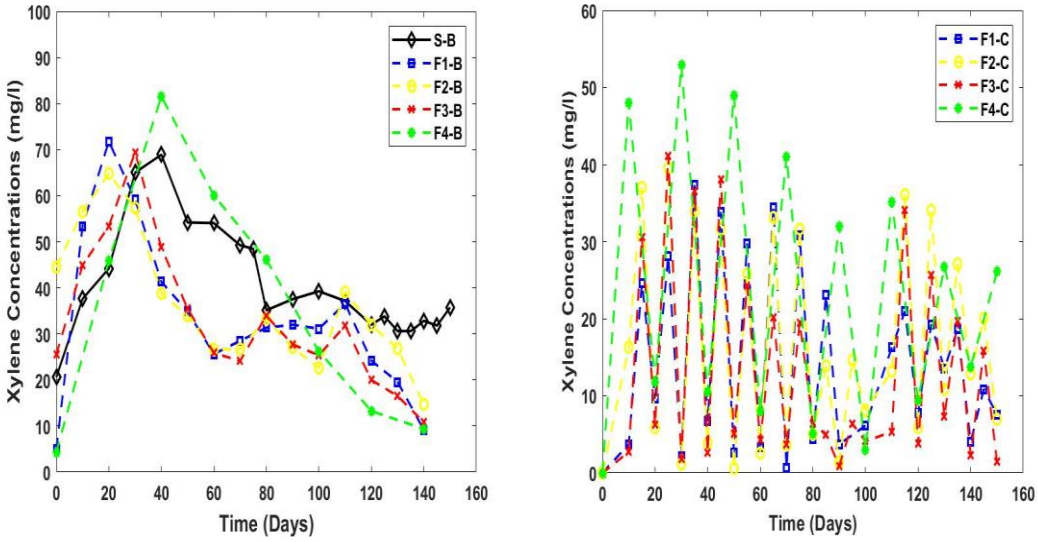

Figure C 4: Xylene Concentrations at the middle (depth B) and the bottom (depth C) of the columns S, F1, F2, F3, and F4

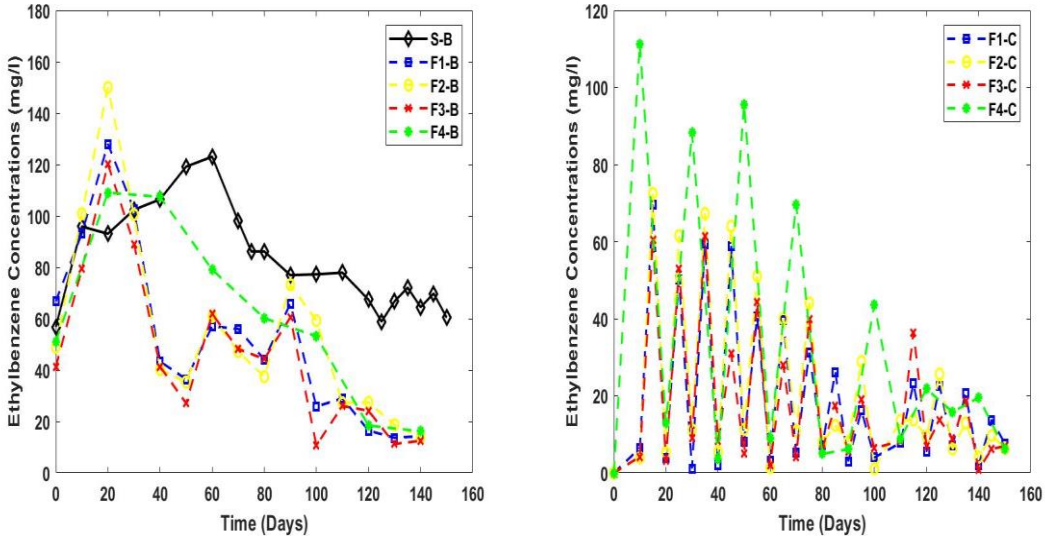

Figure C 3: Ethylbenzene concentrations at the middle (depth B) and the bottom (depth C) of the columns S, F1, F2, F3, and F4

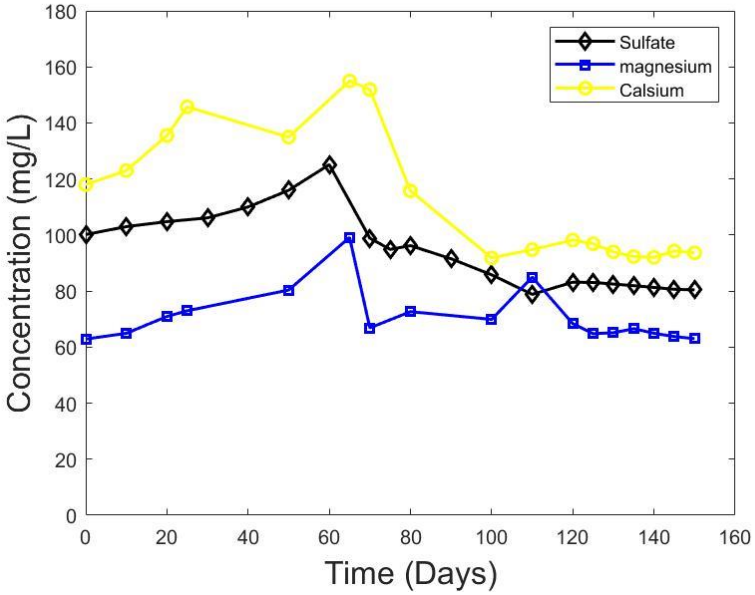

Figure C 5: Sulfate, Magnesium, and Calcium concentrations at the middle (Depth B) of the stable column (S)

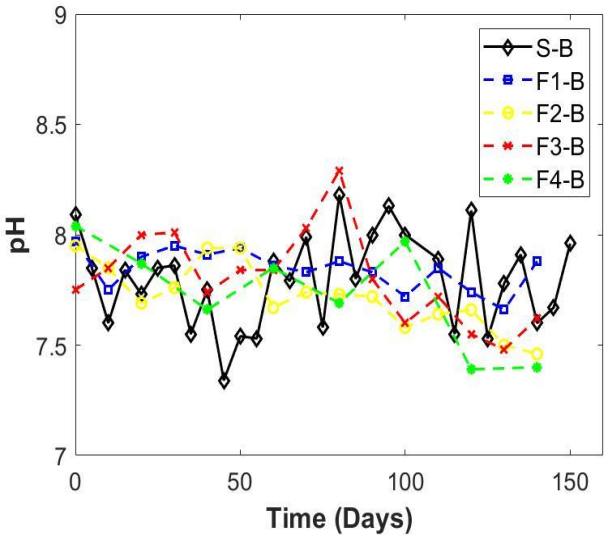

Figure C 6: pH at the middle (Depth B) of all columns (higlighted P-value > 0.05)

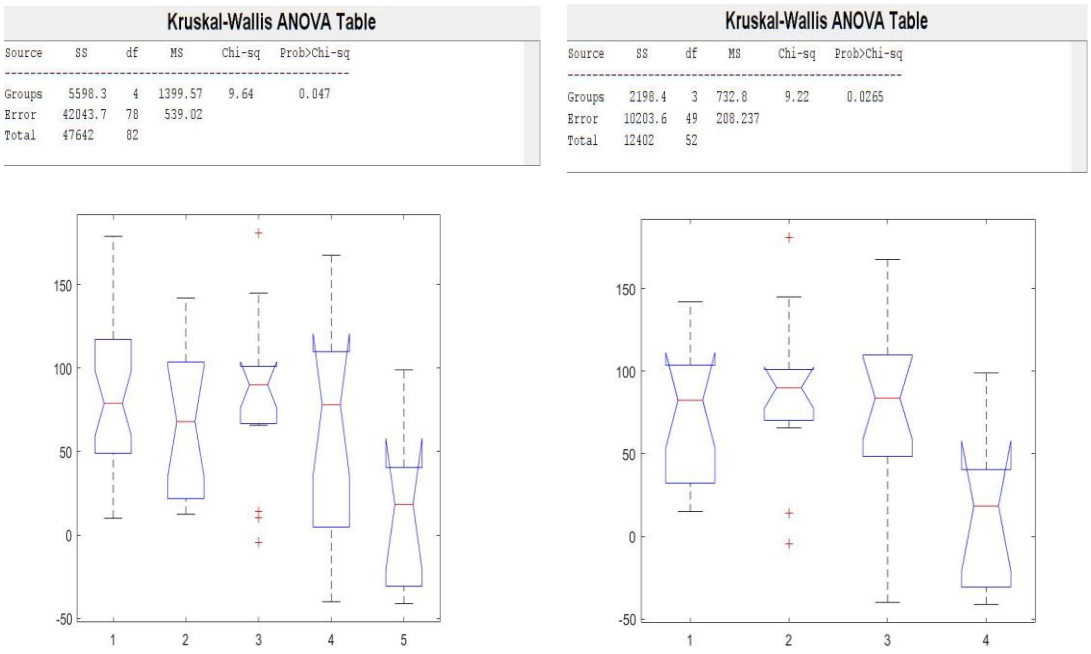

Figure D 1: P-values of ORP for the (left) middle of all columns (i.e., S, F1, F2, F3, and F4), and (right) for only the fluctuating columns (i.e., F1, F2, F3, and F4).

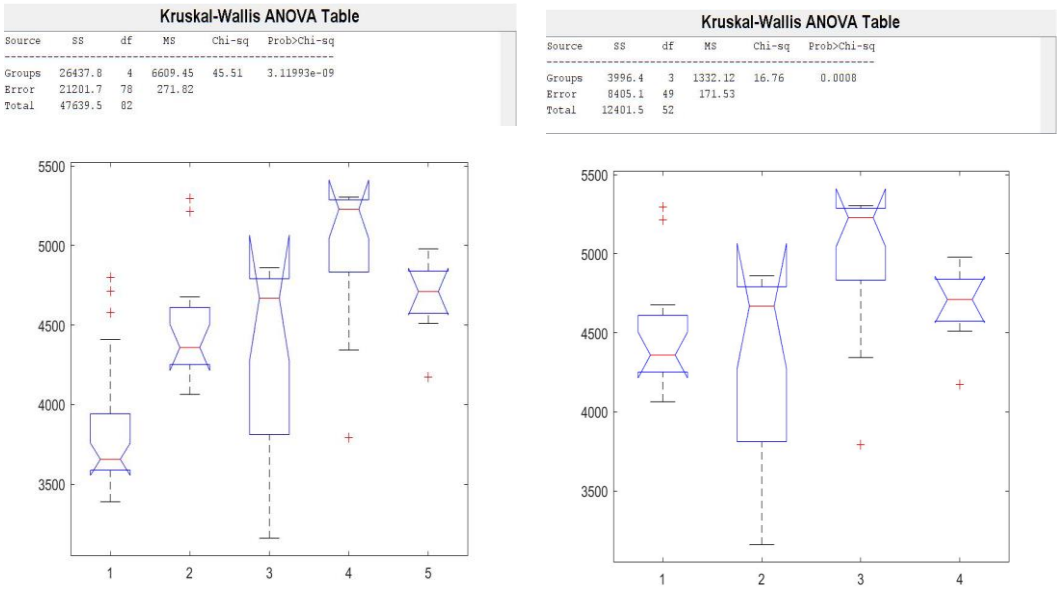

Figure D 2: p-values for the (left) EC values at the middle (depth B) of all columns (i.e., S, F1, F2, F3, and F4), (right) at the middle (depth B) of only fluctuating columns (i.e., F1, F2, F3, and F4),

APPENDIX E: CHAPTER 6 FIGURES

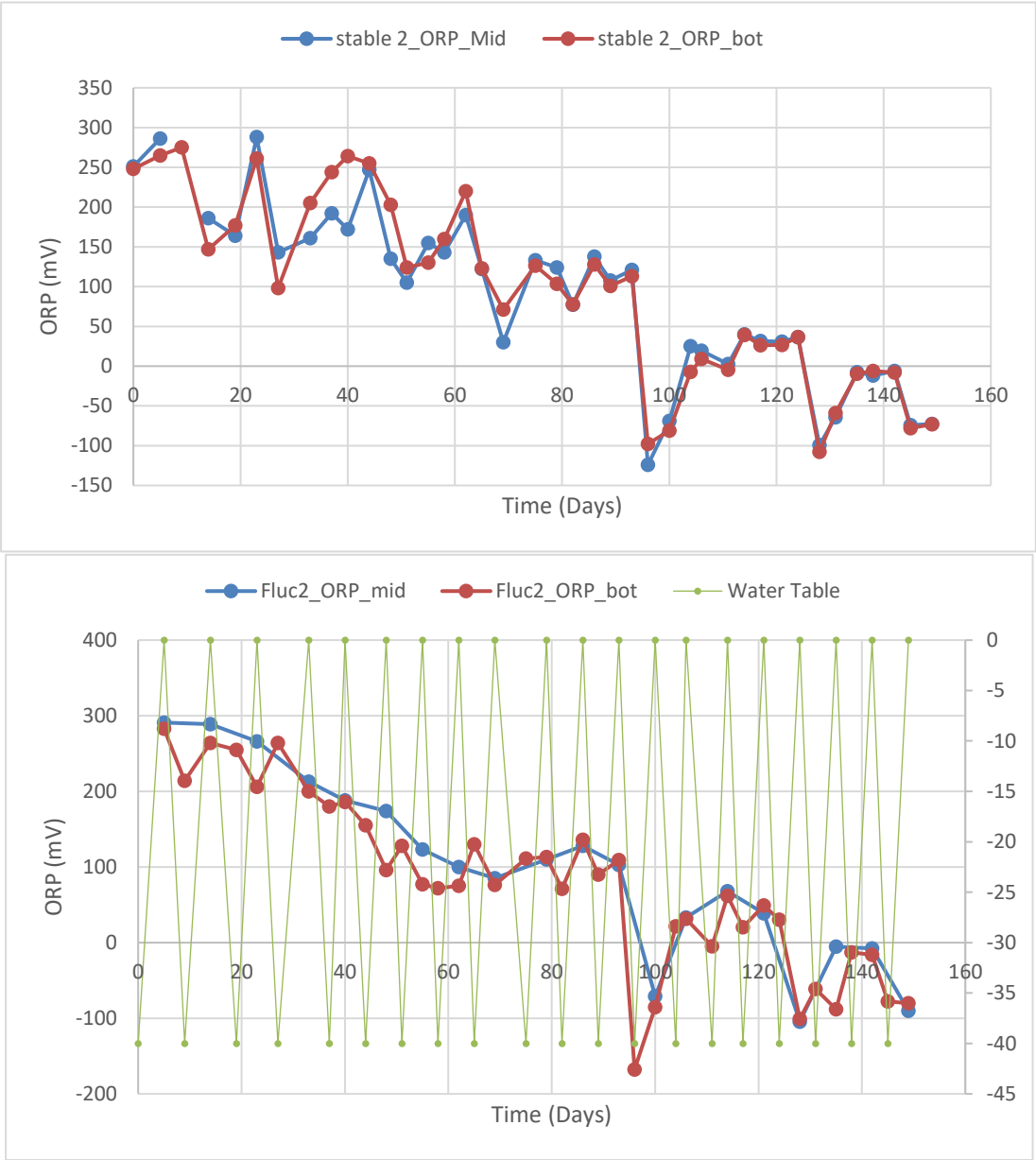

Figure E 1: Oxidation reduction potential (ORP) at the middle (depth B) and the bottom (depth C) of the columns S21 and F2

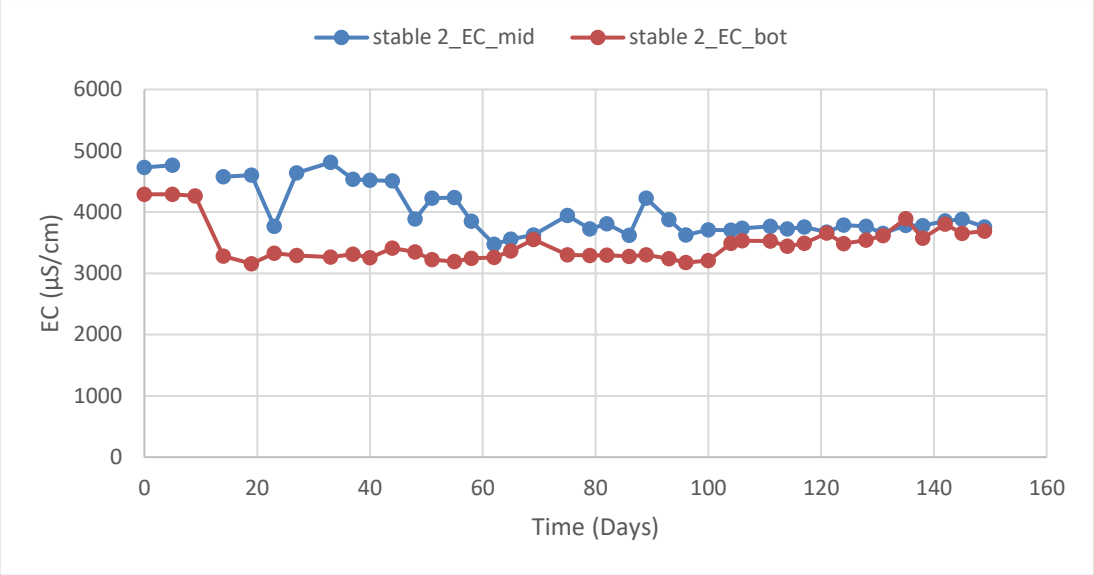

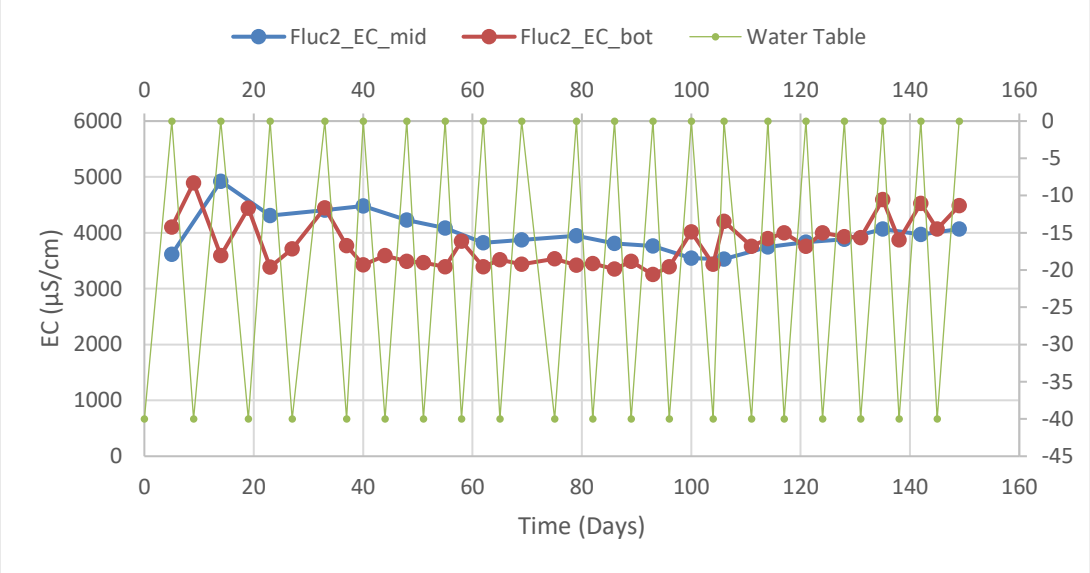

Figure E 2: Electric conductivity (EC) at the middle (depth B) and the bottom (depth C) of the columns S2 and F2

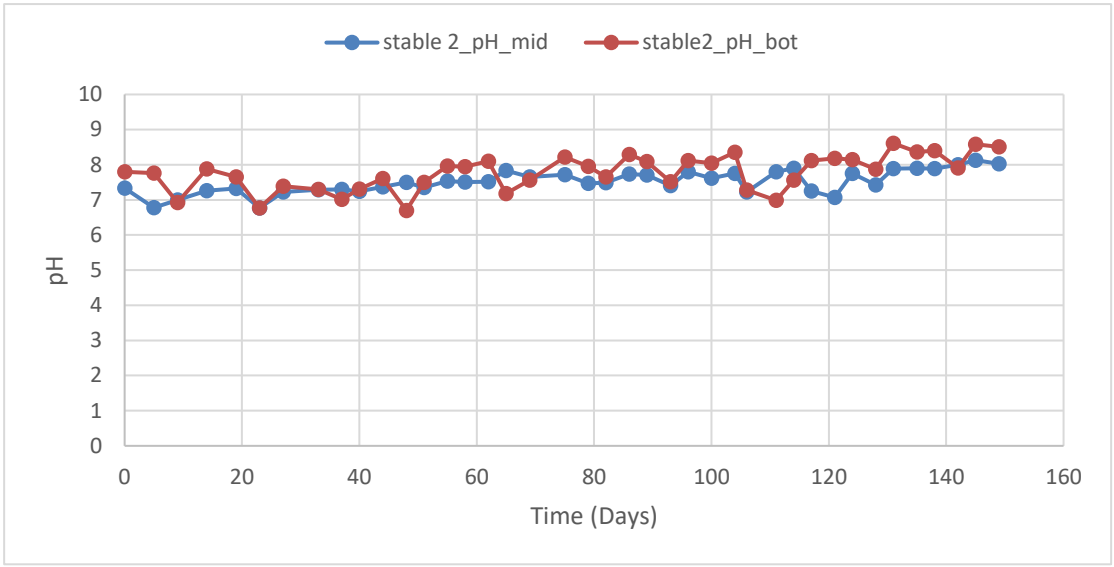

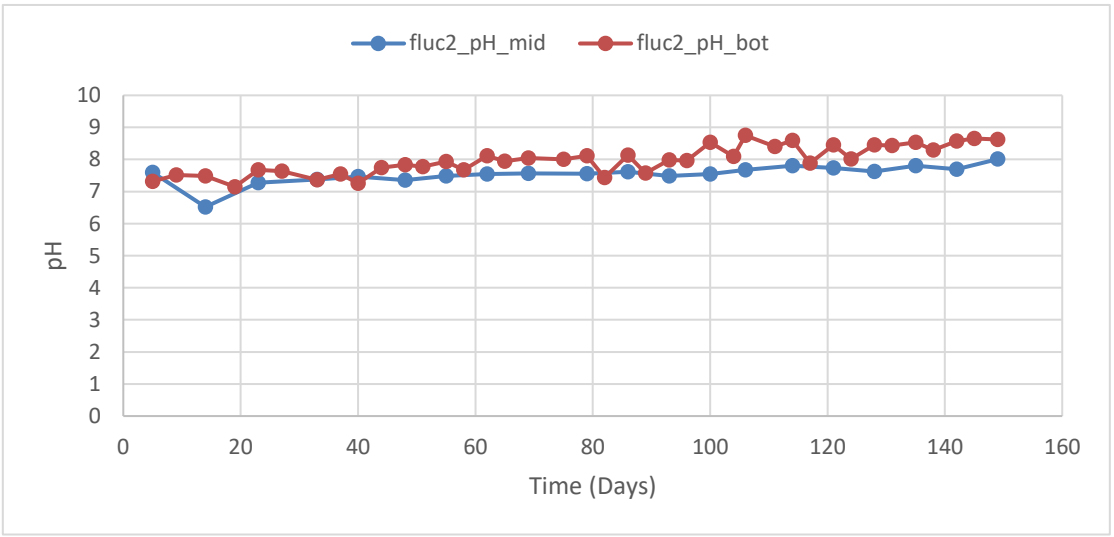

Figure E 3: pH values at the middle (depth B) and the bottom (depth C) of the columns S2 and F2

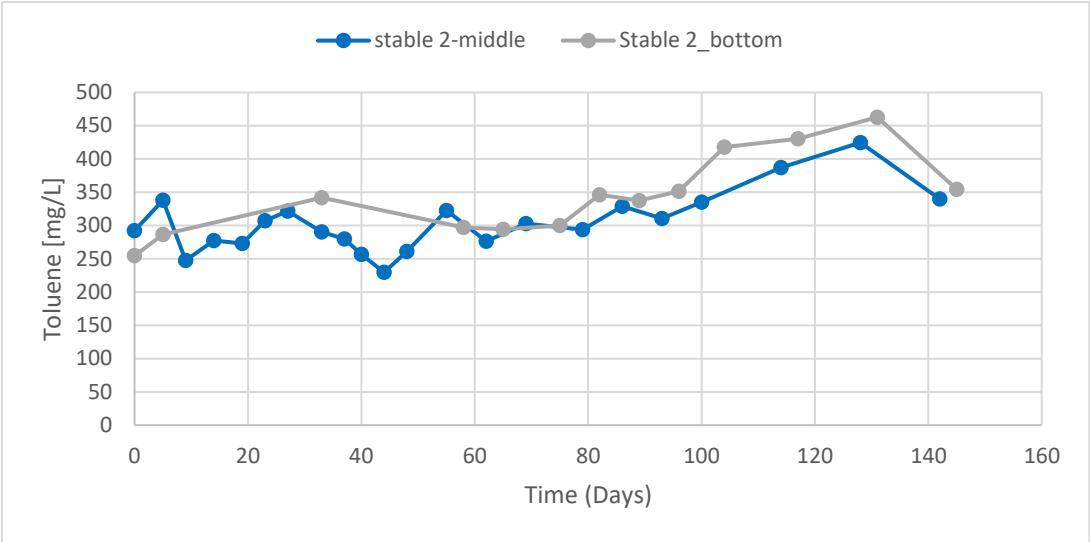

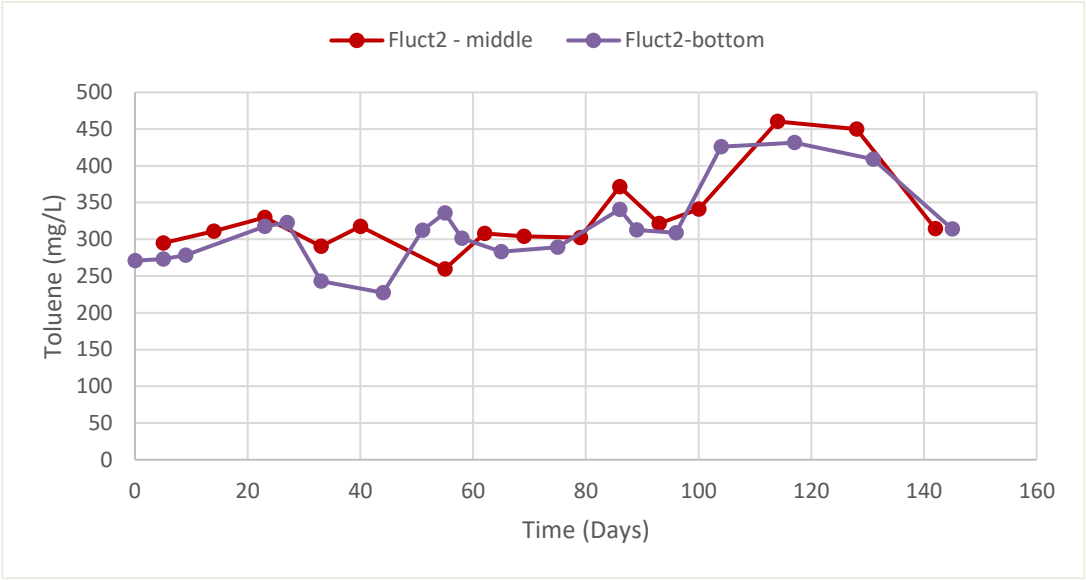

Figure E 4: Toluene concentrations at the middle (depth B) and the bottom (depth C) of the columns S2 and F2

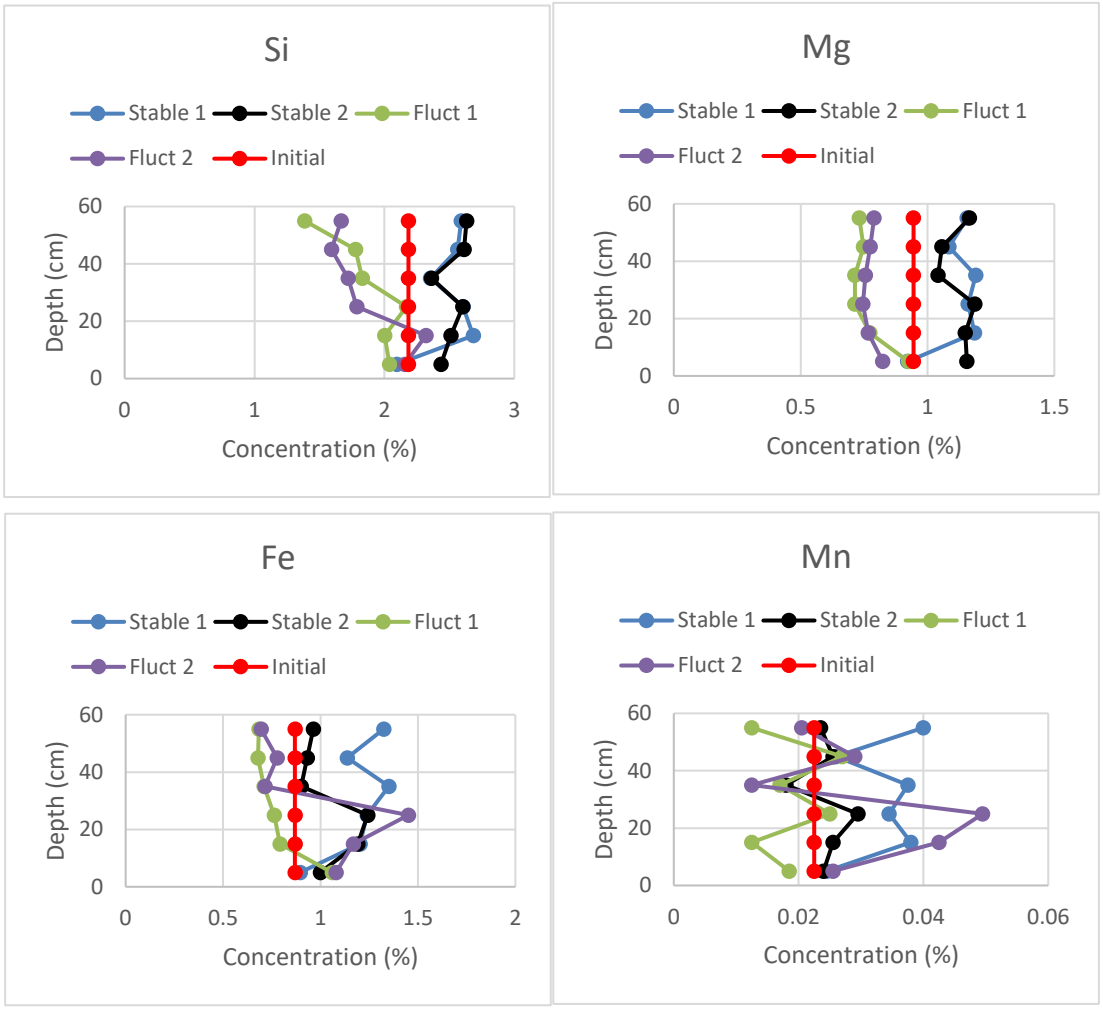

Figure E 5: Si, Mg, Fe, and Mn for the initial soil, and for the columns S1, S2, F1, and F2